



Title: Evaluating animal-free approaches to the testing of skin sensitisers

Name: Nora Naser Eddin

This is a digitised version of a dissertation submitted to the University of Bedfordshire.

It is available to view only.

This item is subject to copyright.



Evaluating Animal-Free Approaches to the testing of skin sensitisers

by

Nora Naser Eddin

2016

University of Bedfordshire

Evaluating Animal-Free Approaches to the testing of skin sensitisers

by

Nora Naser Eddin

supervised by Dr Zheyang Zhu

A thesis submitted to the University of Bedfordshire in partial fulfilment of the requirements for the degree of Master of Philosophy

November 2016

Academic Thesis: Declaration Of Authorship

I, Nora Naser Eddin

declare that this thesis and the work presented in it are my own and has been generated by me as the result of my own original research.

Evaluating Animal-Free Approaches to the testing of skin sensitisers

I confirm that:

1. This work was done wholly or mainly while in candidature for a research degree at this University;
2. Where any part of this thesis has previously been submitted for a degree or any other qualification at this University or any other institution, this has been clearly stated;
3. Where I have cited the published work of others, this is always clearly attributed;
4. Where I have quoted from the work of others, the source is always given. With the exception of such quotations, this thesis is entirely my own work;
5. I have acknowledged all main sources of help;
6. Where the thesis is based on work done by myself jointly with others, I have made clear exactly what was done by others and what I have contributed myself;
7. Either none of this work has been published before submission, or parts of this work have been published as indicated on [insert page number or heading]:

Name of candidate: Nora N. Eddin

Signature: Nora N. Eddin

Date: 10/11/2016

Evaluating Animal-Free Approaches to the testing of skin sensitisers

by

Nora Naser Eddin

ABSTRACT

With the implementation of the 7th Amendment of the EU Cosmetics Directive in 2013, Local lymph node assay (LLNA) assay can no longer be used for testing cosmetic ingredients. The current thesis focused on three aspects for further understanding and elucidating the sensitisation process in order to contribute to the reduction, refinement and replacement (“3Rs”) of the animal models with alternative non-animal approaches.

The performed quantitative whole human skin proteome analysis was established and identified total of 260 proteins. The applied GeLC-MS/MS identified proteins with diverse biological functions, sub-cellular locations and involvement of toxicological pathways at cellular and molecular levels.

An *in chemico* approach, utilising Top-down MS technique, was applied, using Apomyoglobin as recombinant protein. Results have shown a shift of the m/z (mass/ charge) ratio towards a higher value after treating with an extreme sensitiser, 1-chloro-2,4-dinitrobenzene (DNCB), indicating haptenisation . Further results have shown more binding sites on Apomyoglobin by DNCB at a physiological condition.

An *in vitro* model utilizing qRT-PCR (real time quantitative polymerase chain reaction) was used to investigate the effect of chemicals with different potencies and binding mechanisms: DNCB (2,4- dinitrochlorobenzen) and Phthalic anhydride (PA) on GST Pi gene expression in HaCaT cells. Experimental data showed DNCB to be a more potent Nrf2 activator in comparison to PA.

Acknowledgement

Firstly I would like to thank my first supervisor Dr Zheyang Zhu, and second supervisor Prof Jan Domin for their guidance, advice and support throughout the whole research project.

Secondly I would like to thank Dr Min Fang from Health Protection Agency in London, where a large part of the research project took place. Dr Fang was extremely supportive and her help has been essential for the success of this work.

Thirdly I would like to thank the University of Bedfordshire, and in particular everyone from the School of Life Sciences, who were always ready to provide me with the support I needed.

I would like to thank my family for their patience, faith and understanding, without whom I would not have overcome the obstacles that I have faced throughout the whole research project.

Finally, my sincere thanks to Christopher Slater-Walker for his diligent proofreading.

List of contents	Page number
Chapter 1. General Introduction.....	13
1.1 Anatomy and physiology of the skin.....	14
1.1.1 Function of the Skin.....	14
1.1.2.Epidermis.....	14
1.1.3. Dermis	15
1.1.4. Hypodermis.....	15
1.1.5. Immune cells of the skin.....	16
 1.2. Hypersensitivity and the use of cosmetics / personal care products.....	 17
 1.3. Allergic contact dermatitis (ACD).....	 20
1.3.1. Mechanism for skin sensitisation.....	20
 1.4. Local lymph node assay (LLNA).....	 23
 1.5. The 7th amendment of the EU Cosmetics Directive in 2013.....	 25
 1.6. Current approaches for testing skin sensitisers.....	 27
 1.7. Aims and objectives.....	 32
 1.8. Main hypothesis.....	 33
 Chapter 2. Human skin proteome profiling.....	 34
2.1. Introduction	35
 2.2. Materials and methods.....	 37
2.2.1.Sample preparation(<i>performed at University of Bedfordshire</i>).....	37
2.2.2.Estimation of protein concentration (<i>performed at University of Bedfordshire</i>).....	37
2.2.3. GeLC-MS/MS (<i>performed at Health protecting Agency London</i>).....	38
2.2.4. Mass Spectrometry analysis (<i>performed at Health protecting Agency London</i>).....	39
2.2.5. Database searching (<i>performed at Health protecting Agency London</i>).....	40

2.2.6. Uniprot analysis (<i>performed at University of Bedfordshire</i>).....	40
2.2.7. Gene Ontology analysis (<i>performed at University of Bedfordshire</i>).....	41
2.3. Results	42
2.3.1. Characterisation of human skin proteome.....	42
2.4. Discussion	47
2.4.1. Characterisation of human skin proteome.....	47
2.4.2 Interaction of different cosmetic products.....	51
Chapter 3. <i>In chemico</i> approach in studying skin sensitisers.	53
3.1. Introduction	54
3.2. Materials and methods	58
3.2.1 <i>In chemico</i> experiment.....	58
3.2.2. <i>Top-down Analysis (Health Protection Agency London)</i>	59
3.3. Results	61
3.3.1. Top-down mass spectrometry.....	61
3.4. Discussion	64
3.4.1. <i>In chemico</i> approach by Top-down mass spectrometry.....	64
Chapter 4. <i>In vitro</i> approach in studying skin sensitisers. Phase II xenobiotic metabolic enzymes	69
4.1. Introduction	70
4.1.1. Regulation of XME phase II- Keap1-Nrf2-ARE.....	73
4.1.2. Gluthation-S-transferase (GST).....	74
4.2. Materials and methods	76
4.2.1. Cell recovery and culture.....	76
4.2.2. MTT [3-(4,5-Dimethylthiazol-2-yl)-2,5-Diphenyltetrazolium Bromide] assay.....	76
4.2.3. Treating HaCaT cells with the same dose of 2,4-Dinitrochlorobenzene (DNCB) and Phthalic Anhydride (PA) at different time incubation.....	77

4.2.4. mRNA extraction and cDNA synthesis.....	77
4.2.5. Primer design.....	78
4.2.6. Qualitative determination of the designed GSTpi primers using PCR reaction.....	78
4.2.7. Quantitative polymerase chain reaction (qRT-PCR).....	78
4.3. Results	79
4.3.1. Cytotoxicity.....	79
4.3.2. Primer design.....	81
4.3.3. Qualitative determination of the designed GSTpi primers using control, DNCB and PA treated samples.....	81
4.3.4. Class pi (GST Pi) mRNA expression.....	82
4.4. Discussion	85
4.4.1. <i>In vitro</i> examination of induced metabolic enzymes (XME phase II).....	85
Chapter 5. Final Discussion and Future Studies	89
5.1. Characterisation of human skin proteome.....	90
5.2. <i>In chemico</i> approach by Top-down mass spectrometry.....	91
5.3. <i>In vitro</i> examination of induced metabolic enzymes.....	93
6. References	95
7. List of Abbreviations	103
8. Supplementary Data	107

List of Figures	Page number
Figure 1. Schematic representation of the composition of the skin	16
Figure 2. Simplified schematic representation of the induction phase of the sensitisation process: Allergen penetrates the epidermis (1), enabling covalent interaction with a protein (2) leading to the formation of complete protein-hapten conjugate, which interacts with keratinocytes (KC,) and (3) triggers dendritic cells (DC) activation and maturation to the lymph nodes (4). There, the antigen is presented to naive T cells. TC differentiates and proliferates in response to the antigen presence (5).....	22
Figure 3. Overview of the local lymph node assay, in which a test substance is applied on the mouse ear for 3 subsequent days, followed by injecting at day 6 into the tail vein with radioactively labeled thymidine (³ H-thymidine). Lymph nodes are removed and processed for measuring the amount of lymphocytes produced as a result of the exposure.	25
Figure. 4. Global cosmetics market is predicted to reach \$265 billion in 2017. From 2012 to 2017 the Global cosmetic market is predicting 4.6 % increase.....	25
Figure 5. Summary of the currently non-animal approaches for sensitisation assessment.....	30
Figure 6. Current evaluated and validated non-animal models for categorization of skin sensitizers by European Union Reference Laboratory for alternatives to animal testing.....	32
Figure 7. Schematic overview of the current research project.....	33
Figure 8. Schematic overview of S9 and NS9 sample analysis by GeLC-MS/MS method.....	42
Figure 9. Cellular location of proteins identified in the soluble and insoluble fractions was annotated to the GOA human GO Slim terms and Generic human GO slim terms for cellular compartment, using GO Term Mapper.....	43
Figure 10. Biological function of all proteins identified from mass spectrometry analysis of human skin. Proteins were annotated with the GOA human Go slim terms for biological process, using GO term Mapper.....	44
Figure 11. MS spectrum of APG-DNCB sample. A:control (APG alone + vehicle); B: APG modified by DNCB incubated at 18 °C (mass shift of 8.74m/z ≈166.06 Da).....	62

Figure 12. MS spectrum of APG-DNCB sample. A: control (APG alone + vehicle); B: APG modified by DNCB incubated at 18 °C (mass shift of 7.64m/z \approx 168.08 Da); C. APG modified by DNCB incubated at 32 °C shows two peaks : The first peak with a mass shift of 7.64 m/z \approx 168.06. The second peak with a mass shift of 15.14 m/z. The 15.14 m/z \approx 333.08.....63

Figure 13. Predictive diagram of the DNCB-apomyoglobin adduct formation following the incubation of apomyoglobin with extreme sensitiser (DNCB) at 18 °C for 24 h. The change of the mass as a result of the incubation with DNCB suggests that the protein-hapten conjugate formation is based on the addition of the DNCB molecule to a single location on the apomyoglobin protein (masses calculated based on the mass spectrometry data) with the loss of a single chlorine.....65

Figure 14. Predictive diagram of DNCB-apomyoglobin adduct formation following incubation of apomyoglobin with extreme sensitiser (DNCB) at 32 °C for 24 h. The change of the mass as a result of chemical incubation suggests that protein-hapten conjugate formation is based on the addition of two DNCB molecules to different locations on the apomyoglobin protein (masses calculated based on mass spectrometry data) with the loss of two chlorines.....66

Figure 15. Schematic representation of drug metabolism. Phase I includes oxidation, hydrolysis, reduction. Phase II includes the formation of hydrophilic compound R-SG, sulfation, acetylation and formation of acetyl Co-A and glucuronidation using glucuronic acid. Phase III involves further metabolism and pump of the product out of the cell.....71

Figure 16. Keap1-Nrf2-ARE pathway. Keap1-Nrf2 complex exist in the cytoplasm. When reacting with hapten, the Keap1 disassociates from Nrf2, leading to Nrf2 translocate to the nucleus. In the nucleus Nrf2 forms a dimer with Maf protein. The haptenised Nrf2-Maf complex bind to DNA and facilitate to the transcription of the target gene.....74

Figure 17. MTT assay: A. Benzalkonium Chloride (BC); B. Benzaldehyde (BZ); C. Phthalic anhydride (PA), D. 2,4-Dinitrochlorobenzene (DNCB). Error bars are mean \pm SD.....80

Figure 18. Qualitative analysis of primer specificity using agarose gel electrophoresis of A- HaCaT cells treated with DNCB and C- HaCaT cells treated with PA with different incubation periods; B- analysis of primer specificity using agarose gel electrophoresis of standard sample of untreated HaCaT cells incubated for 24h.....82

Figure 19. Standard cDNA melting curve, A and standard curve, B performed on untreated HaCaT cells using the designed GSTpi primers.....83

Figure 20. mRNA expression level of Gluthatione-S-transferase (Pi), phase II metabolic enzyme (GST-pi) of keratinocytes (HaCaTa cell line) using qRT-PCR treated with DNCB at different incubation time.....84

Figure 21. mRNA expression level of Glutathione-S-transferase (Pi), phase II metabolic enzyme (GST-pi) of keratinocytes (HaCaT cell line) using qRT-PCR treated with PA at different time incubation.....85

Figure 22. The certificates of analysis of the 8 human skin samples provided by Biopredict International, France used in the skin proteome analysis.....114

Figure 23. Proposed regulation of Nrf2 and NF- κ B by protein modification or GSH depletion.....127

Figure 24. Standard cDNA melting curve, A and standard curve, B performed on untreated HaCaT cells using the designed GAPDH primers

List of Tables	Page number
Table 1. Identification and quantitative expression overview of the top ten most abundant proteins identified in S9 & NS9 fractions, based on the presence of tryptic peptides in all 8 donors and based on the presence of ≥ 2 different tryptic peptides identified in all the 8 donors, respectively.....	45
Table 2. Toxicological pathways in which the proteins from S9 and Non S9 fractions are involved, and identified by the ToxProfiler software using WikiPathways and Biocarta databases as reference.....	46
Table 3. List of chemicals tested in the <i>in chemico</i> experiment.....	59
Table 4. Designed Primers for GST-pi and GAPDH genes.....	81
Table 5. Identification and quantitative expression overview of all proteins identified in S9 & NS9 fractions, based on the presence of ≥ 2 different tryptic peptides identified in all the 8 donors.....	115
Table 6. Quantitative expression overview of all proteins identified in S9 & NS9 fractions, based on the presence of ≥ 2 different tryptic peptides identified in all the 8 donors.....	121
Table 7. Summary of the GST Pi gene expression of control and DNCB treated HaCaT cells.....	128
Table 8. Summary of the GST Pi gene expression of control and PA treated HaCaT cells.....	129
Table 9. Summary of the GAPDH gene expression of control, DNCB and PA treated HaCaT	

Chapter 1

General Introduction

1. Anatomy and physiology of the skin

1.1.1 Function of the Skin

The skin is the largest and heaviest organ in the body. Its main function is to protect the body from mechanical injuries, variation in the ambient temperature, radiation, invasion of pathogenic microorganisms, and the effect of external chemicals. The thermal regulation of the body starts with the involvement of the skin via sweat and body hair movement. The skin is a sensitive organ enriched with nerve receptors that are able to detect many changes in the environment, leading to involuntary responses with the final outcome of protecting the body from any harm (Tončić et al., 2011).

The skin is composed of three main layers: epidermis, dermis and hypodermis (Montagna, 1974; Brohem et. al., 2010)

1.1.2. Epidermis

The epidermis forms the outer layer of the skin, providing a waterproof barrier and determining the skin colour. It has a thickness of approximately 50 cells in areas of thin skin, and around 100 cells in areas of thick skin. The epidermis is approximately 0.1 mm thick, and has the ability to renew itself totally every 28 days. The cells composing the epidermis are mainly keratinocytes, melanocytes and Langerhans cells (also known as dendritic cells), which are antigen-presenting immune cells that protect against infections.

The epidermis itself is made of few sub-layers. The deepest layer of the epidermis, located immediately above of the dermis - is known as the Stratum basale. The Stratum basale is composed of cube-shaped cells: keratinocytes and melanocytes. Keratinocytes in this layer constantly undergo division for regeneration, which contributes to the skin renewal process. On the other hand melanocytes, also called protective cells, are responsible for the syntheses of melanin, an important pigment that determine the tones of the skin colour and protects from the UV-radiation of the Sun.

The Stratum spinosum is the second layer of the epidermis, and is composed mainly of keratinocytes.

The third layer is Granulosum and it contains a protein called keratin. Keratin is tough, fibrous protein with protective properties. The fourth epidermal layer is called the Stratum Lucidum; it is found in specific parts of the body such as fingertips, palms of the hands and soles of the feet. The fifth and top outer layer of the epidermis is called Stratum Corneum and it is composed of dead keratinocytes. This layer is continuously regenerated by the formation of new keratinocytes from the deeper layers. The Stratum Corneum and the keratinocytes are separated by epidermal lipids. The epidermal lipids perform adhesion between the skin cells. The keratinocytes and the epidermal lipids together form a waterproof layer, preventing water loss and keeping the skin moist. The surface of the Stratum Corneum appears to be slightly acidic with a pH range from 4.5 to 6.5. The acidic pH is maintained by the secretion of sebaceous and sweat glands to sustain the hardness of the keratin and to prevent the growth of harmful bacteria and fungi (Tortora and Grabowski, 1993).

1.1.3. Dermis

The Dermis is the middle skin layer, located between the epidermis and the hypodermis. This layer is 2 mm thick and is responsible for maintaining the structure and resilience of the skin. The dermis is made of structural proteins called collagen and elastin, forming a mesh-like structure, as well as blood and lymph vessels, mast cells and fibroblasts surrounded by glycosaminoglycans (a gel-like substance). The glycosaminoglycans provide moisture to the epidermis and enable the collagen fibres to retain water. The fibroblasts are cells that produce collagen and elastin, whereas blood vessels in the dermis help with the body's thermal regulation. Mast cells are specialised cells with an important immunological role and ability to trigger skin immune response as a result of contact with allergens and harmful microorganisms.

1.1.4. Hypodermis

The Hypodermis is the inner skin layer, rich with fat tissues, hair follicles, blood vessels, sweat glands and connective tissues. The fat tissues help in regulation of body temperature,

shock absorption and the provision of nutrients and energy to surrounding cells (Millington and Wilkinson, 2009) (Siemionow and Einsenmann-Klein, 2016).

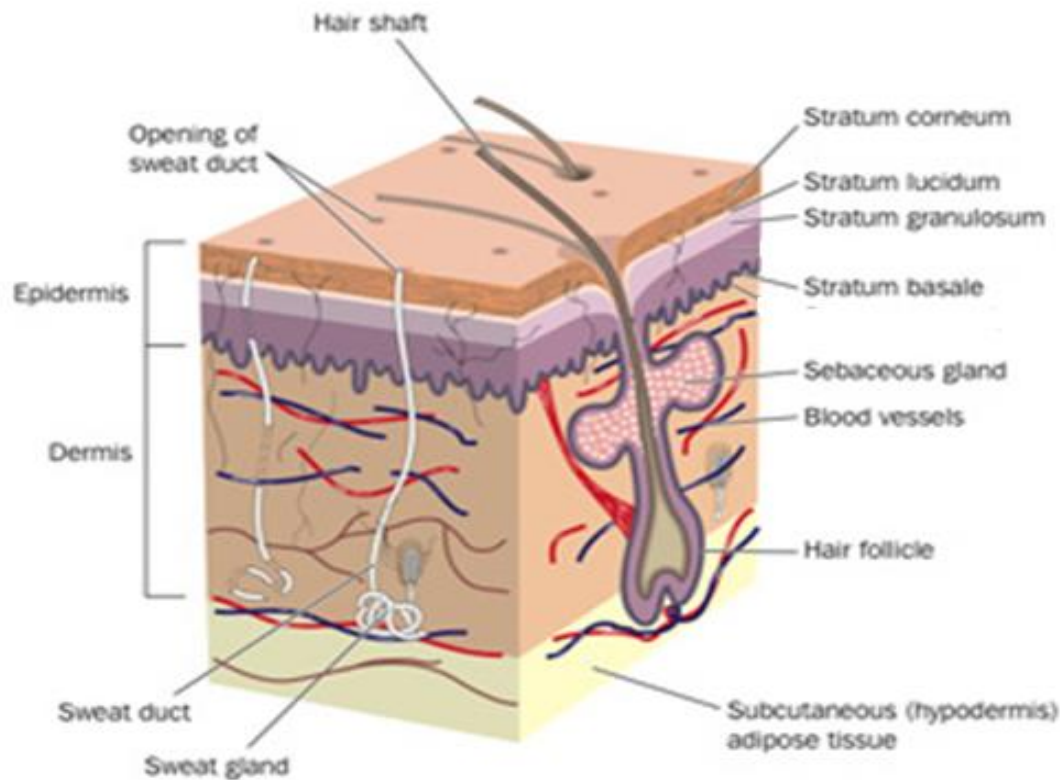


Figure1. Schematic representation of the composition of the skin (Tortora and Grabowski, 1993)

1.1.5. Immune cells of the skin.

The skin is the primary barrier against physical insults and microbial pathogens.

It represents a unique environment where immune cells interact with skin cells to keep tissue homeostasis and induce immune responses. A diverse and multifunctional immune cells populate the skin.

In the epidermis a specialised subset of Dendritic cells (DC) known as Langerhan cells (LC) sample antigens such as toxins. LC cells appear to have both anti-inflammatory and activatory role in the skin, depending on the event. DC cells in the dermis are highly efficient of capturing dead cells, and presenting antigens such as viruses and other pathogens to the T

cells. DC cells can be described as the immune vehicle, that represent antigen to T cells, where T cells are the immune effectors. In healthy skin the amount of T cells is double in comparison with the T cells present in the blood. Most of them are T cells that have previously recognised Ag (antigens) and can be quickly reactivated. T cells in the epidermis are mostly CD8 + T cells, which as a result of their activation can kill target cells.

T cells in the dermis are mostly CD4+ T cells, with a modulatory role (reduce tissue destruction) as a result of the immune response. In addition, NK (natural killers), mast cells and eosinophil cells are present in the dermis and are involved in skin immune reactions.

In the case of Ag invasion the keratinocytes presented in the epidermis start secreting AMP (antimicrobial peptide) that can kill bacteria directly and/or secrete inflammatory mediators such as IL1 (interleukin 1) which activate DC cells and chemokines that recruit macrophages, T cells and neutrophils (different types of cells involved in the immune response). Activated DC cells migrates to the LLNA (local lymph node), representing the antigen to the available there naive cells which in turn become activated and turn into effectors T cells. Activated T cells return to the epidermis and kill the affected keratinocytes or secrete signals to recruit additional immune effectors cells. Following antigen clearance the memory CD8+ T cells remain in the epidermis to provide immunity for future encounters with the same antigen (Galli and Tsai, 2013).

1.2. Hypersensitivity and the use of cosmetics / personal care products

Any substance that triggers an allergic response is referred to as an allergen. Allergens can be substances secreted by microorganisms; plants; animals; or any other naturally occurring chemical. The allergy can be caused by exposure to an agent in the atmosphere (pollen); contact with skin (cosmetics); ingestion (food) or injection (insect bite or drug) . Allergic hypersensitivity is an immune response by the body resulting from an exposure to a certain dose-specific stimulus, which may, however, be well-tolerated by other individuals. Different factors can affect the nature and

severity of an allergic reaction, such as route of exposure, skin condition, degree of sensitisation in addition to various genetic factors which are not yet very well understood. Hypersensitivity can be considered both allergic and non-allergic. Non-allergic hypersensitisation, also known as "pseudo-allergy," does not lead to an immune reaction due to contact with certain allergens. Allergic hypersensitivity appears when the individual develops an immune response as a result of contact with the allergen. Allergic hypersensitivity can be antibody-mediated or non-antibody-mediated. Antibody-mediated hypersensitivity involves antibodies such as IgE, IgG, IgM (immunoglobulins E, G and M), and mast cells, where the immune response can develop within hours. Allergic contact dermatitis belongs to the non-antibody-mediated hypersensitivity also known as cell mediated immune reaction (CMIR), which is regulated by the proliferation of T cells. The immune response caused by non-antibody-mediated hypersensitivity usually develops within one to three days following exposure to allergens (Janeway et al., 2003).

Immune reactions can be classified into four main groups, known as Types I, II, III and IV.

Type I immune reaction known as an immediate hypersensitivity that can develop typically within few minutes of the exposure to an antigen. This type of immune response is lead mainly by IgE (immunoglobulin E) and mast cells. Mast cells are type of granulocytes derived from myeloid stem cells. Mast cells play an important protective role from allergy, wound healing and defence against pathogens.

Type II immune response is based on antibody binding to membrane- bound antigen leading to inflammation. This type of immune response usually develops within 20 min as a result of exposure to an antigen.

Type III immune response takes place when the antibody binds to a soluble antigen forming immune complex. In this immune response the immune reaction develops within seven to ten hours as a result of antigen exposure.

Type IV immune response include cell-mediated reaction. The reaction evolves slower in comparison to the antibody mediated reactions usually within few days post exposure to an antigen.

The allergen immune response can be divided into two main events: sensitisation event and reaction event.

During the sensitisation event the presence of antigen triggers the immune response by the activation of IgE antibodies alongside with T cells, B cells and macrophages. The induced IgE antibodies bind to the tissue mast cells through the Fc mast cell receptors. The Fc's receptors on the surface of the mast cells have a very high affinity towards IgE antibodies.

Re-exposure to the same allergen triggers the reaction event of the immunological response. The antigen is recognised by the mast-cell-bound-IgE antibody complex and attaches to it. As a result the large basophilic granules presented in the mast cells are released into the tissue, a process known degranulation. The released by the mast cells pharmacologically active compounds (mediators) can have different effect on different tissues as a result of the antigen exposure (Janeway et al., 2003).

The market provides huge variety of different cosmetic and personal care products. Each product contains different substances that come into contact with the which in some cases lead to allergic reactions. Many different substances are added to wide range of cosmetic products, detergents and personal care products to enhance the product's fragrance and quality. The main allergenic substances available in cosmetic and personal care products have been listed by Schnuch et al.; in 2004, around 5000 different substances were in use as fragrances in different cosmetics and personal care products (shampoo, body lotions, perfumes, crèmes, toothpastes). For example p-Phenylene diamine is a substance used in hair dyes and temporary tattoos (henna additives); formaldehyde or formaldehyde liberators/resins, a substance used as a preservative in cosmetics; rubber products containing mercaptobenzthiazol which triggers a type IV hypersensitivity immune response. To

ensure product safety to customers, all cosmetics industries are required to undertake toxicity testing on all new and current chemicals (Schnuch et al., 2004).

There are two main approaches to the reduction of contact allergies. Firstly, testing of the substances used in the production of cosmetics and personal care products; more specifically, those substances that come into direct contact with the skin. Secondly, the use of available information to develop models which aim to predict more accurately the skin sensitisation potency of different substance (The Adverse Outcome Pathway for Skin Sensitisation Initiated by Covalent Binding to Proteins, 2014).

1.3. Allergic contact dermatitis (ACD)

Contact allergy, known as Allergic Contact Dermatitis (ACD), is a type IV delayed hypersensitivity reaction. It is considered to be a challenging immunological disease in the public health context, as it affects a large section of the public. It is based on environmental, domestic and occupational contact with chemicals, and affects up to 15-20% of the population of Europe. The majority of cases belong to allergies caused by chemicals used in cosmetics and personal care products (Tončić *et al.* 2011). ACD is considered the second most widespread occupational illness. It entails an annual cost of up to \$1 billion in terms of employment compensation, cost of medical treatment and lost working time (Anderson et al., 2011).

1.3.1. The mechanism of skin sensitisation

Allergic Contact Dermatitis (ACD) is a type IV delayed hypersensitivity reaction, occurs after direct contact of the skin with allergens known also as haptens. Allergens are molecules small enough to pass through the epidermis and so reach the dermis. The haptens on their own are unable to trigger any immune response by the body. However, if the allergens (haptens), on reaching the dermis, bind covalently with local proteins, they form a

so-called protein-hapten conjugate (or complex), which in its turn as a complex can lead to allergic response. The extent to which the haptens are able to pass through the skin is known as their bioavailability.

ACD process is based on the ability of an allergen to penetrate the skin and to bind to an endogenous epidermal protein, thereby forming a protein-hapten conjugate. Some chemicals (pro-haptens) require enzymatic activation, whereas other chemicals (pre-haptens) have to be oxidised in order to become active haptens, with the ability to bind to the proteins available in the skin. This process is known as haptensisation. As a result of the protein-hapten formation, the keratinocyte cells (KC) available in the epidermis are capable of producing a cocktail of pro-inflammatory cytokines as a response to a chemical stress. The protein-hapten conjugate (known also as modified protein) is recognised by the Langerhans cells (LC), which are a type of hapten-presenting immune cells. The Langerhans cells recognise the protein-hapten conjugate, engulf it and migrate to the nearest lymph node. The LC cells, having matured and migrated to the local lymph nodes present the protein hapten conjugate (or part of it) on its surface using MHC class molecule (major histocompatibility complex). The protein-hapten adduct is recognised by the CD4⁺ T helper cells (white blood cells with a crucial role in the body's immune response). As soon as the recognition between the CD4⁺ T cells and the protein-hapten conjugate, now attached to the LC cells happens, the LC cells start to release IL-12 (interleukin 12). IL-12 causes the CD4⁺ to mature and differentiate, and form Th1 (T cell helper cells). The mature Th1 cells start releasing interleukin 2 (IL-2), causing proliferation of the Th1 cells. Th1 cells start secreting IFN γ (interferon gamma), which helps to activate macrophages and causes proliferation of T cells. Activated macrophages start releasing pro inflammatory cytokine (TNF, IL1, IL6) which causes more T cells to reach the areas affected by allergen. When the skin undergoes subsequent exposure to the same allergen, the T cells recognise the haptensised protein as a

foreign molecule and lead to skin inflammation (local redness, edema and fever). (Goebel et al., 2012; Ryan et al., 2007; Saint-Mezard et al., 2004; Haniffa et al.,2015) (Figure 2).

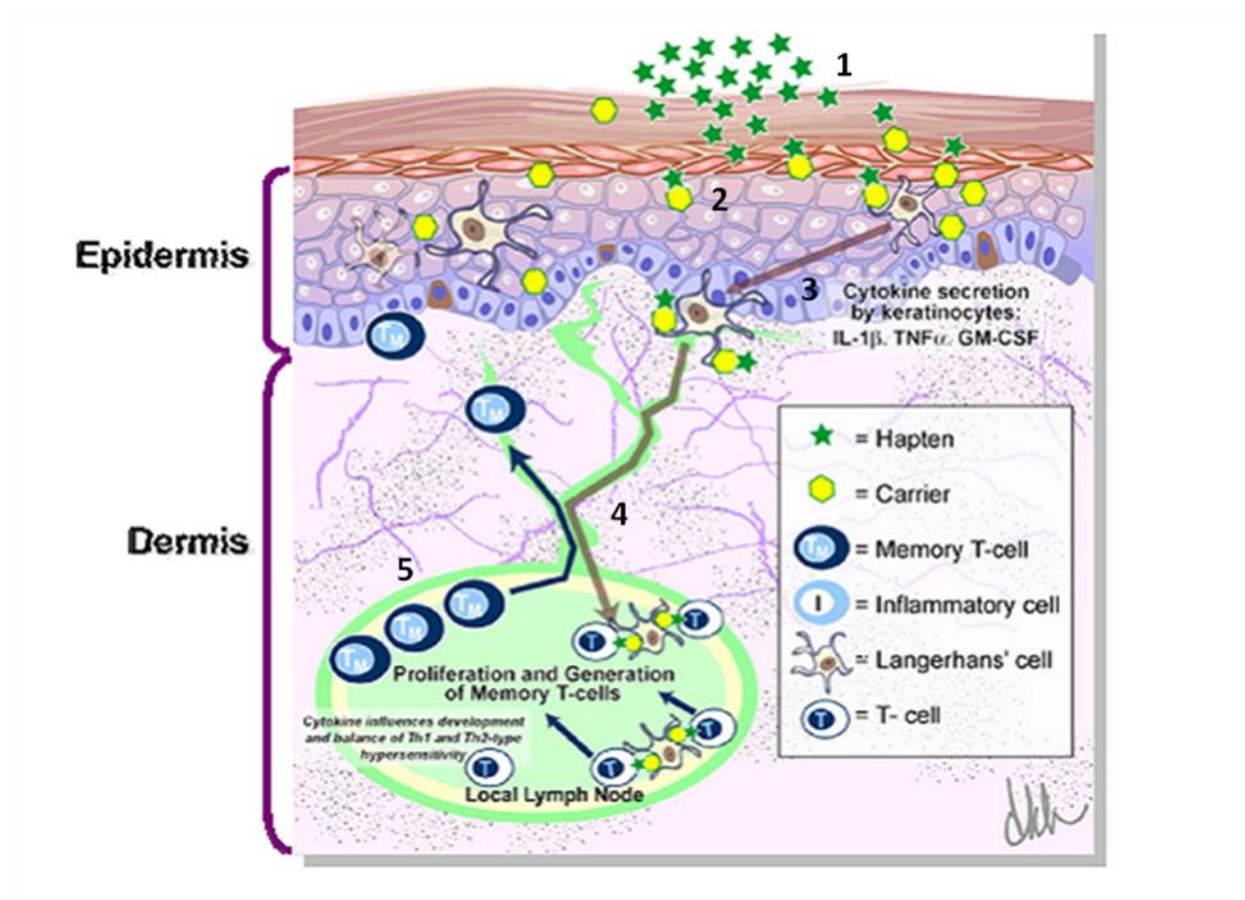


Figure 2. Simplified schematic representation of the induction phase of the sensitisation process: Allergen penetrates the epidermis (1), enabling covalent interaction with a protein (2) leading to the formation of complete protein-hapten conjugate, which interacts with keratinocytes (KC,) and (3) triggers dendritic cells (DC) activation and maturation to the lymph nodes (4). There, the antigen is presented to naive T cells. TC differentiates and proliferates in response to the antigen presence (5). Source: The Adverse Outcome Pathway for Skin Sensitisation Initiated by Covalent Binding to Proteins (2014).

Figure 2 shows the induction of skin sensitisation as a multi-stage process driven by several toxicity pathways including disposition, biotransformation, haptens and immune-reactivity in skin.

The formation of protein-hapten conjugate is one of the key events in the skin sensitisation process. The ability of the hapten to covalently bind and modify a protein is due to the different physico-chemical properties amongst haptens and proteins. Haptens appear to act as

electrophiles this word is formed from the word “electron” and the Greek word *philos* (love), meaning that electrophiles have a strong tendency to attract electrons)

whereas some proteins can act as nucleophiles (which donate electrons) due to the nucleophilic properties of their side chains. It is important to highlight the fact that the haptens (electrophiles) are unable to cause a skin sensitisation unless bound to a protein (a nucleophile) available in the skin (Aleksic et al., 2007)

Despite the importance and diverse functions of the skin, relatively little is known about its proteome composition. As the covalent modification of skin proteins by allergens plays a crucial role in the skin sensitising process, a full characterisation of the skin proteome, detailed understanding of the protein-hapten binding mechanism and the specificity of its reaction will lead to the development of new approaches in testing contact allergens (Aleksic et al., 2008).

The key to the risk assessment of skin sensitisation is to understand the molecular pathways involved in the process. Although many details of hapten-modified protein immune recognitions and the complex pathophysiology of skin sensitisation have been clarified, several aspects remain unclear and require further investigation. In particular, detailed information on biotransformation and haptensisation on a molecular level is limited and remains as the most challenging area (Chipinda et al., 2011).

The process of haptensisation is regarded as a crucial step in sensitising human T cells.

1.4. Local lymph node assay (LLNA)

Different *in vivo* models have been used to evaluate skin allergens by their toxicity and potency. Local Lymph Node Assay (LLNA) is the preferred method for evaluating sensitisers based on their potency developed in 1989. It is currently one of the most appropriate and successfully validated sensitisation test methods to evaluate chemicals with regards to skin

sensitisation based on the use of animal models. Local lymph node assay (LLNA) is the main and standard testing method to measure the skin sensitising potency of low molecular weight chemicals, and is performed on mice.

The chemical undergoing risk assessment is injected into the ear of an animal model (mouse) for three subsequent days. At day six of the chemical exposure the mouse is injected with the radioactive nucleoside ^3H -thymidine. Thymidine is an essential nucleoside for DNA synthesis, hence Radioactively labelled thymidine can be used to determine the change in the number of lymphocytes produced. Based on this technique a chemical can be classified as a sensitizer if it has caused a threefold increase in the number of proliferate lymphocytes in the lymph nodes in comparison with a control (Anderson et al.2011) . The method determines the concentration of the chemical leading to sensitisation by measuring the proliferation of lymphocytes in the lymph nodes and hence classifying chemicals as strong, moderate, weak, irritant and non-sensitisers (Gerberick et. all 2007; Troutman et al., 2011). LLNA can provide reliable results based on quantitative and dose dependent data and predict chemical potency (Figure 3). Despite the benefits of using the LLNA assay, researches show that the assay has a few disadvantages, such as false positive results, in addition to the variation due to the animal model used and the ethical issues arising from the use of animal models (Anderson et al., 2011).

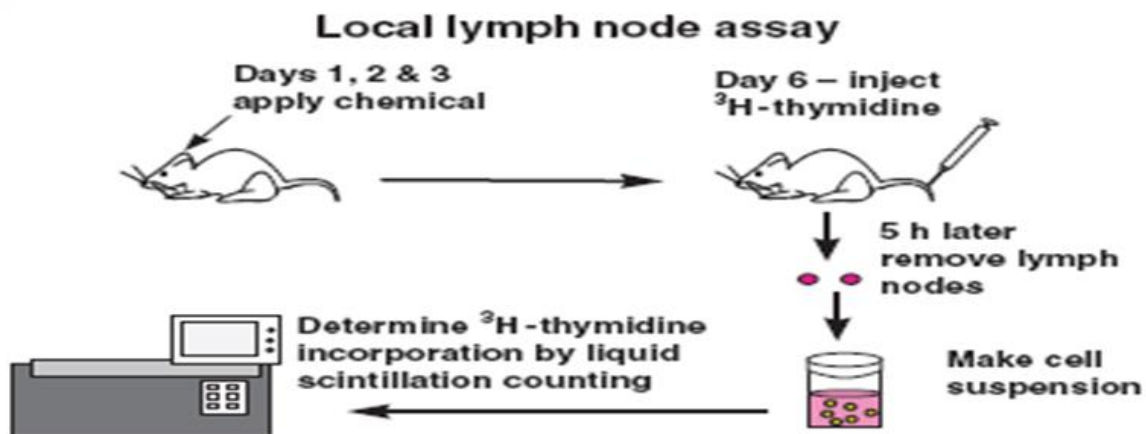


Figure 3. Overview of the local lymph node assay, in which a test substance is applied on the mouse ear for 3 subsequent days, followed by injecting at day 6 into the tail vein with radioactively labeled thymidine (^3H -thymidine). Lymph nodes are removed and processed for measuring the amount of lymphocytes produced as a result of the exposure. Source: (Basketter, 2008)

1.5. The 7th amendment of the EU Cosmetics Directive in 2013

The Global Cosmetics Market is predicted to reach \$292 billion in 2017 due to the increase in the consumer income and changing people's life style (Figure.4).

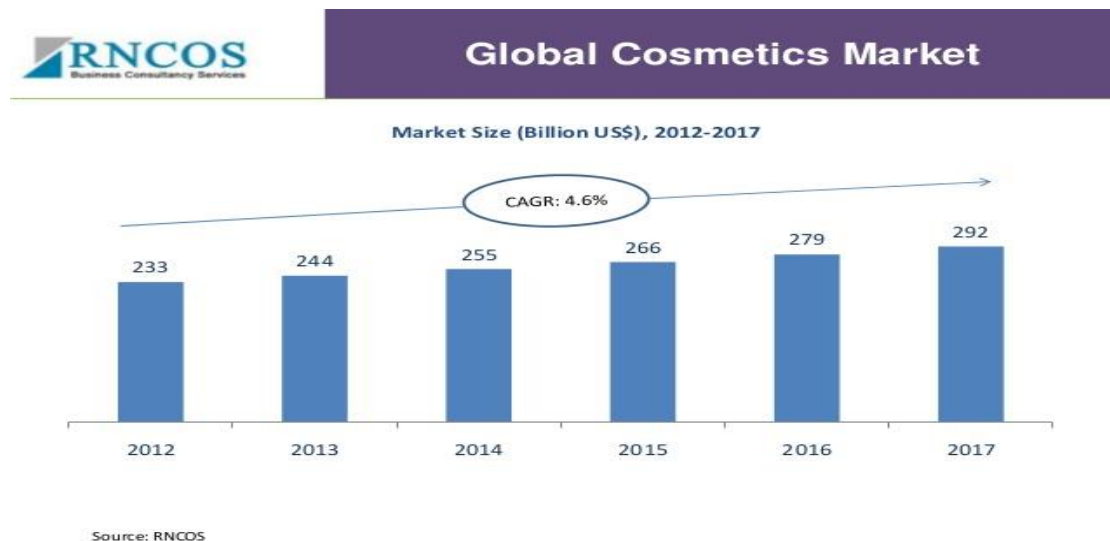


Figure. 4 Global cosmetics market is predicted to reach \$265 billion in 2017. From 2012 to 2017 the Global cosmetic market is predicting 4.6 % increase. Source: (Maheshwari, 2013) by RNCOS

The Registration, Evaluation and Authorisation of Chemicals (REACH) has to assess thousands of chemical substances yearly for environmental and health risks. REACH was established in 2006 (Regulation (EO) No 1907/2006), aiming to control any chemical

substances used in the EU market. The regulation aims to ensure a high level of human health and environmental protection ; to guarantee free movement of chemical substances in the European market; to ensure that the necessary risk assessment of using the chemicals has been appropriately undertaken; to encourage the use of alternatives to the currently used methods for testing sensitisers and to promote innovation within and competitiveness of the European chemical industry (REACH - Growth - European Commission, 2017).

Skin sensitisation is one of the key endpoints for safety testing on cosmetic products before they are licensed.

The proposed from the European Union (EU) Directive to ban the use of animal models for testing cosmetics and personal care products was first issued in 1993.

Cosmetic companies were asked to find alternatives to the currently used methods, such as LLNA, for testing the sensitisation potency of chemicals by 1998. However, at that point the researchers had failed to develop alternative models that could replace the available animal models, hence the deadline was extended by two more years.

In 2003 the new Directive proposed a set of provisions where screening any developed cosmetic products and cosmetic ingredients on animals would be banned. The EU continued to work hard on establishing a total ban on the use of the animals as chemical testing models and in 2009 (6 years later), the ban entered into force in the EU.

In March 2013 the ban was officially applied under the 7th amendment of the EU Cosmetics Directive. The ban included two aspects: firstly a testing ban, where cosmetic products and ingredients are prohibited for testing on animals. The second aspect referred to a marketing ban, stated that any cosmetics products and ingredients tested on animals are prohibited for the EU market (Ban on Animal Testing - Growth - European Commission, 2017).

With the implementation of the 7th amendment of the EU Cosmetics Directive in 2013, the currently powerful LLNA technique for safety testing of skin sensitisation on animals can no longer be used for chemical ingredients used in cosmetics or personal care products. On the other hand REACH has the aim to assess approximately 30,000 chemical substances which need to comply with this ban and undergo alternative to the *in vivo* examination (REACH - Growth - European Commission, 2017).

Therefore there is an urgent need to reduce, refine and replace (*the “3 Rs”*) animal models with alternative non-animal approaches. Currently there are a few alternative approaches to the animal methods for testing chemicals, known as *in chemico*, *in vitro*, *in silico*; some have been validated and others are still under study. In addition to the above, there is also the possibility of developing integrated testing strategies with a combination of different mechanistically-based testing models (*in chemico/in silico/in vitro*), to test toxicities including skin sensitisation (Troutman et al, 2011; Basketter, 2012).

1.6. Current approaches for testing skin sensitisers.

Hypersensitivity is a complex response by the body to allergens that can be analysed and described on a molecular and cellular level. The pathway of events leading to the body's response to stimuli is known as the Adverse Outcome Pathway (AOP). Many research groups are working extensively on establishing non-animal models for testing sensitisers by focusing on the different AOP key events. AOP includes four main key events, detailed study of which would contribute to the identification and characterisation of skin sensitisers. The first key event of AOP is the bioavailability, the ability of the allergen to penetrate the skin, pass through the epidermis and reach the dermis. All these events can be explained with a detailed knowledge of the physico-chemical features of the skin. Antibody mediated and cell-mediated immune responses lead to the activation of T cells by activation of class I and II

MHC molecules located on the surface of antigen-presenting cells such as LC cells. However, this event can take place only if the body's immune system is able to recognise the skin-penetrating allergens. As allergens (haptens) are small molecules, they can lead to an immune response only if they bind to proteins available in the skin, thereby forming a protein-hapten adduct (this is the second event of the AOP). Allergens can be reactive and directly bind to skin proteins, while in some cases allergens need to be activated either by enzymatic modification (pro-haptens) or oxidative modification (pre-haptens) in order to induce a chemical response. The third AOP key event is the activation of LC cells that upregulate the expression of cell surface biomarkers (CD83, CD86) and/or monitoring of DC gene expression at the transcriptional level as a result of chemical sensitisation. Many DC cell line based assays have been developed using the U937 myeloid cell test, the human Cell Line Activation test (h-CALT), and the U937/CD86 assay, evaluated by different leading cosmetic companies (L'Oreal, P&G, Shiseido, Kao, Henkel). The final event of the AOP pathway is measurement of the proliferation of T cells in the local lymph nodes, where LLNA is still considered to be the leading approach for quantitative sensitisation endpoint (The Adverse Outcome Pathway for Skin Sensitisation Initiated by Covalent Binding to Proteins, 2014; Maxwell and MacKay, 2011; Aebly et al., 2007).

The OECD (Organisation for Economic Co-operation and Development) is a multinational organisation, established in 1961, with a membership from 35 different countries. The main aim of the OECD is to improve economic outcomes / to improve economic situations across the world, by assuring the social well-being of the population. OECD tries to seek solutions to common international problems of the current century in broad economic, social and environmental areas, including the safety of chemicals (About the OECD - OECD, 2017).

OECD in regards to the AOP for skin sensitisation has reported that various non animal approaches are at different stages of acceptance, validation, development and use.

However with the current data, it is impossible to rate the chemicals on their sensitisation potency (Corsini et al., 2016).

The main three studied alternative to the animal approaches are *In chemico*; *in vitro* and *in silico* (Figure 5).

The *In chemico* approach is developed on the basis of studying the mechanism of haptens, i.e. the ability of the allergen (haptens) to penetrate and bind to proteins available in the skin. This approach is built on the basis of the use of recombinant proteins or peptides (sequence of amino acids) as a model for studying chemical potency. This approach is based on measuring peptide depletion as a result of protein-hapten formation and/or measuring the reactivity of the proteins towards the allergens, after the allergens have been metabolised by enzymes or by oxygen (prohaptens and prehapten respectively). The *in chemico* approaches are simple and easy to perform; the protein-hapten formation can be easily explained with the knowledge of organic chemistry. Despite the above advantages this approach faces a very important drawback, the discrepancy between the behaviours of the proteins in the real system (in the body) and when isolated (in a tube), where it is not possible to consider any interactions between the proteins under analysis and those in the surrounding body tissues (Gerberick et al., 2007; Gerberick et al., 2009; Troutman et al., 2011;).

The *In vitro* approach is based on measuring the complex mechanism of the body response on a molecular, cellular and tissue level as a result of the sensitisation process. Studying the interaction between the allergens and the different compartments of the immune system underlies the *in vitro* approaches. Keratinocytes (KC cells) play a crucial role in triggering the immune response as a result of contact with sensitisers. KC cells produce a large quantity of inflammatory cytokines that can alert LC cells to the presence of allergens. *In vitro* assays aim to measure any chemical-induced changes as a consequence of a chemical

exposure. On the other hand measuring the maturation of Dendritic cells has been intensively studied in the last 20 years, by measuring changes in cell surface receptor expression. T cell proliferation is another sensitisation endpoint covered within the *in vitro* approaches, following co-culture of DC or LC with chemical sensitisers (Maxwell and MacKay, 2011).

The *In silico* approach is based on the use of different computer programs to predict skin sensitisation. The computer programs are usually developed based on information (data) gathered from experiments performed either *in chemico*, or *in vitro*, or both. Following the established predictions, scientists can make assumptions and apply these assumptions to other chemicals in order to categorise them as sensitisers or non-sensitisers. “Structure Activity Relationship” (SAR) is an example of an *in silico* approach, which studies the relationship between the chemical structure of the allergens and the biological activities of proteins as a result of exposure to that allergen. An *in silico* model additional to SAR is the so-called “Quantitative Structure Activity Relationship” (QSAR), which uses statistical methods to analyse biological data. The main limitation of such an approach is that it is based on predicting “yes or no” sensitising outcomes, without physically interpreting the chemical compound’s behaviours Figure 5 (Thyssen et al., 2012)

Current non-animal sensitisers assessment

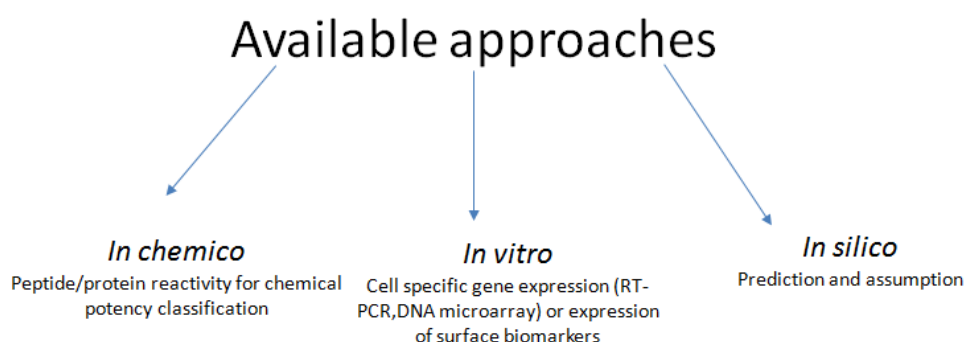


Figure 5. Summary of the currently non-animal approaches for sensitisation assessment

The development and evaluation of non-animal models suitable for the categorisation of skin allergens is one of the most current strategies at the European Union Reference Laboratory for Alternatives to Animal Testing (EURL ECVEM), of which the intention is to finalise and validate the existing models over the next few years (Casati et al., 2013; Zuang et al., 2013).

More than 4000 chemicals with a molecular weight below 500 Da have been proven to cause Allergic Contact Dermatitis (ACD). It is crucial from a toxicological point of view to estimate and categorise the potency of these chemicals in order to determine their hazardous effect on human health.

EURL ECVEM was established in 2011 with the aim to scientifically validate the proposed non-animal models for testing skin sensitisers. The methods which have so far been validated for testing chemical potency by EURL ECVEM are DPRA (Direct Peptide Reactivity Assay), an *in chemico* method, which measures the depletion of lysine and/or cysteine peptides in the presence of chemicals; the KeratinoSen assay, an *in vitro* assessment which measures the expression of the luciferase gene as a result of the activation of the Keap1-Nrf2-ARE pathway using HaCaT cells. The third method validated by EURL ECVEM is the Human Cell Line Activation Test (h-CLAT), an *in vitro* method based on measuring the expression of surface biomarkers such as CD86 and CD84 using human monocytic leukemia cells (THP-1) (Figure 6) (Corsini et al., 2016).

Validated non-animal methods for testing sensitisers

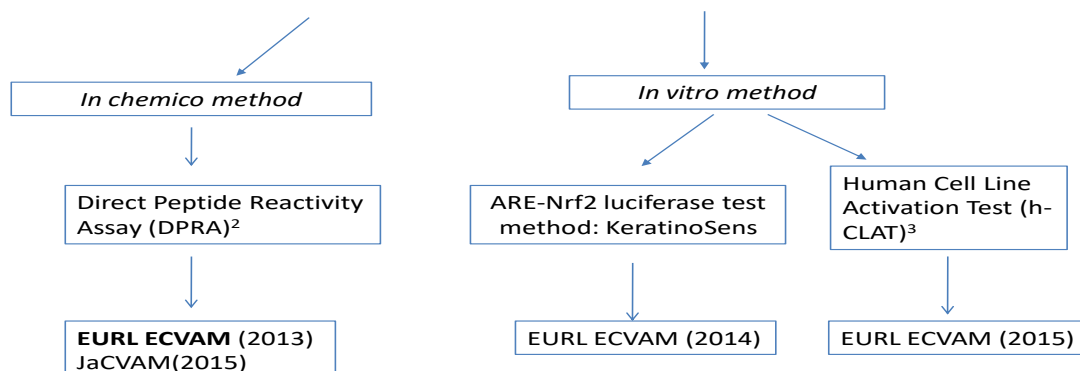


Figure 6. Current evaluated and validated non-animal models for categorization of skin sensitisers by European Union Reference Laboratory for alternatives to animal testing

1.7. Aims and objectives.

A schematic representation of the scheme of the current work and a summarized description of each outcome and how it is to be achieved is represented in Figure 7. The current research project was established through a series of experiments aiming to contribute to the “3 Rs” (Refine, Reduce and Replace) the animal as a model for assessing skin sensitisers.

1. To determine and characterise constitutively expressed proteins in the whole human skin by utilising the established label free quantitative GeLC-MS/MS proteomic technique.
2. To develop a new *in chemico* approach to examine intact protein-hapten interactions and identify potential new haptens pathways by using the top-down mass spectrometry technique.

- To investigate mRNA expression of metabolic enzymes (Phase II) induced by chemical sensitisers with different binding mechanisms and sensitising potency over time course using quantitative polymerase chain reaction (qRT-PCR).

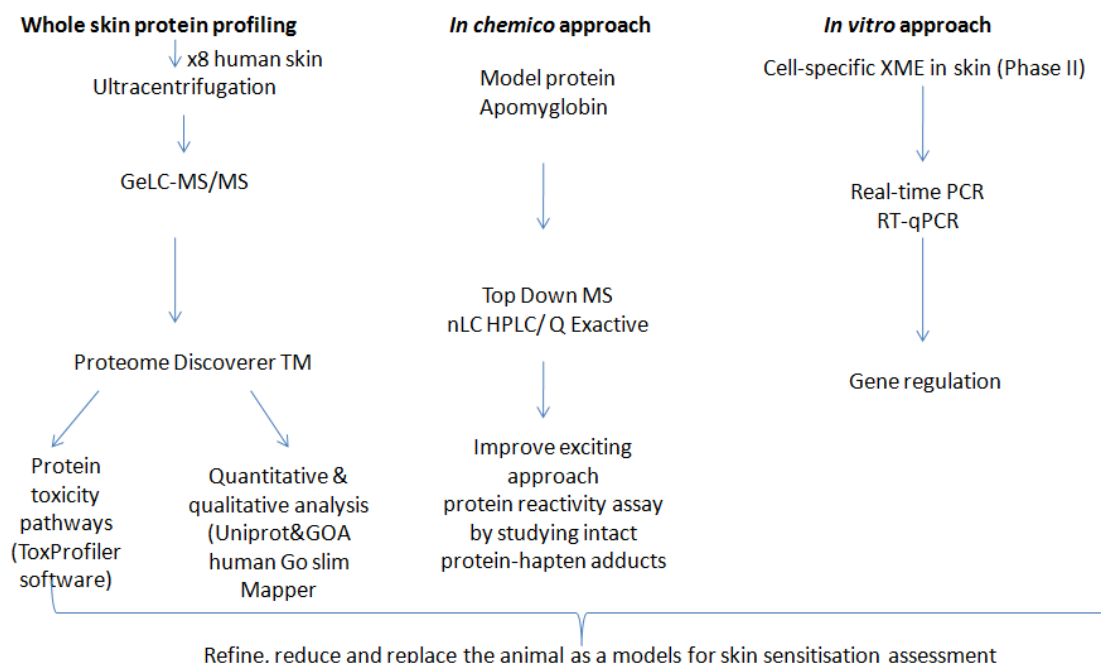


Figure 7. Schematic overview of the current research project.

1. 8. Main hypothesis

A detailed study of the human skin proteome and possible improvements to existing non animal approaches (*in chemico*, *in vitro*) can help in the aim of refining, reducing and replacing the use of animals as an existing model for chemical risk assessments.

Chapter 2

Human skin proteome profiling

2.1. Introduction

Skin cells are able to grow, renew themselves and differentiate throughout their life, and provide physical barrier to the environment, in that they limit the inwards and outward passage of water, electrolytes and various substances, while providing protection against microorganisms, ultraviolet radiation, toxic agents and mechanical injuries. (Zaidi, 2010). Despite the importance and diverse functions of the skin, relatively little is known about its proteomic composition. As the covalent modification of skin proteins by allergens plays a crucial role in the skin sensitising process, a clear picture of the protein composition of the skin, and identification of the toxicological pathways involved could lead to the development of new approaches to testing contact allergens (Aleksic et al., 2008).

Quantitative and qualitative characterization of the skin proteome could provide detailed information about the structure and function of skin proteins, leading to better explanation of the skin changes in response to sensitisers. The current research is particularly interested in those skin proteins involved in Toxicity pathways that could be determined as “specific markers” in response to chemical exposure.

GeLC-MS/MS, also known as SDS-PAGE-gel digestion-LC-MS/MS is a powerful technique for differential analysis of complex protein mixtures. Briefly, the protein complex mixture is separated based on the size of the proteins using SDS-PAGE Polyacrylamide gel followed by protein digestion and NanoLC-MS/MS. The received data of each individual fraction are searched against a database, leading to identification and quantification of the whole complex protein sample, an approach already successfully applied by different research groups (Zhu et al., 2008b; van Eijl et al., 2012; Parkinson et al., 2014). Van Eijl and co-worker successfully applied this approach in identifying and comparison studies between xenobiotic metabolic enzymes of whole human skin and available *in vitro* skin models. In addition, Parkinson and his research group worked out and analyzed whole human skin proteome which identified 150 skin proteins (Parkinson et al., 2014).

The complexity of the sensitisation process and the diversity of skin proteins directed many of the current *in vitro* researches to be focused on the different AOP (adverse outcome pathways) leading to the toxicity endpoint. Identifying, studying and analyzing the whole human skin proteome in addition to the explication of toxicity pathways involved therein, could explain in detail the skin responses toward chemicals and hence distinguish between sensitisers and non-sensitisers (Vandebriel et al., 2010; Van den Veer et al., 2012).

In this research, detailed quantitative and qualitative description of the whole human skin proteome was provided by utilizing the well-established GeLC-MS/MS techniques. The identified proteins were subjected to further analysis in a toxicological context with the aim of finding “markers” that may work as cellular endpoints for skin sensitisers at the level of transcriptomics and/or proteomics.

Furthermore, little is known about which proteins in the human skin are targeted by haptens, due to the absence of information about the whole human skin proteome. A more detailed picture and characterisation of the human skin proteome would lead to the development of better approaches for testing cosmetics and personal care products (Aleksic et al., 2008). In the current project, protein separation, identification and quantification in the subcellular fractions of the human skin samples were performed by using label-free quantitative proteomics GeLC-MS/MS. This methodology was established by Zhu et al., 2008a and has been successfully applied in the Cosmetics Europe Skin Metabolism project by van Eijl et al., 2012. This technique allows assessment of the global expression profile of proteins, unlike other approaches.

2.2. Materials and method

2.2.1. Sample preparation (performed at University of Bedfordshire)

Samples of abdominal human skin homogenate fractions from healthy females, aged between 30 and 60 , and having undergone reduction mammoplasty (n-8) were obtained from Biopredic International (Paris, France). The abdominal skin homogenate samples represented two different races: four Caucasian and four African. To my knowledge there is no record provided by Biopredic International (Paris, France) in regards to whether any of the donors has suffered from any allergic reactions (Human skin certificate of analysis, see appendix figure 22). The homogenates were provided in corresponding buffer (10mMTris-Cl, 1mM EDTA, 250mM Sucrose, protease inhibitors, pH 7.4) and stored in liquid nitrogen for further usage.

The 8 samples were ultracentrifuged at 10 000 rpm for 25 min at 4°C for the separation of the soluble S9 and insoluble non-S9 fractions. One of the technical difficulties faced during the experiment was to solubilise the proteins in the non S9 fractions. To achieve that the insoluble Non S9 fractions were dissolved in 9M Urea/2 %Chap followed by centrifugation at room temperature for 20 min at 3000 rpm. The insoluble non-S9 fractions were dissolved in 9M Urea/2 %Chap followed by centrifugation at room temperature for 20 min at 3000 rpm. The supernatant was collected and used to determine the protein concentration using BCA assay.

2.2.2. Estimation of protein concentration (performed at University of Bedfordshire)

The BCA assay method (Sigma Aldrich, UK) using bicinchoninic acid was performed to determine the protein concentration of the 8 samples (S9 and non-S9 fractions separately). BSA (bovine serum albumin), used as a standard was prepared as per the manufacturer's requirements. 25 µl of each standard and unknown samples in replicates were added to a 96

microplate well. 200 μ l of working reagent (prepared according to the manufacturer's methodology) was added to each well and the plate was mixed on a shaker for 30 min. The plate was covered and incubated at 37 °C for 30 min. Absorbance was measured at 570 nm. A standard curve was plotted showing absorbance at 570 nm vs. concentration in μ g/ml. The plotted graph was used to determine the protein concentrations of the unknown samples.

2.2.3. GeLC-MS/MS sample preparation (performed at University of Bedfordshire)

The whole protein of S9 and the non-S9 samples were separated on Nu-Page 4-12% Bis-Tris gel purchased from (Invitrogen/UK) at 200 V for approximately 45 min. The loading capacity for each well for S9 and non-S9 samples were 20-30 μ g/well and 20 μ g/well respectively. One of the difficulties faced during this step was determining the concentration of S9 and non S9 samples to be loaded onto the SDS gel. This experimental part was repeated many times until good protein separation of both skin fractions was obtained. Following staining with Coomassie blue to visualize the protein bands, the gels were cut into 2-4 mm and each piece subjected to *in situ* trypsin digestion using method described by (Zhu et al., 2008a). S9 and non-S9 gel pieces were incubated with 0.5-1ml of 25mM AmBic 50% methanol at 37 °C for 30 min. The process was repeated until the blue dye washed off. The destined gel was washed with 0.5-1 ml distilled water. The gel pieces were dehydrated using 1 ml 100 % (Acetonitrile) for 15 min. Separated proteins were incubated with trypsin (1 ng/ μ l) at 37 °C for 16 h until complete digestion. The extracted proteins were aspirated and stored at -80 °C for nano-capillary LC-MS/MS analysis.

2.2.4. Mass Spectrometry analysis (performed at Health Protection Agency London)

Tryptic peptide mixtures from in-gel trypsin digestion were separated using nanoflow reversed phase liquid chromatography and analysed using tandem mass spectrometry (nLC-MS/MS) on an Ultimate™ 3000Dionex nano/capillary HPLC system (Thermo Scientific Dionex™) coupled online to a LTQ Orbitrap™ mass spectrometer (Thermo Scientific).

For peptide separation, buffer A (98/2 water/CH₃CN containing 0.1% formic acid) and buffer B (10/90 water/acetonitrile containing 0.1% formic acid) were used as mobile phases for gradient. Peptide mixtures (10 µl) were first trapped and desalted on a reversed phase trap column (Acclaim PepMap100, 300µm i.d. x 5mm, C18, 5µm, 100Å, Thermo Scientific) using Buffer A at a flow rate of 25 µl/min and further separated on an C18 reversed-phase nanocolumn (Acclaim PepMap100, 75 µm i.d. × 15 cm, C18, 3 µm, 100 Å, Thermo Scientific) at 35°C. Separation was achieved using a 45-minute gradient: from 10% to 45% solvent B over 45 min, followed by 45% to 90% solvent B over 0.5 min, maintained at 90% B for an additional 5 min, then returned to 10% B over 0.5 min at a flow rate of 300 nl/min. The total run time was 60 min.

MS/MS data were acquired on the LTQ Orbitrap mass spectrometer controlled by Xcalibur™ (version 2.1.0, Thermo Scientific). The instrument was operated in positive ion mode and a data-dependent ‘top 6’ method was used. MS1 survey scans (m/z 440–2000) were acquired in the Orbitrap with a resolution R = 60,000 at m/z 400. The six most abundant multiply charged precursor ions detected in the preceding survey scan were selected for MS/MS using collision-induced dissociation (CID) with detection of fragment ions in the linear ion trap. General mass spectrometric conditions were set as follows: spray voltage at 1.6 kV, capillary voltage at 38 V, capillary temperature at 200°C, tube lens at 125 V. Helium was used as

collision gas but no sheath or auxiliary gas were applied. CID normalised collision energy was set to 35%, activation of $q = 0.25$, and activation time of 30 ms. The lock mass option was enabled using the polydimethyl-cyclosiloxane ion generated in the electrospray process from ambient air, protonated $(\text{Si}(\text{CH}_3)_2\text{O})_6$ at m/z 445.120025, was used for internal calibration in real time to enable accurate mass measurement (method previously used and described by Mirza and Gaulton, 2015).

2.2.5. Database searching (performed at Health Protection Agency London)

MS data were generated in the form of RAW files (Thermo Finnigan file formats), which contain all the spectra detected from the LC-MS/MS analysis for each sample. Spectra acquired were searched against the non-redundant Swiss-Prot protein database using Proteome DiscovererTM (Version 1.4, Thermo Scientific). The search parameters used were: Enzyme: trypsin; Fixed (or static) Modifications: carbamidomethylation of cysteine; Variable Modifications: oxidation of methionine; Missed Cleavage Sites: 2; peptide mass tolerance \pm 10 ppm. The search results were filtered using Scaffold (Version 4, Proteome Software, USA) to minimize the number of false positives, as indicated by a false discovery rate of < 2 %. Protein identifications were accepted with at least 1 identified peptide (method previously described by Ru et al., 2006).

2.2.6. Uniprot analysis (performed at University of Bedfordshire)

Genes were identified based on the obtained proteins by MASCOT searching cross-referenced with Uniprot identifier using the open access Protein Identifier Cross Reference Tool (<http://www.ebi.ac.uk/Tools/picr/>) with search limited to human proteins and mapped to Swiss-Prot and TrEMBL database (method previously used by Parkinson et al., 2014).

2.2.7. Gene Ontology analysis (performed at University of Bedfordshire)

Uniprot identified proteins from the GeLc-MS/MS analysis were submitted into Gene ontology Go Term Mapper (<http://go.princeton.edu/cgi-bin/GoTermMapper>) and were searched against the goa_human (GOA GO slim) and the goa_human(Generic GO slim), for cellular compartment and biological process (method previously used by Parkinson et al.,2014).

2.3. Results

2.3.1. Characterisation of human skin proteome

Eight human skin samples were analysed for whole skin proteome. Proteomic analysis was performed on both S9 and Non S9 fractions. Schematic overview of the gel digestion procedure and the S9 and non S9 protein separation are represented on Figure 8.

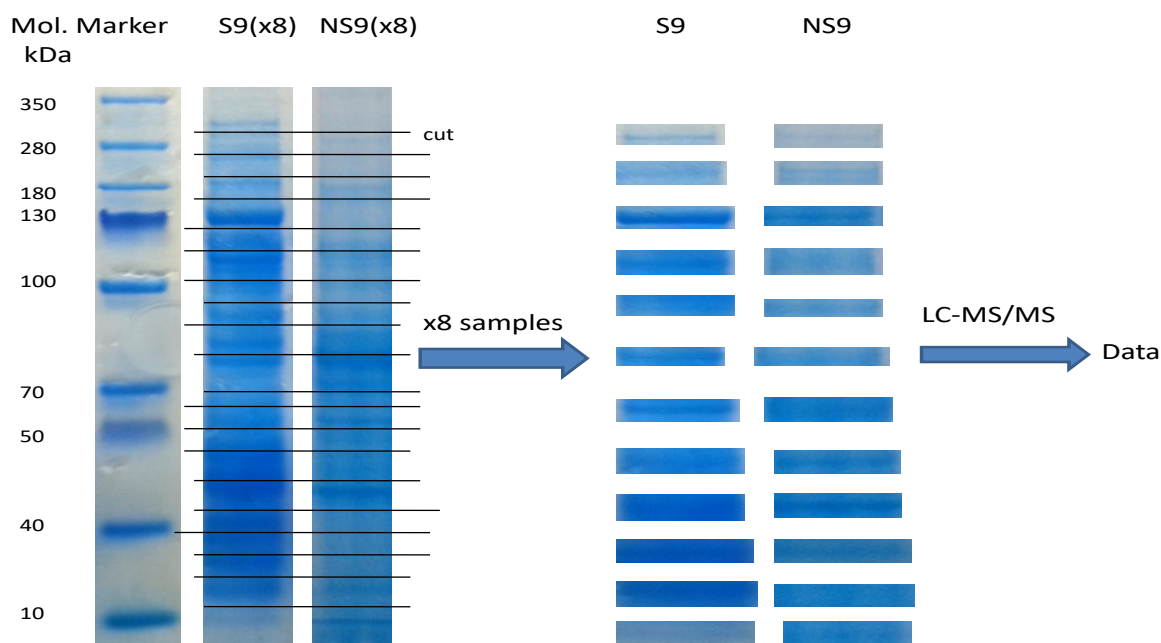


Figure8. Schematic overview of S9 and NS9 sample analysis by GeLC-MS/MS method

Proteins of the human skin samples were separated by SDS –PAGE gel and subjected to LC-MS/MS analysis, which led to the identification of 1491 tryptic peptides in total, corresponding to 260 proteins in total (row data available in appendix table 6). The results were analysed based on the presence of at least 2 peptides in all 8 human skin samples. The received data were further refined by selecting the proteins with the same tryptic peptides identified across all 8 human skin samples for S9 fractions and based on the presence of ≥ 7 tryptic peptides identified across all 8 human skin samples for non S9 fractions (row data available in appendix table 6). As a result total of 260 proteins corresponding for S9 and non S9 fractions were further considered for analysis.

The identified proteins in both fractions were compared with Gene Ontology (GO) in terms of cellular compartments (Figure 9).

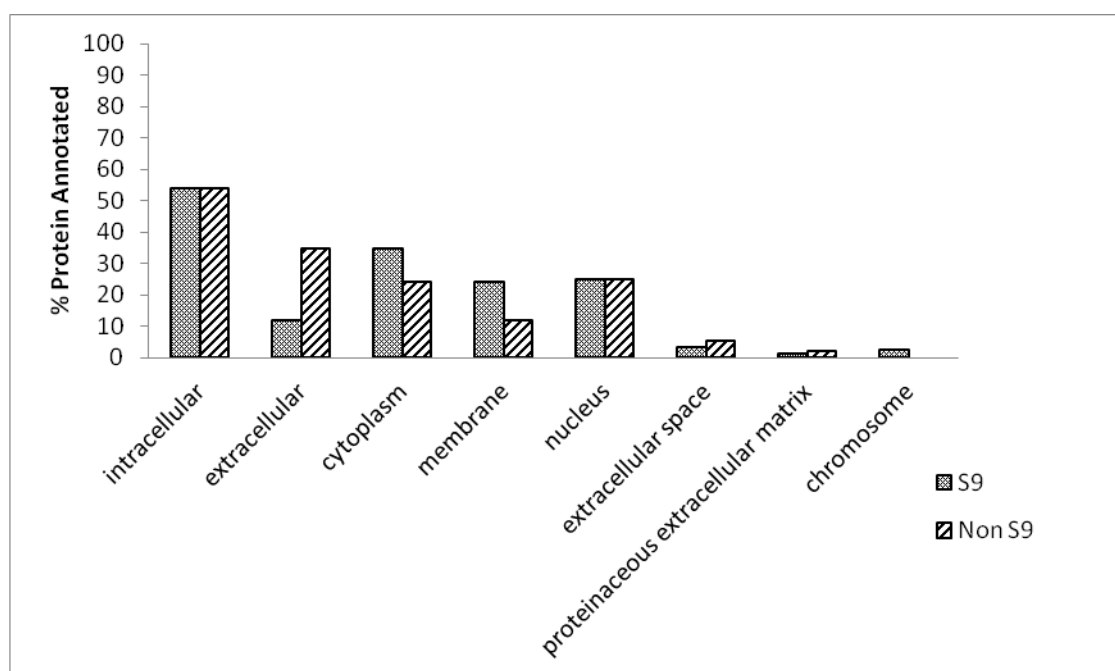


Figure 9. Cellular location of proteins identified in the soluble and insoluble fractions was annotated to the GOA human GO Slim terms and Generic human GO slim terms for cellular compartment, using GO Term Mapper (<http://go.princeton.edu/cgi-bin/GOTermMapper>)

Of the 260 proteins identified, 142 and 118 proteins were determined from the soluble (cytosol and microsome) and insoluble (membrane, nuclei etc.) fractions respectively. The revealed proteins have diverse physico-chemical properties, with 105 and 82 found exclusively in the soluble (cytosol and microsome) and insoluble (membrane, nuclei etc.) fractions respectively.

The skin proteome appears to contain components involved in a number of different biological processes, including regulation, transport and metabolism etc. (Figure 10).

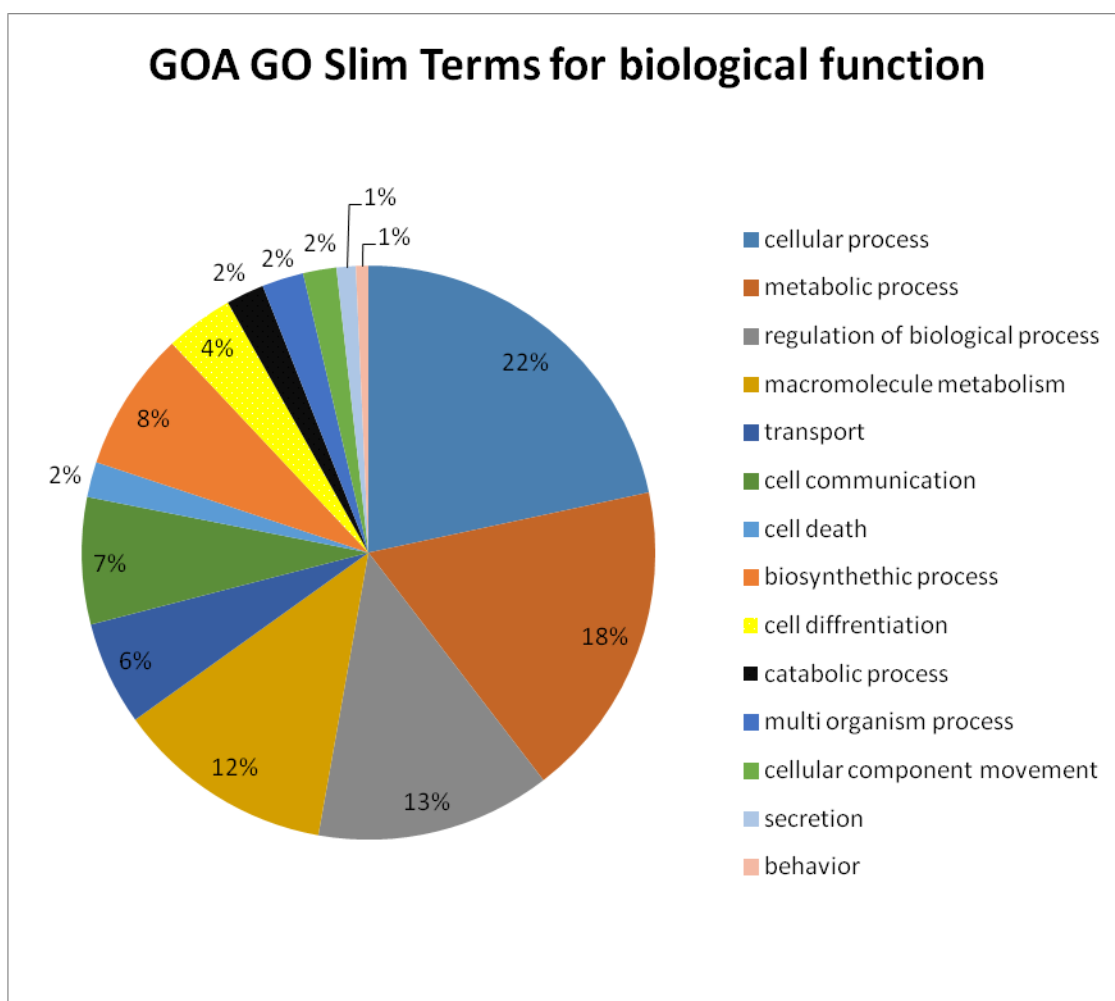


Figure 10 Biological function of all proteins identified from mass spectrometry analysis of human skin. Proteins were annotated with the GOA human Go slim terms for biological process, using GO term Mapper (<http://go.princeton.edu/cgi-bin/GOTermMapper>).

The identification and quantitative expression level of the proteins, as two examples, are represented in Table 1, which estimates relative level of the protein to the most abundant protein (considered as 100 %) in the S9 and Non S9 fraction respectively. Each protein level was calculated as an average of its peptide levels quantification, analysed by the Thermo Protein Centre software (From data set to meaningful biology, 2017) . The calculated averages peptide levels of each protein grouped the proteins of the analysed 8 human skin samples in order based on their abundance, from highest to lowest. Table 1 displays the most abundant proteins in S9 and non S9 fractions based on the calculated average peptide level in each one of them (raw data table 6, available in the supplement data).

Table 1. Identification and quantitative expression overview of the top ten most abundant proteins identified in S9 & NS9 fractions, based on the presence of tryptic peptides in all 8 donors and based on the presence of ≥ 2 different tryptic peptides identified in all the 8 donors, respectively.

S9 fraction proteins	Numbers of Peptides identified	MW (Da)	NCBI identification	Relative abundance (%)
Keratin, type II cytoskeletal 2 epidermal	18	65,433	NP_000414.2	100
Histone H4	6	11,269	NP_778224.1	97
IG gamma-1 chain C region	6	36,105	PT0368	60
Glyceraldehyde-3-phosphate dehydrogenase	3	36,053	CAA25833.1	45
IG kappa chain C region	3	11,608	P01834.1	42
Histone H2B type 1-N	4	13,950	NP_003511.1	42
Keratin, type II cytoskeletal 1	17	66,040	NP_006112.3	38
Hemoglobin subunit beta	2	15,998	NP_000509.1	37
Serum albumin	24	69,366	NP_000468.1	36
IG alpha-1 chain C region	2	37,754	B45874	28

Non S9 proteins	Numbers of Peptides identified	MW (Da)	NCBI identification	Relative abundance (%)
Histone H4 type VIII	4	11439	NP_778224	100
Galectin-7	3	15074	NP_002298	67
Keratin, type II cytoskeletal 2 epidermal	15	45000	NP_000414.2	65
ATP synthase subunit beta, mitochondrial	2	137923	NP_001677.2	59
Keratin, type II cytoskeletal 1	17	66040	NP_006112.3	53
Keratin, type I cytoskeletal 10	20	58828	NP_000412.3	52
Annexin A2	20	38606	AAH68065.1	43
Desmoglein-3	4	113748	NP_001935.2	30
Desmoglein-1	14	99970	NP_001933.2	27
Fatty aldehyde dehydrogenase	6	54849.8	NP_00102697.1	27

All the identified 260 proteins were put into toxicological pathway context analysis by using ToxProfiler with the WikiPathways and Biocarta database as references (Table 2).

Table 2 Toxicological pathways in which the proteins from S9 and Non S9 fractions are involved, and identified by the ToxProfiler software using WikiPathways and Biocarta databases as reference.

NCBI No	S9 proteins	Pathway
NP_001211.3	Beta chain associated protein kinase	inflammatory response
NP_476508.2	collagen type 3	inflammatory response
NP_000085.1	Collagen alpha	inflammatory response
NP_036246.1	Caspase 1	IL-1 signaling
NP_001185798.1	Calpain-1 catalytic subunit	IL-1 signaling
NP_031381.2	Heatshock protein 90	IL-6 signaling
NP_003861.1	Ras protein activator	IL-4 signaling
NP_112598.3	Epiplakin	EGFR1 Signaling
NP_000840.2	Glutathione transferase	KEAP 1-NRF2
NP_001743.1	Catalase	oxidative stress
AAF87085.1	Thioredoxine	oxidative stress

NCBI No	Non S9 proteins	Pathway
NP_008839.2	Ras-related C3 botulinum toxin substrate 1	Wnt Signalling
NP_000691.1	Annexin A1	Prostaglandin Synthesis and Regulation
NP_001145.1	Annexin A5	Prostaglandin Synthesis and Regulation
NP_001144.1	Annexin A4	Prostaglandin Synthesis and Regulation
AAH68065.1	Annexin A2	Prostaglandin Synthesis and Regulation
NP_001265853.1	Annexin A8-like protein 2	Prostaglandin Synthesis and Regulation
NP_112598.3	Epiplakin	EGFR1 Signaling
ADZ75461.1	Epidermal growth factor receptor	EGFR1 Signaling
P30453.1	HLA class I histocompatibility antigen, A-34 alpha chain	Cytokines and inflammation response
ADZ75461.1	Epidermal growth factor receptor	Regulation of Actin cytoskeleton
NP_005337.2	Heat shock 70 kDa protein 1A/1B	MAPK Signalling
NP_054768.2	Acyl-CoA dehydrogenase family member 9, mitochondrial	Fatty acid beta oxidation

2.4. Discussion

2.4.1. Characterisation of human skin proteome

The skin has the ability to grow, renew and differentiate throughout life, providing a physical barrier to the environment which limits the inward and outward passage of water, electrolytes and various substances, while providing protection against microorganisms, ultraviolet radiation, toxicological agents and mechanical injuries. Despite these crucial roles, relatively little is known about the global protein composition of skin and how it changes in response to exposure to stimuli (Bensouilah et al., 2006).

The proteins of the S9 and Non S9 fraction in each of the analysed 8 human samples were separated using the well-known SDS PAGE electrophoresis. SDS PAGE electrophoresis is a powerful technique to separate proteins based on their size using a porous gel matrix. To enhance the separation technique and maximise the number of identified proteins, the SDSPAGE electrophoresis of the S9 and non-S9 fraction was repeated several times using gels with various pore sizes. In the experiment a gel matrix with pore size from 4 to 12 % Bis-Tris gel was purchased from (Invitrogen/UK). The use of a gel matrix with pore size from 4 to 12% facilitated the separation of proteins with different sizes using the same gel. SDS PAGE electrophoresis is a powerful technique, as it relies on the full solubilisation of the proteins by SDS (sodium dodecyl sulphate), high tolerance to salts, buffers and detergents and consistent digestion by trypsin. The electrophoresis removes from the protein extracts buffers, salts and detergents from the protein extracts that may interfere with the mass spectrometry. As a result of the trypsinisation, all the tryptic peptides remain in a single fraction. Coomassie blue stain, used to visualise the separated proteins, provides quality control prior to the in-gel digestion (Piersma et al., 2013). The separation of the proteins in the non-S9 fraction was a challenging process. Initially the separation of the proteins in the non-S9 fraction relied on their solubility in SDS, however the resulted SDSP PAGE gel electrophoresis did not provide

good protein separation. The solubility of the non-S9 fractions was improved by the use of 9M Urea/2 % Chaps. The collected supernatant was used to determine the protein concentration using a BCA assay, followed by SDS-PAGE electrophoresis. The established GeLC-MS/MS identified 260 proteins with a broad range of molecular weights and biological functions. The study by Taverna and co-workers was focused on the use of LC-MS/MS for detection and definition of protein signature in normal human epidermis and dermis by MALDI-MS profiling and MALDI-MS imaging respectively by discrete location based on histology. The experiment determined the protein differences between epidermis and dermis and the slight differences between the papillary and reticular dermis. Furthermore, it identified proteins unique to human skin, as well as those associated with unique markers of individual variability (Taverna et al., 2011). On the other hand, van Eijl and co-workers used the proteomic profiling approach to successfully elucidate enzymes responsible for drug metabolism in human skin microsomes and cytosols by utilising the GeLC-MS/MS methodology (van Eijl, 2012).

In the current research the GeLC-MS/MS was applied to the analysis of both S9 and non-S9 fractions, leading to the identification of whole human skin proteins with diverse biological functions, sub-cellular locations and involvement of toxicological pathways at cellular and molecular levels.

Several Annexin proteins were discovered in both the S9 and non-S9 fractions such as annexin 1,2,4,5 and 7, which was proved to be over-expressed in the presence of glucocorticoids such as cortisol which inhibits inflammation (Busher, et al., 2002). Members of the Heatshock proteins 70, 90 were identified, their expression was previously found to be altered by cysteine binding skin sensitisers (Natash, 2010). The heat shock protein-90 family is known to protect tissues from various environmental insults and participate in repairing damaged tissues (Jayaprakash et al., 2015).

Epidermal adhesion is mediated primarily by integrin-associated proteins. Numerous *in vitro* reports have implicated the involvement of those proteins in the regulation of a plethora of cellular processes other than adhesion, such as signal transduction, re-epithelialisation during wound healing, hair growth, and stem cell maintenance. A study of the epidermal growth factor suggested that human-like epidermal growth factor protein could improve visible signs of photo damage and aging in facial skin (Schouset et al., 2012). Mutations to the gene which encodes desmoplakin have been proved to be linked with skin defects, the expression of which in turn is regulated by the involvement of cellular pathways, and which can be targeted (Pigors, et al 2014).

Several 14-3-3 family proteins were identified that regulate diverse cellular processes by binding to proteins with numerous functions. It has been shown that the 14-3-3 protein is over-expressed in a number of skin diseases such as psoriasis, condylomata acuminata and actinic keratosis (Lodaygin et al., 2003). A protease such as caspase 14 was identified to be involved in filaggrin processing and activated during keratinocyte cornification. Caspase 14 is mainly involved in inflammation and apoptosis, and plays an important role in the correct degradation of (pro) filaggrin and the formation of the epidermal barrier (Deneker et al. 2009). Thioredoxins are antioxidant enzymes that play important roles in many health-related cellular processes by facilitating the reduction of other proteins. Van der Veen and co-workers demonstrated that the protein is under control of the ARE/EpER element and up-regulated after its subsequent treatment with cysteine-binding electrophiles (skin sensitiser) (Collet and Messens, 2010; Van der Veen et al., 2012).

The calculated relative abundance of each protein per fraction in Table 1 shows that the highest abundance percentage belongs to Keratin type 2 cytoskeleton and Histone H4 protein in the S9 fraction, where *as* the highest proportion from the non-S9 fraction belongs to Histone H4. The proteins identified at relatively high proportions can be further analyzed

through their physico-chemical properties and used as model proteins in the ongoing *in chemico* approaches of replacing the current animal models for assessing skin chemicals.

The proteins identified by GeLC-MS/MS and analysed through ToxProfiler, showed that proteins from both fractions (S9 and non-S9) are involved in various toxicological pathways such as inflammation, IL-1/4/6- signalling, KEAP 1-NRF2, oxidative stress, EGFR1 signalling, MAPK signalling, prostaglandin synthesis and regulation (Table 2). These findings may lead to further in-depth studies of those proteins and target them *in vitro* as specific ‘‘sensors-markers’’ at specific toxicological endpoints (Natsch, 2010).

There is continuously increasing demand for the screening of chemicals used in cosmetics and personal care products. Research projects are carried out and focused on studying the transcriptomes and proteomes as a result of skin allergy with the ultimate aim of filling the knowledge gaps in the topic.

The data and information obtained from skin protein profiling can be further extended to quantify reversible post-translational modification of the proteins, e.g. phosphorylation as well as irreversible modification such as haptenisation. The data can also be used to deeper understanding of the skin proteome. For example, knowledge of the relative abundance of proteins allow the design of better strategies for the depletion of common proteins, thereby allowing low abundance proteins to be uncovered.

In addition to the above, the received data set could provide valuable insight into the level of key protein nucleophilic residues that are potential targets for the electrophilic chemicals or metabolites, the product of which leads to delayed types of hypersensitivity reaction. Information obtained from single protein models (Alekcis et al., 2008) showed that chemical modification of proteins occurs in specific microenvironments within the 3D protein structure. That is why more efforts need to be focused on the role of the 3D protein

configuration in determining the ultimate availability of nucleophilic amino acid side chains for reaction with exogenous chemicals in relevant physiological conditions.

2.4.2. Interaction of different cosmetic products

Since ancient times people used to mix various organic and inorganic sources to develop and enhance the effect of different drugs and cosmetic products. With the advancement of the life science, the understanding of the human biology on genomic and proteomic levels scientists have begun to combine chemicals used in different products carefully in order to increase the product's efficiency and reduce any possible side effects. The effect of combining different chemicals (ingredients) when developing drugs or cosmetic products has been studied for more than a century.

There are three types of actions as a result of the chemical combination in a product.

- a). Similar action (dose/concentration addition)- chemicals have same mechanism of action but different potencies.
- b). Dissimilar action known as independent action - chemicals have different mode of action, but have no influence on each other.

Both the similar and dissimilar modes of action are based on the assumption that chemicals in the mixtures do not influence each other's toxicity and each has its own biological target.

- c). Different chemical interactions. The interactions can be divided into strong (synergetic, potentiating, supra- additive) or weak (antagonistic, sub-additive, inhibitive, infra- additive). The interaction of the chemicals can vary based on the dose, duration of exposure and the biological molecules targeted by those chemicals (Scientific Committee on Health and Environmental Risks, 2011)

The identified skin proteins as a result of the skin proteome characterisation, can be used as model proteins to study the effect of the drug combination. Skin samples can be treated with individual chemicals followed by a treatment with a combination of two or more chemicals at

the same time to monitor any protein modifications and determine the effect of the drug combination. It is crucial to highlight few suggestions by Fouquier and Guedj, 2015 when studying drug interactions: the design of the analytical methods has to be appropriate for the classified drug interaction; A standard framework has to be used when analysing drug combinations. The framework has to be clear and targeting the different types of interaction and established based on well understood mechanism of drug's action, not based on any assumptions as well as being an easy to perform by other scientists. The analysis has to be adapted to the different stages of the research process(discovery, preclinical and clinical stages) (Fouquier and Guedj, 2015).

Chapter 3

***In chemico* approach in studying skin sensitisers**

3.1. Introduction

One of the most intensely studied non-animal approaches aiming to substitute *in vivo* testing is the *in chemico* approach. This approach is based on experimental physicochemical measurements of the nucleophilic protein and electrophilic hapten in order to study the specificity and correlation between the protein reactivity and chemical potency (Cronin et al., 2009).

Studies of the relationship between sensitisation and chemical-protein reactivity have been carried out using nucleophile molecules, peptides containing mostly lysine and cysteine, and protein models by measuring peptide depletion as a consequence of the protein-hapten formation. Residues such as lysine, tyrosine, cysteine, histidine and arginine have been proved to be involved in the peptide-haptenisation process leading to skin allergy (Aeby et al., 2007)

Covalent modifications of skin proteins by allergens play a crucial role in the skin sensitising process, and a full understanding of the protein-hapten mechanism and specificity of reaction will lead to an improvement in development of *in chemico* approaches for testing chemicals in cosmetics and personal care products. The current *in chemico* reactivity assays for screening chemicals suggest that a large amount of peptide depletion needs to be recorded in order to categorise a chemical as a sensitiser. This leads to performing *in chemico* experiments using peptide: chemical reactivity in the presence of an excessive amount of chemicals. Therefore, the nucleophile (peptide) :electrophile (chemical) ratio used in *in chemico* experiments is of high importance. Roberts and Basketter suggested that an important aspect when developing an electrophile-nucleophile reactivity assay is to consider whether the tested chemical is pure with no other impurities, or whether it is impure with a combination with other chemicals that could present as a trace or in higher quantities. If the tested chemical sample is impure, then the reactivity assay has to be developed with an

excess of the sample, because if the chemical of interest is unreactive a significant nucleophilic depletion will still be observed. If the tested chemical is a pure substance, an excess of the nucleophile has to be used, so any trace impurity in the sample will not interfere with the final results and cause confusion (Roberts and Basketter, 2009; Pease et al., 2010).

Studies of the relationship between sensitising potency and chemical-peptide reactivity have been carried out using peptides containing mostly lysine and cysteine or model proteins (further trypsinised to peptides), followed by measuring peptide depletion by using HPLC, UV spectrometry and mass spectrometry (Aeby et al., 2007; Jeonge et al 2013). Due to the lack of knowledge in terms of the skin proteome, and which proteins exactly can be targeted by the sensitisers, the current investigations using *in chemico* approaches are mostly based on the use of model nucleophiles, synthetic peptides and recombinant proteins (Aleksic et al., 2008)

Although all chemicals with reactive electrophiles will form a covalent adduct with nucleophilic proteins, the mechanism of action is different for different chemicals, therefore it can be used to distinguish between the strength and the type of many chemicals (Chipinda et al., 2011).

The *in chemico* approaches are simple to perform and easy to based on the incubation of peptides and model proteins with different chemicals at different times and temperatures. This will help to determine the nucleophile reactivity and the study of the protein-chemical mechanism of interaction. *In chemico* approaches are practical and the chemical reactivity can be explained by established facts in organic chemistry.

A major drawback of *in chemico* approaches is the dissimilarity between the behaviour of the protein in a real system and during the experiment. During *in chemico*, the proteins are considered as separate biomolecules with no consideration of the surrounding real systems (bioavailability of the skin, water solubility, metabolic transformation and immune

recognition). Very often (another source of error) the proteins may be modified by the non-physiological conditions of the experiment (Astoriol and Worth, 2011).

The *in chemico* approaches can be used as a tool along with other *in vitro* methods to build up a full understanding of the electrophile-nucleophile interaction and hence contribute to the total replacement of the current *in vivo* assessments on the various chemicals used in cosmetics and personal care products (Chapin et al., 2013).

Many studies have started focusing and studying the correlation between the reactivity of proteins and chemical potency using recombinant proteins.

A study by Aleksic et al., 2007 using Human Serum Albumin (HSA) incubated with different chemicals: strong sensitizer, moderate, irritant and non-sensitizer led to very promising results. The samples were further analysed by HPLC/MS, showing that the amino acids lysine, histidine, tyrosine and cysteine were modified by both strong and moderate sensitizers, whereas HSA treated with irritant and non-sensitisers did not show any protein modification under any conditions. The results suggested the *in chemico* approach can be used to distinguish between sensitizers and non-sensitizers (Aleksic et al., 2007).

Maja Aleksic and co-workers further extended their investigation and worked on two more protein models, i.e. Cytokeratine 14 (K14) and Cofilin, using sensitizers with different potency: strong, irritant and non-sensitisers (DNCB, BC and DCNB). The samples were further analysed by MALDI/MS and Nano-LC/MS/MS, and as a result protein depletion was not detected on the proteins treated both with non-sensitizers and with irritant chemicals. The study has also proved that the reactive chemicals target the nucleophilic amino acids residing in specific microenvironments of the 3D protein structure (Aleksic et al., 2008)

The current study is performed to investigate nucleophile reactivity using model recombinant protein Apomyoglobin with sensitisers of different potencies, aiming to develop an

understanding of the mechanism of protein-hapten formation and to find any specific binding locations, considering different doses and time incubation.

Apomyoglobin (APG) MW16951 is a protein synthesised in the Endoplasmic reticulum (ER), this protein is able to bind to the heme on the mitochondrial outer membrane to form holomyoglobin, which keeps and transports oxygen into muscle tissues. The ApoMb structure is highly helical and its hydrophobic core is tightly packed (Basova et al., 2004)

Top down Mass Spectrometry is a novel technique of measuring intact protein. It is a measuring tool based on the mass/charge ratio (m/z) of charged molecules which pass through an electric and magnetic field. The Top Down MS gives us detailed information about the presence of a particular protein as well as its amino acid composition and any post-translational modification (e.g. phosphorylation of the protein). The Top Down approach differs from the already available MS techniques, as it is possible to measure molecules with high molecular weight without those molecules requiring previous proteolytic digestion, and hence it measures the mass/charge ratio of the intact protein-chemical adduct. In addition, Top Down MS also provides high resolution and accuracy in presenting the results data (Kellie et al., 2010).

Top-down MS techniques are increasingly being applied for high-throughput protein analysis, in particular to characterise more complicated combinations of intact protein-chemical interactions (Kelleher et al., 2004; Kellie et al., 2010), with the clear advantage that the quantification of multiple protein forms with combinations of chemicals is straightforward when the mixture is measured intact. This new technology applied in this project (with collaboration with Health Protection Agency, England) may provide crucial information about the haptenisation pathways.

The aim of the experiment is to apply the novel technique of Top Down MS with higher resolution and accuracy, in order to measure protein depletion as a result of the protein-

hapten adduct formation with the purpose of elucidating the mechanism of protein-hapten formation and studying any specific binding between sensitisers and model proteins.

3.2. Materials and Methods

3.2.1. *In chemico* experiment

Apomyoglobin(APG) protein (MW 16.5 kDa, Sigma Aldrich, UK) as a lyophilised powder was dissolved in Tris buffer at a working solution of 10µg/µl. The effective nucleophile: electrophile molar ratio of APG:chemical is 1:2.5, which was calculated based on the number of nucleophile side chains of APG. Initially APG was incubated with four chemicals with different potency: 2-4-Dinitrochlorobenzene (DNCB) (potency: strong); Phenyl Salicylate (PS) (moderate), Benzaldehyde(BZ) (a non-sensitiser) and Benzalkonium Chloride (BC) (an irritant). Samples were prepared by mixing protein and chemical in the following ratios: 1:500, 1:100, 1:50, 1:2.5, 10:1 and 100:1, and incubated at 18°C for 24h, 3 days, 7 days and 15 days, separately. Subsequently, 21 chemicals with known skin sensitising potency from the LLNA database with name and class defined by LLNA were selected (Table 3). Samples were prepared at a 1:500 protein:chemical ratio. The samples were incubated at 18°C for 24 hours. In addition to the above, one of the samples treated with DNCB, and the control were incubated at 32°C and 37°C in order to replicate the skin and body physiological conditions respectively. Control samples were prepared by using acetone/water in buffer containing same amount of the protein.

Table 3 List of chemicals tested in the *in chemico* experiment

No	Chemicals	Class (LLNA)
1	Maleic acid (MA)	False-positive (Irritant)
2	Sodium Dodecyl Sulphate (SDS)	False-positive (Irritant)
3	Benzalkonium chloride (BC)	False-positive (Irritant)
4	Chlorobenzene (CB)	Non-sensitiser
5	Methyl salicylate (MS)	Non-sensitiser
6	Benzaldehyde (BZ)	Non-sensitiser
7	Coumarin (CM)	Non-sensitiser
8	Ethyl acrylate (EA)	Weak sensitiser
9	Methyl methacrylate (MM)	Weak sensitiser
10	Eugenol (EG)	Weak sensitiser
11	2,4-dichloronitrobenzene (DCNB)	Weak sensitiser
12	2-Mercaptobenzothiazole (MB)	Moderate sensitiser
13	Diethyl Maleate (DM)	Moderate sensitiser
14	Dihydrocoumarin (DC)	Moderate sensitiser
15	Phenyl Salicylate (PS)	Moderate sensitiser
16	2-4-Dinitrochlorobenzene (DNCB)	Strong sensitiser
17	Dibenzoyl peroxide (DP)	Strong sensitiser
18	p-Benzoquinone (BZ)	Strong sensitiser
19	p-Phenylenediamine (PD)	Strong sensitiser
20	Isoeugenol (IE)	Strong sensitiser
21	Formaldehyde (FA)	Strong sensitiser

3.2.2. Top-down Analysis (Health Protection Agency London)

Online chromatography was performed with the Thermo Easy nLC 1000 ultra-high pressure HPLC system (Thermo Fisher Scientific) coupled online to the Q Exactive (Thermo Scientific). The instrument was controlled by Xcalibur (Q Exactive Plus 2.3, Thermo Scientific).

For chromatographic separation, buffer A (water containing 0.1% formic acid) and buffer B (acetonitrile containing 0.1% formic acid) were used as mobile phases for gradient separation. 2 µl of samples (diluted in water/acetonitrile (1:1, v:v)) were loaded into a reversed phase Nano Trap Column (Acclaim PepMap 100, 100µm i.d. x 2cm, C18, 5µm, 100 Å) and further separated on an C18 reversed-phase nanocolumn (Acclaim PepMap100, 75 µm i.d. × 15 cm, C18, 3 µm, 100 Å, 75 µm i.d. × 15 cm, Thermo Scientific) with a linear gradient of 4-

65% buffer B at a flow rate of 300 nL/min over 12 min. Due to loading, lead-in and washing steps, the total time for an nLC-MS/MS run was 21 min.

For top down data acquisition, the instrument was operated in positive ion mode and a data-dependent ‘top 4’ method was used. Survey scans (400 – 2000) were acquired at a resolution of 70,000 at m/z 200 with maximum IIT of 100 ms. MS/MS was performed by HCD fragmentation using CID. Resolution for HCD spectra was set to 17,500 at m/z 200 with maximum IIT of 50 ms. Normalized collision energy was set as 20. The ‘underfill ratio’, specifying the minimum percentage of the target ion value likely to be reached at maximum fill time was defined as 1.0 %. Charge exclusions of unassigned and 1 – 3 were selected, in order to exclude precursor ions with 1 - 3 and unassigned charge states from fragmentation selection. A Default dynamic exclusion of 15.0 s was selected to prevent an ion from triggering a subsequent data-dependent scan after having already triggered a data-dependent scan. Furthermore, the S-lens RF level was set at 70, which gave optimal transmission of the m/z region occupied by intact proteins.

Top down data were processed and analysed using Xcalibur (Q Exactive Plus 2.3, Thermo Scientific).

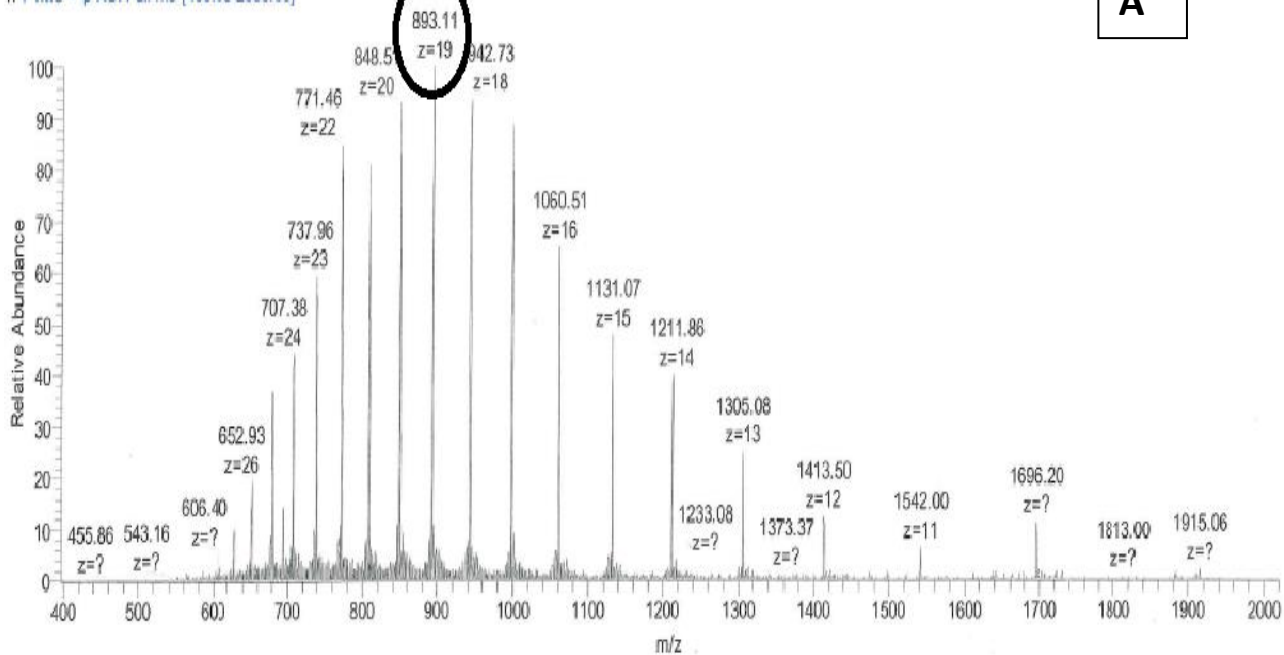
3.3. Results

3.3.1. Top-down mass spectrometry

APG was incubated at 18 °C for 24 h with 2,4-dinitrochlorobenzene (DNCB), as a strong sensitizer, which has been used as a model hapten in a number of studies. The data received from top down MS (Figure 11) shows a clear shift of the m/z ratio towards 8.74 m/z ($=166.06$ MW), i.e. towards higher values of the intact protein-hapten conjugate in comparison with the chemically untreated APG sample (control). The highest peak on the DNCB-treated sample corresponds to 901.85 ($z=19$) (Figure 11 B), whereas on the control sample (untreated), the highest peak is 893.11 ($z=19$) (Figure 11 A). Subtracting 893.11 from 901.85 gives a shift of 8.74 m/z shift. This shift suggests that the difference in molecular weight between control and treated sample is ≈ 166.06 MW. This can be explained by nucleophilic substitution on the DNCB aromatic ring with the loss of chlorine atom. The shift of m/z ratio towards higher values corresponds exactly with the mass addition of the reacted DNCB chemical molecule (with chlorine atom excluded), as a result of the formation of a protein-hapten adduct .

Min_ZY_Apo_15Oct2013_02 #4220-4299 RT: 10.11-10.26 AV: 16 NL: 5.07E7
T: FTMS + p NSI Full ms [400.00-2000.00]

A



Min_ZY_Apo_15Oct2013_02 #4322-4468 RT: 10.32-10.61 AV: 30 NL: 5.80E7
T: FTMS + p NSI Full ms [400.00-2000.00]

B

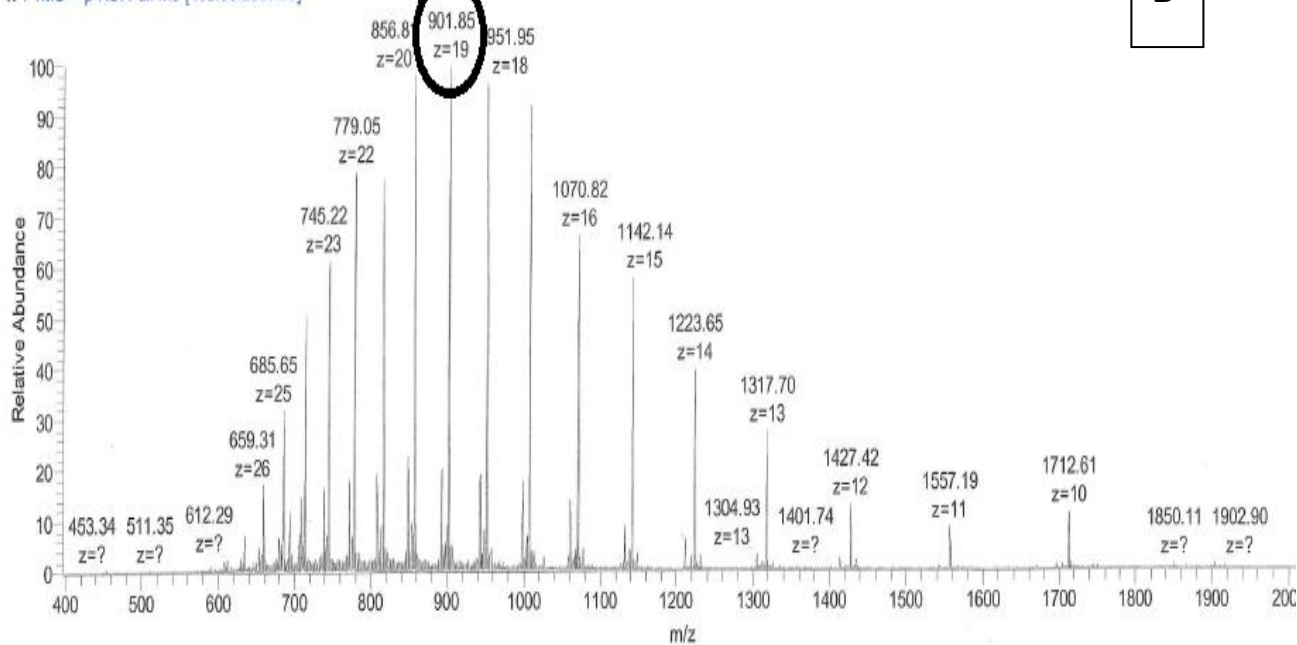


Figure 11. MS spectrum of APG-DNCB sample. A: control (APG alone + vehicle); B: APG modified by DNCB incubated at 18 °C (mass shift of 8.74m/z \approx 166.06 Da).

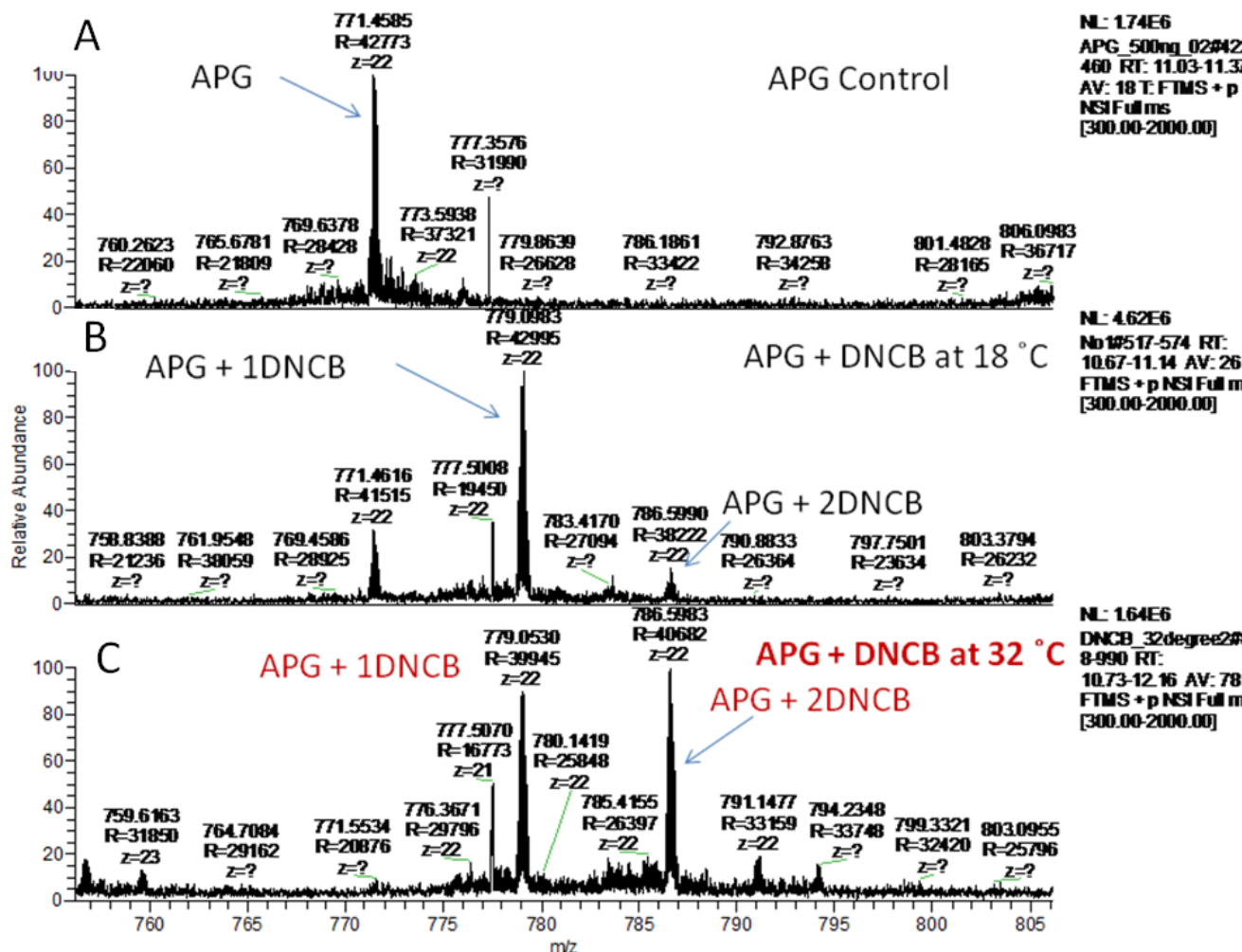


Figure 12. MS spectrum of APG-DNCB sample. A: control (APG alone + vehicle); B: APG modified by DNCB incubated at 18 °C (mass shift of 7.64 m/z \approx 168.08 Da); C: APG modified by DNCB incubated at 32 °C shows two peaks: The first peak with a mass shift of 7.64 m/z \approx 168.06. The second peak with a mass shift of 15.14 m/z. The 15.14 m/z \approx 333.08.

APG was incubated with a strong sensitizer (DNCB) at 32 °C (skin physiological condition) for 24h. The experiment was repeated at 18 °C and 32 °C for comparison analysis. The received mass spectra (Figure 12) at 18 °C show a clear shift in the mass spectrum, corresponding to an m/z ratio of 7.64 m/z ratio \approx 168.06 MW between the control (untreated) APG sample and the treated one. At 32 °C the mass spectrum shows two shifts (two peaks): one corresponding to 7.64 m/z (\approx 168.06 MW) and an additional peak corresponding to 15.14 m/z (\approx 333.08 MW) (Figure 12). The two shifts suggest that most probably two DNCB molecules are bound to the APG molecule.

Analysis of the time and dose courses of DNCB interacting with APG is still ongoing, together with the outcomes from 21 other chemicals incubated with the protein.

3.4. Discussion

3.4.1. *In chemico* approach by Top-down mass spectrometry

In the current experiment, the new top-down MS technique developed at HPA was applied. Top-down MS is a novel technique for measuring intact proteins, providing detailed information about the interaction between protein and ligand as well as post-translational modifications (Compton and Kelleher, 2012; Rose et al., 2012). The current experiment gave encouraging results which promised to distinguish between sensitisers and non-sensitisers, shown by a clear shift of the m/z ratio towards higher values where the APG protein was treated with a strong sensitiser chemical (DNCB) (Figure 11). The control sample incubated at 18°C shows a peak at 893.11 ($z=19$) as the most abundant molecule. The peak at the control sample corresponds exactly to the mass of the APG ($893.11 \times 19 \approx 16969\text{Da}$). The APG chemically treated with DNCB 18°C shows a peak at 901.85 ($z=19$) as the most abundant molecule. The peak at the treated sample corresponds to a mass higher than the mass of APG ($901.85 \times 19 \approx 17135.15\text{ MW}$). This shift in the m/z ratio can be explained based on the physicochemical properties of APG and DNCB, as well as established facts in organic chemistry. The m/z shift ratio (Figure 11) corresponds to an m/z ratio of 8.74 ($901.85-893.11 = 8.74$), which, converted to mass, gives 166.06 MW (8.74×19). The molecular mass of DNCB is 202.65 MW, hence the increase in the mass of the treated sample corresponds to the addition of a DNCB molecule (202.65 MW) to the mass of APG, with a loss of 35 MW ($202.65 - 166.06 \approx 35$), which corresponds to the mass of a single chlorine atom (Figure 13).

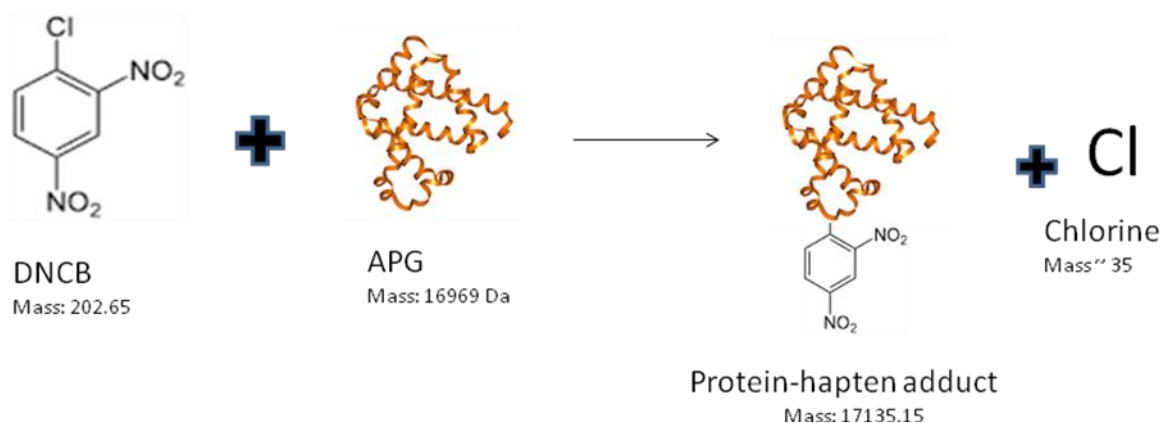


Figure 13. Predictive diagram of the DNCB-apomyoglobin adduct formation following the incubation of apomyoglobin with extreme sensitiser (DNCB) at 18 °C for 24 h. The change of the mass as a result of the incubation with DNCB suggests that the protein-hapten conjugate formation is based on the addition of the DNCB molecule to a single location on the apomyoglobin protein (masses calculated based on the mass spectrometry data) with the loss of a single chlorine.

The experiment was repeated at 18°C and 32°C (skin physiological condition). The incubated control sample shows a peak at 771.458 ($z=22$) as the most abundant molecule. The peak at the control sample corresponds exactly to the mass of APG ($771.458 \times 22 \approx 16972$ MW). APG chemically treated with DNCB at 18 °C shows a peak at 779.098 ($z=22$) as the most abundant molecule. The peak at the treated sample corresponds to a higher mass than the mass of APG the mass of APG ($779.098 \times 22 \approx 17140.156$ MW). This shift in the m/z ratio can be explained based on the physicochemical properties of the APG and DNCB as well as the knowledge of the organic chemistry. The shift in the m/z ratio (Figures 12 A and B) corresponds to ($779.098 - 771.458 \approx 7.64$) 7.64 m/z , and ratio converted to mass gives 168.08 MW (7.64×22). The molecular mass of DNCB is 202.65 MW, hence the increase in the mass corresponds to the addition of a DNCB molecule to the APG (202.65 MW) with a loss of 35 MW ($202.65 - 168.08 \approx 35$), which corresponds to the mass of a single chlorine.

APG chemically treated with DNCB at 32° C shows two peaks: one at 779.053 ($z=22$) and another one at a higher shift corresponding to 786.598 ($z=22$). The first peak can be

explained with a mass shift equal to 7.59 m/z (779.053 - 771.458), which, converted to molecular weight, gives $7.59 \times 22 = 166.98$ MW. By subtracting this from the molecular weight of DNCB (202.65), a figure of 35 is obtained ($202.65 - 166.98 = 35$); thus it can be concluded that a molecule of DNCB is added to APG, with the loss of one chlorine atom. The second peak clearly shows a double shift ($786.598 - 771.458 \approx 15.14$), 15.14 m/z. The 15.14 m/z ratio converted to molecular weight corresponds to 333.08 MW (15.14×22) (Figures 12 A and C). The change in the molecular mass corresponds to the addition of two DNCB molecules, each with 166.5 MW, and the loss of two chlorines ≈ 72.16 MW (2×36.08 MW) (Figure 14).

Interestingly, the new results (Figure 12) have shown more binding sites on APG available to by DNCB under physiological condition (32° C), which can be studied possibly over temperature, time or dose course. Further analysis is ongoing, together with the analysis of 21 more chemicals with different potencies.

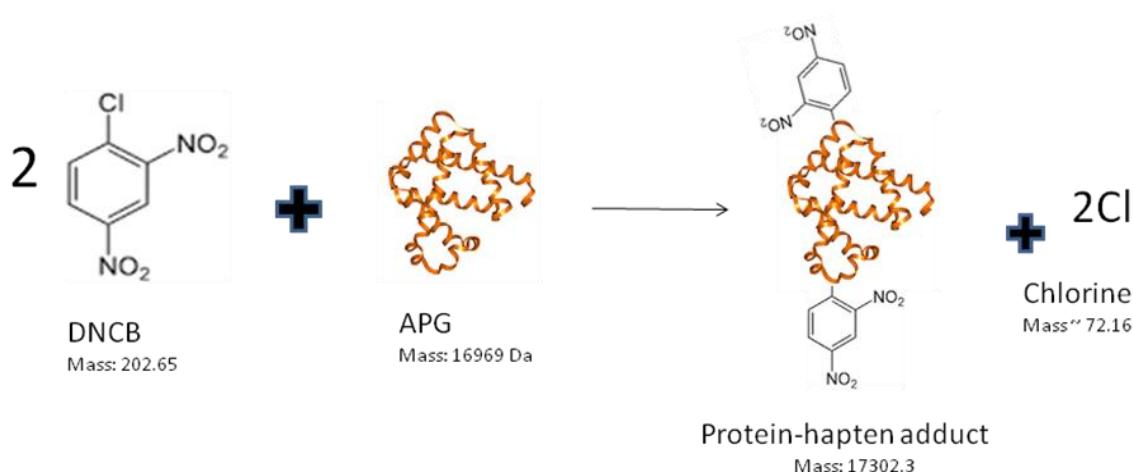


Figure 14. Predictive diagram of DNCB-apomyoglobin adduct formation following incubation of apomyoglobin with extreme sensitizer (DNCB) at 32 °C for 24 h. The change of the mass as a result of chemical incubation suggests that protein-hapten conjugate formation is based on the addition of two DNCB molecules to different locations on the apomyoglobin protein (masses calculated based on mass spectrometry data) with the loss of two chlorines.

The sensitiser's reactivity using recombinant proteins as model proteins has been studied (Aleksic et al., 2007), in which human serum albumin was incubated with chemicals of different potencies followed by MALDI-TOF-MS analysis. The results showed that Nucleophile residues, of which the recombinant protein is composed were covalently modified in selective ways with different modes of action towards high and moderate sensitiser (DNCB and PS respectively) and no reactivity towards non-sensitiser (DCNB) including irritants (SDS and BC). The same research group, one year later, used MALDI-TOF-MS analysis to investigate the reactivity of two model proteins, Cytokeratine 14 and Cofilin, towards strong sensitiser (DNCB), irritants (BC) and non-sensitiser (DCNB). The study showed that reactive chemicals targeting nucleophilic amino acids reside in specific microenvironments of the 3D protein structure that are conducive to reactivity (Aleksic et al., 2008). Here it is very important to highlight that Aleksic and co-workers used the MALDI-TOF-MS technique, in which protein was trypsinised into peptides before performing mass spectrometry.

Information obtained from the single protein model (Aleksic et al., 2008) showed that chemical modification of proteins occurs in a specific microenvironment within the 3D protein structure. Aleksic and co-workers used Insight II software to prepare computer-based images, and to show the location of the DNCB binding, and the number of the modified protein amino acid residues. That is why future studies need to be focused on the role of the 3D protein configuration in determining the ultimate availability of nucleophilic amino acid side chains for reaction with exogenous chemicals under relevant physiological conditions.

Protein Centre is a computer-based software provided by Thermo Scientific as a web-based interpretational tool which is able to compare proteins data. Protein Centre provides comparative information between identified proteins, reveals the biological context of different protein data sets, provides protein quantitative analysis and studies protein involvements in different biological pathways. The software can be used to compare treated and untreated

samples, which makes it a suitable tool to analyse APG, both untreated, and treated with the 21 chemicals listed in table 3. In this way Protein Centre will not only provide a comparative study between treated and untreated samples using MS raw data, but also will provide a wider overview about the characterisation of intact protein(s) (From data set to meaningful biology, 2017).

Chapter 4

In vitro approach in studying skin sensitisers

Phase II xenobiotic metabolic enzymes

4.1. Introduction

The metabolic detoxification of xenobiotics is a crucial body function usually performed by phase I and phase II enzymes called xenobiotic metabolic enzymes (XMEs). Considering the liver as the main metabolising and detoxifying organ in the body, most research activities are based on liver xenobiotic enzymes. There is a lack of research when it comes to cell-specific metabolic enzymes, in particular in the human skin, considering its important role against chemical exposure (Esser and Gotz, 2013).

Recent studies suggest that chemical-induced changes in the expression of some metabolic processes in the skin may be a characteristic of skin sensitisers (Natsch, 2010). Despite some research publications that documented mRNA expression of enzymes or quantifying enzymatic activity in human or rodent skin (Gotz et al., 2012a & 2012b), very little information is available documenting metabolic enzyme expression levels, other than that performed by the Cosmetics Europe (formerly COLIPA) skin metabolism initiative. The results not only demonstrated equivalent enzymatic activity of various phase I and II metabolising enzymes in native or reconstructed 3D human skin (Gotz et al., 2012a & 2012b), but also an equivalent expression level of metabolising proteins (van Eijl et al., 2012). However, no work on chemical sensitiser-induced expression at molecular levels (mRNA or protein) has been undertaken and this key knowledge gap remains (Hewitt et al., 2013).

The skin protection role does not stop at preventing harmful substances from entering the body. Metabolising these chemicals into simpler compounds in order to pump them out of the cells is performed mainly by phase I and II xenobiotic metabolic enzymes (XME) available in the skin.

Drug metabolism can be divided into 3 phases. The first phase involves a group of XMEs such as cytochrome P450 oxidases, known as XME phase I, which introduce polar or reactive groups into the xenobiotic (hapten). The modified compound then conjugates with another polar compound under the catalysis of enzymes such as Glutathione-S-transferases,

known as XME phase II. In phase III the xenobiotic conjugate can be further recognised by efflux transporters and pumped out of the cells (Ioannides, 2002) (Figure 15).

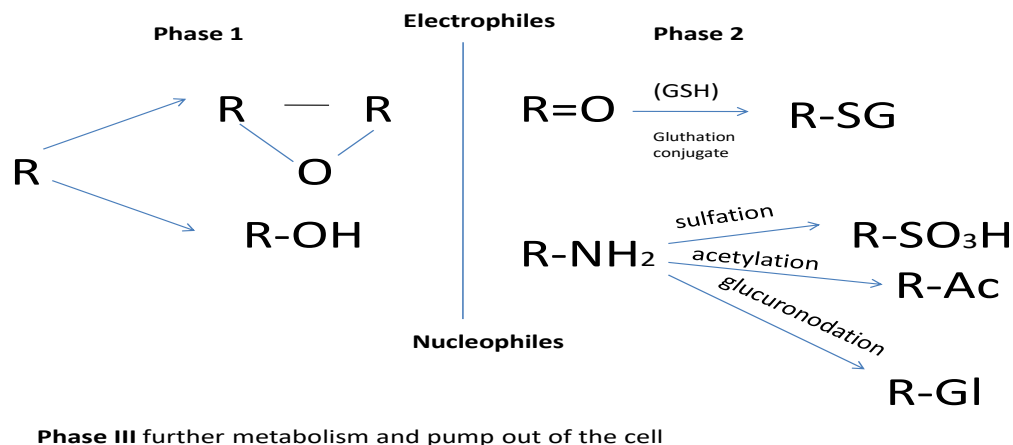


Figure 15. Schematic representation of drug metabolism. Phase I includes oxidation, hydrolysis, reduction. Phase II includes the formation of hydrophilic compound R-SG, sulfation, acetylation and formation of acetyl Co-A and glucuronidation using glucuronic acid. Phase III involves further metabolism and pump of the product out of the cell.

Despite the important role of the XME in detoxification of various xenobiotics, there is a surprising lack of research on skin XME. Cosmetics and pharmaceuticals used occupationally, accidentally and intentionally, contain chemicals which, in many cases, lead to skin irritation, inflammation, allergy and even cancer (Esser and Gotz, 2013).

The increased interest in studying skin metabolism, especially since the establishment of the 7th amendment to the European Cosmetic Directive for the replacement of animal models of chemical assessment, has led to extensive investigation of the skin as an active metabolising organ in many toxicological studies. The whole human skin, especially the keratinocytes in the epidermis, proved the presence of both phase I and phase II XME (Gotz et al. 2012a,b).

COLIPA (European Cosmetic, Toiletry and Perfumery Association) has studied various phase I and II XMEs in order to establish the XME profile in the human skin, and compare it with developed *in vitro* skin models.

In vitro models for assessing skin irritation and toxicity have a number of disadvantages, from species-specific metabolism to the ethical issues and risk assessment associated with such research. COLIPA has generally worked on two projects. One project focused on protein expression of XME *in vitro* in whole skin, 3D skin models and keratinocytes monolayer using a label-free proteomic technique.

The second project involved measuring the activity of the XME phase I and II *in vitro* using 3D skin models, whole ex-vivo human skin and epidermal keratinocytes. Some XME phase I were not detected, or if detected they were at a low level, such as cytochrome P450 monooxygenases in whole skin. However, XME phase II GST (glutathione-S-transferase), N-acetyltransferase and UDP glucuronosyl-transferase were detected on mRNA and protein level in the whole skin and 3D models at levels similar to those in liver.

It is important here to highlight that the presence of mRNA which encodes a specific enzyme is not a definite indication of the presence of the respective protein or even a measure of its activity (Hewitt et al., 2013)

GST (Glutathione-S-transferase) represents a phase II XME involved in catalysing the reaction of glutathione and an electrophilic substrate, hence preventing toxic injuries in many tissues.

Currently much research shows interest in studying the GST enzymes in organs frequently exposed to toxic electrophiles such as liver, intestine and skin.

Despite the importance of the skin as a barrier against toxic chemicals, very little is known about the XME in the skin, especially the epidermis. The epidermis is mainly composed of

keratinocytes, so they can be used as suitable model for studying XME phase II enzymes (Blacker et al., 1991).

4.1.1. Regulation of XME phase II- Keap1-Nrf2-ARE

The Keap1-Nrf2-ARE pathway is involved in the regulation of the transcription of mainly phase II XME. The Keap1-Nrf2-ARE pathway is highly expressed in many cell types, including keratinocytes (Esser and Gotz, 2013).

The Keap1-Nrf2-ARE pathway can be activated by different chemicals (haptens). In an uninduced condition, Keap1 is associated with the Nrf2 factor, forming a Keap1-Nrf2 conjugate. In the presence of a hapten, the Keap1 protein disassociates from the Nrf2 factor, where the hapten covalently binds to the cysteine residues of the Keap1 protein. Human Keap1 protein has been proved to contain 25 cysteine residues, however modification of some of them can lead to the release of Nrf2 from the Keap1-Nrf2 conjugate. The free Nrf2 migrates to the nucleus where it binds to the ARE regulatory element and regulates the transcription of a series of XME (Figure 16), (Natsch, 2010; Jacquilleot et al., 2015).

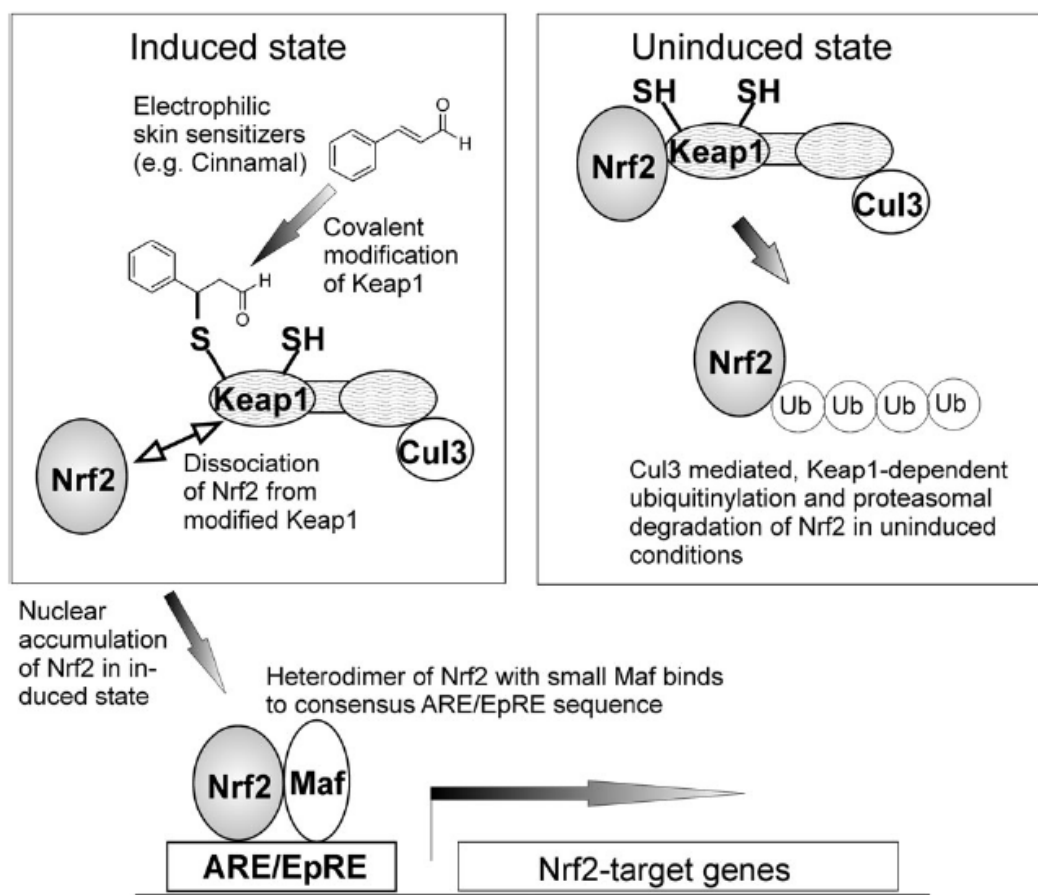


Figure 16. Keap1-Nrf2-ARE pathway. Keap1-Nrf2 complex exist in the cytoplasm. When reacting with hapten, the Keap1 disassociates from Nrf2, leading to Nrf2 translocate to the nucleus. In the nucleus Nrf2 forms a dimer with Maf protein. The haptenised Nrf2-Maf complex bind to DNA and facilitate to the transcription of the target gene (Natsch, 2010).

Many researchers have focused on developing new or on improving existing *in vitro* models for testing sensitisers, aiming for complete replacement of animal models with non-animal models. Regardless of the different approaches used to achieve this goal, their common aim is to study changes in the cell-specific response towards potentially different chemicals, utilising genomics and/or proteomics techniques, leading to the development of alternative techniques for chemical risk assessment.

4.1.2. Glutathione-S-transferase (GST)

Glutathione-S-transferase (GST) is considered to be one of the most important phase II xenobiotic metabolic enzyme given its role in detoxifying allergen, and preventing tissue

damage by oxidative stress (Kimura et al., 1998). GST is characterised by its ability to conjugate xenobiotics by being activated through small molecular weight organic donor molecules such as glutathione; as a result the allergen is detoxified and eliminated from the body. HaCaT cells are known to express higher levels of GST when exposed to varying quantities of electrophiles (Jacquilleot et al., 2015).

Despite the fact that studying and experimentally monitoring the protein expression level and activity are commonly used and considered accurate, studies based on gene expression at the mRNA level using advanced qRT PCR still can provide results with high sensitivity and reliability (Luu-The et al., 2009).

The GST xenobiotic metabolic enzyme can exist in five different isoforms: alfa (GST A), mu (GST M), theta (GST T), pi (GST P) and Z (GST Z), with GST P being the predominant epidermal isoform (Gotz et al., 2012a)

Studies by Gotz et al., 2012a and Luu-The et al., 2009 investigated the expression of GST in reconstructed skin models and in human skin (dermis, epidermis) demonstrated a high level of GST P isoform expression in response to potential sensitisers.

Hewitt et al., 2013 performed a comparison between XME phase I and II protein expression and activity across various skin models, cells lines and native skin. As a result, GST P protein expression and activity were detected across HaCaT cells, native skin and NCTC cells. The same study was extended by looking at the mRNA expression of various quantities of XME, including GST P and omega (xenobiotic metabolic enzyme phase II) expressed in 3D skin models and HaCaT cells. The mRNA level expression of GST P and omega detected in HaCaT cells showed the potential to metabolise a wide spectrum of xenobiotics at the same rate as NCTC and NHEK cells. Interestingly, GST alfa and mu were detected in native human skin, but they were not detected in HaCaT cells. This had been proved earlier by Blacker et al., 1991.

The aim of the experiment was to study the regulation by chemicals of the expression of phase II XMEs, in order to enhance the understanding of metabolic pathways. The research was primarily intended to discover any pattern or consistency in the “induced behaviours” of phase II metabolic enzymes in response to chemicals of differing sensitising potency and binding mechanisms.

4.2. Materials and Methods

4.2.1. Cell recovery and culture:

HaCaT cell line (Cell Line Service, CLS, Germany) was recovered from liquid nitrogen.

HaCaT cells were cultured in DMEM (Dulbecco's Modified Eagle's medium), supplemented with 10% of foetal bovine serum, 1% of penicillin-streptomycin and 2mM L-glutamine at 37 °C/ 5% CO₂ up to 80 % confluence.

4.2.2.MTT [3-(4,5-Dimethylthiazol-2-yl)-2,5-Diphenyltetrazolium Bromide] assay:

Before the chemical exposure, the cells (5×10^4 cells/100µl) were cultured into each well of a 96-well plate for 24h. HaCaT cells were then treated with chemicals with different potency [2,4-dinitrochlorobenzene (DNCB) (extreme); phthalic anhydride (PA) (strong); benzalkonium chloride (BC) (irritant) and benzaldehyde (BZ) (non-sensitiser)] prepared in DMSO. For each chemical a range of concentrations (0.01µM; 0.1µM; 1µM; 10µM; 100µM) was used to treat the cells for 24h to determine cytotoxicity. Following chemical incubation in each well, 25 µl MTT [3-(4,5-Dimethylthiazol-2-yl)-2,5-Diphenyltetrazolium Bromide] solution prepared in sterile PBS (Phosphate buffer saline was added). The microtitre plate was incubated at 37 °C for 2 hours. 100µl of lysing buffer was added to each well and left overnight. Absorbance was measured at 590-600 nm using a spectrophotometer (methods

described previously by Zhu et al., 2008b). Statistical analysis was performed using Graph Pad prism software. Ordinary one way ANOVA non-repeated measures analysis was performed on all the concentrations per each chemical used to treat HaCaT cells. The analysis then was corrected for multiple comparisons using Tukey's multiple comparison test. Maximal 20% death was defined as the criteria of selecting chemical concentrations for further analysis.

4.2.3. Treating HaCaT cells with the same dose (10 μ M) of 2,4-Dinitrochlorobenzene (DNCB) and Phthalic Anhydride (PA) at different incubation periods

2,4-Dinitrochlorobenzene (DNCB) and phthalic anhydride (PA) were prepared in DMEM medium at 10 μ M final concentration based on MTT assay. Maximum 20% death is the criterion for choosing the above chemical concentration. Control was prepared using sterile DMSO (dimethyl sulfoxide) in DMEM medium. HaCaTa cells were subcultured 5x10⁵ cells/ml in 6 well plates and incubated with DNCB and PA over a range of incubation periods 0.5h; 1h; 2h; 3h; 4h; 6h and 24 h at 37 °C, 5% CO₂.

4.2.4. mRNA extraction and cDNA synthesis

HaCaT cells treated with DNCB, PA, and the control cells had their mRNA extracted using RNeasy MiniKit (Qiagen, Germany). mRNA concentration was determined using NanoDrop T009 (ThermoScientific, UK) as per manufacturer requirements.

cDNA was synthesised with a final concentration of 1 μ g using PCRBIO cDNA Synthesis Kit (PCRBiosystem, UK).

4.2.5. Primer design: One pair of primers per GST Pi gene and GAPDH gene were designed by the NCBI website (<http://www.ncbi.nlm.nih.gov>). The GSTpi gene accession number was entered into the “Enter accession” section on the <http://www.ncbi.nlm.nih.gov> website. The PCR product size was selected to be between 70 and 500 bp. Two of the primers were selected based on the generated results and copied into a word document for manual annotation.

4.2.6. Qualitative determination of the designed GSTpi primers

Primers were received in a lyophilized state and the primer pellet was resuspended with PCR water to generate 100 μ M stock solution, using the information provided on the primers' tubes. Working solution 20 μ M was generated by dilution the stock solution at a 1:5 with 10mM Tris, pH 8.8. The designed primers underwent qualitative analysis on the standard, control and treated samples for different incubation periods. The qualitative analysis was performed using normal PCR: PCR BIO Taq Mix red (PCRBiosystem, UK) kit as per as per the manufacturer recommendation. cDNA with a final concentration of 1 μ g from each sample (DNFB and PA treated) was used. The condition of the PCR reactions were 40 cycles and included: hold at 90 °C for 1 min, denaturation at 95 °C for 15 sec, annealing at 62°C for 15 sec and elongation at 72°C for 30 sec.

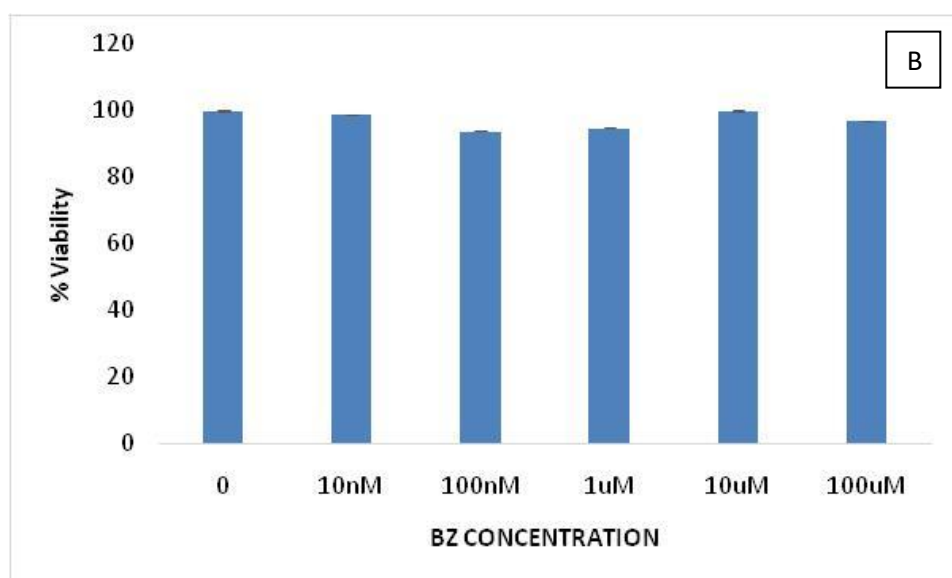
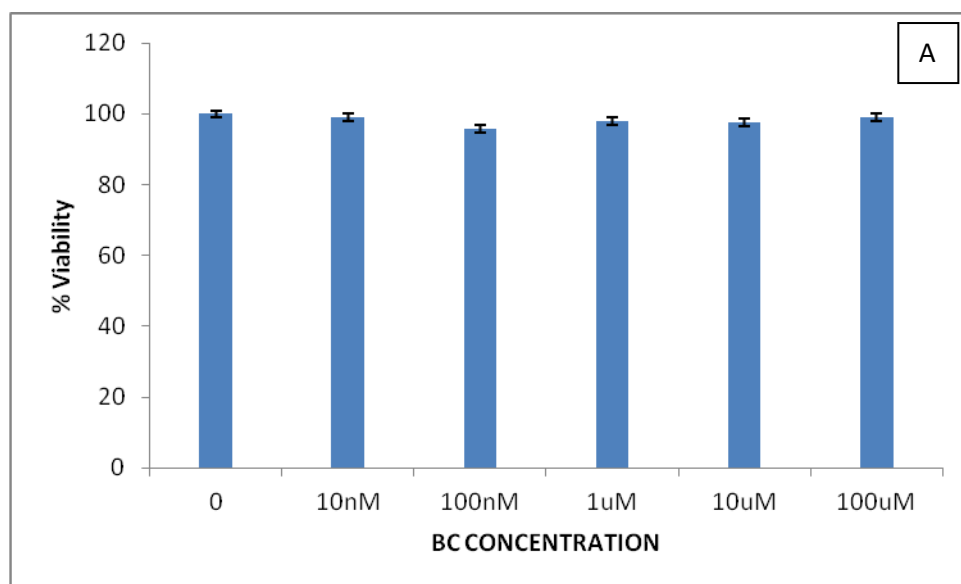
4.2.7. Quantitative polymerase chain reaction (qRT-PCR).

1 μ g of total cDNA was used to perform fluorescence-based Real Time PCR quantification, using 2xqPCR BIO SyGreen Mix Lo-Rox (Pcrbiosystems,UK). The condition of the PCR reactions were 40 cycles including: hold at 90 °C for 2 min, denaturation at 95 °C for 5 sec, annealing at 62°C for 28 sec and elongation at 72°C for 30 sec. The data were normalised using the mRNA expression of the housekeeping gene named GAPDH.

4.3. Results

4.3.1. Cytotoxicity

The highest concentration of the chemicals DNCB, PA, BZ and BC showing no cytotoxicity or 80% cell viability in the HaCaT cells was selected from the MTT assay (Figure 17), 10 μ M for each chemical.



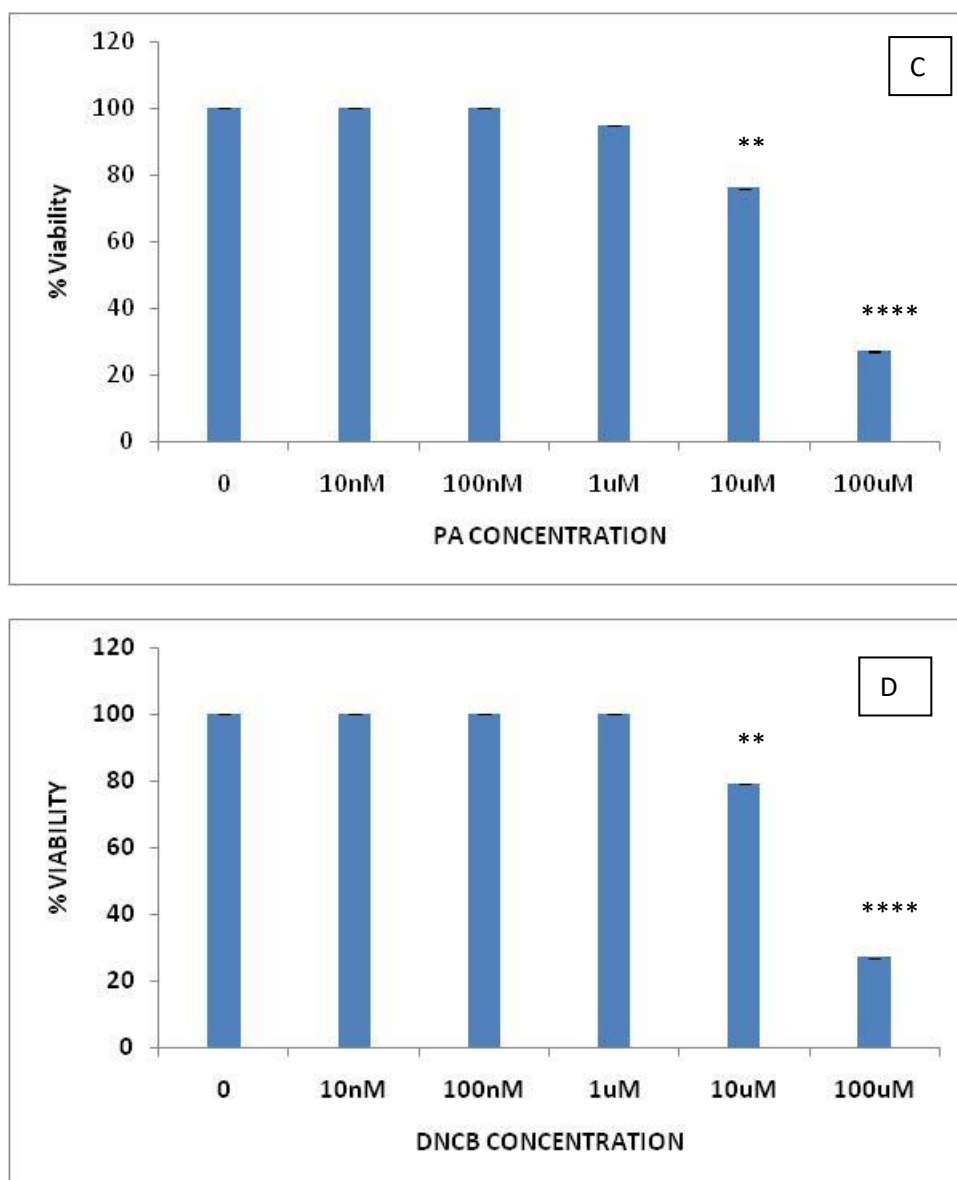


Figure 17. MTT assay: A. Benzalkonium Chloride (BC);B. Benzaldehyde (BZ); C. Phthalic anhydride (PA), control vs. 10uM, $p=0.0025$ and control vs 100uM, $p<0.0001$; D. 2,4-Dinitrochlorobenzene (DNCB), control vs. 10uM, $p=0.0025$ and control vs 100uM, $p<0.0001$. Error bars are mean \pm SD.

4.3.2. Primer design

Two pairs of primers were designed by NCBI software (<http://www.ncbi.nlm.nih.gov>) based on the mRNA nucleotide sequences for each of GST-pi and GAPDH (housekeeping gene) gene as follows:

Table 4. Designed Primers for GST-pi and GAPDH genes

GST-pi (1)	Primer1
Reverse primer	CAACCCTCACTGTTTCCCGT
Forward primer	GGAGACCTCACCTGTACCA

GAPDH (1)	Primer1
Reverse primer	TGCAACCGGGAAGGAAATGA
Forward primer	TTCCCGTTCTCAGCCTTGAC

4.3.3. Qualitative determination of the designed GSTpi primers using control, DNCB and PA treated samples

Agarose gel electrophoresis was used for qualitative analysis of the specificity of the designed GST-pi primers using the standard, control, DNCB and PA treated samples. The expected product corresponds to a size of 460 bp. The images of the agarose gels, visualised using a UV spectrophotometer, have shown the expected product in all the samples (treated with DNCB and PA and control), including the used standard (Figure 18).

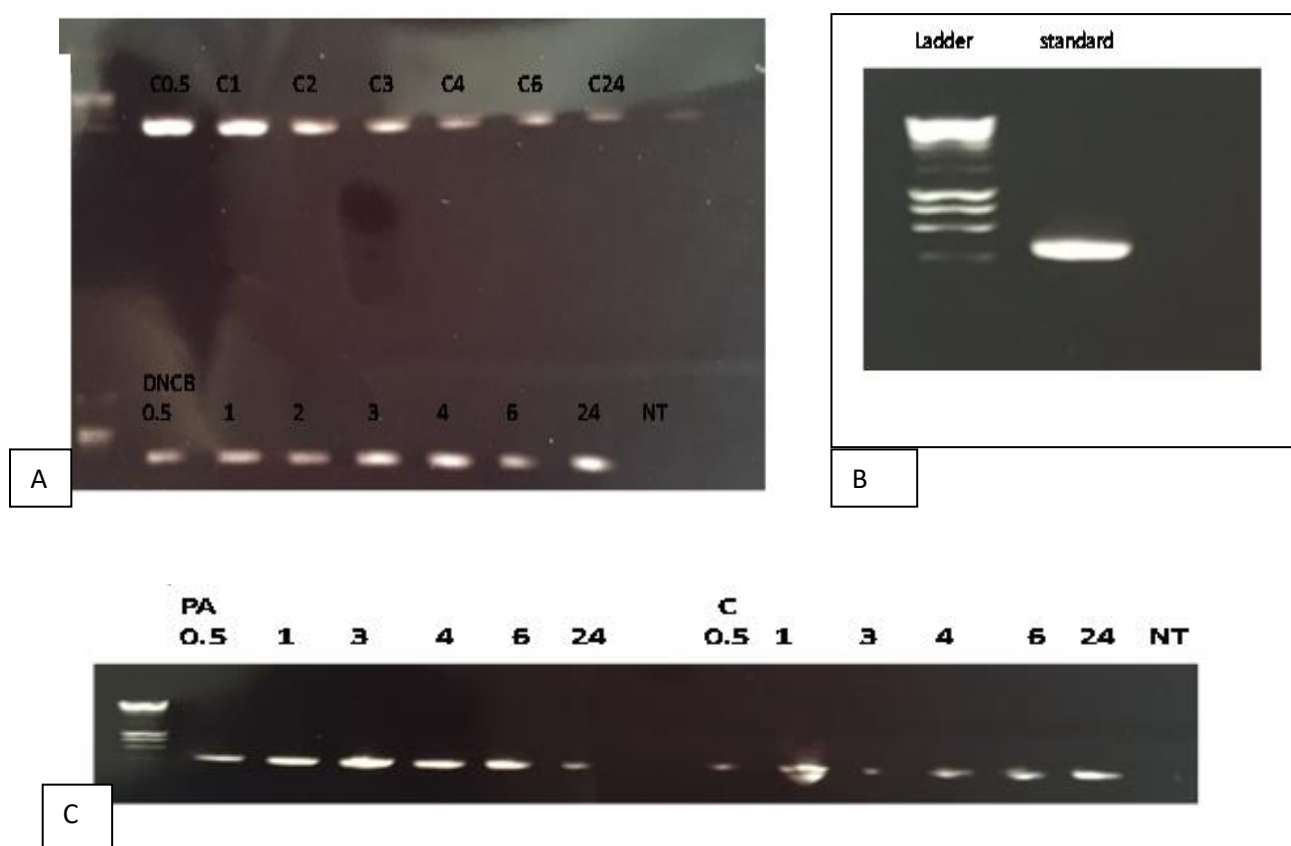


Figure 18. Qualitative analysis of primer specificity using agarose gel electrophoresis of A- HaCaT cells treated with DNCB; B- analysis of primer specificity using agarose gel electrophoresis of standard sample of untreated HaCaT and C- analysis of primer specificity using agarose gel electrophoresis of HaCaT cells treated with PA with different incubation periods; cells incubated for 24h

4.3.4. Class pi (GST Pi) mRNA expression

Although measuring protein expression and activity is a more accurate method to determine gene function, monitoring the mRNA level still can be easier, sensitive enough and convenient to be performed in the laboratory. Keratinocytes, HaCaT cells (CLS cell line

service, Germany) were subjected to DNCB and PA treatment (same dose) for different incubation periods. The expression level of mRNA was recorded using the Real Time PCR (qPCR) technique, generating a standard curve using untreated standard HaCaT cells incubated for 24 h at 37 °C, 5% CO₂ (Figure 19).

The standard curve was obtained by performing qPCR on samples (HaCaT untreated cells for 24 h) with known DNA concentration (30ng/μl stock cDNA). A series of DNA standard dilutions were prepared in the following ratios: 1:5; 1:25; 1:125; 1:625; 1:3125 and no NT -template sample (no DNA sample). The control and chemically treated samples were prepared at a 1:100 ratio and their expression calculated based on the plotted standard curve.

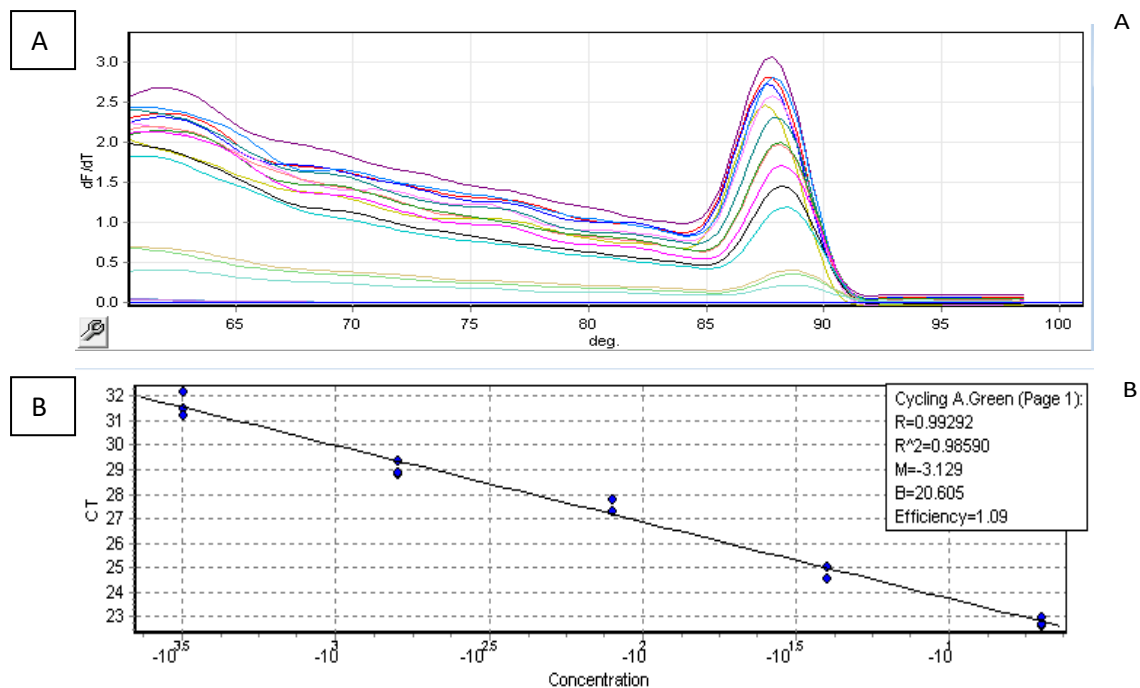


Figure 19. Standard cDNA melting curve, A and standard curve, B performed on untreated HaCaT cells using the designed GSTpi primers.

The analysed expression level of mRNA of treated (DNCB and PA) and untreated (control) cells are represented in figure 20 and figure 21 respectively.

The mRNA level of the DNCB treated cell - dramatically increased during the first 30 minutes of the treatment, reaching approx. 0.125 copies/μg. During the second 30 minutes the level of mRNA started to reduce sharply with more than 50% reaching 0.05 copies/μg.

Interestingly, the decrease in the level of mRNA continued up to 2h of incubation, followed by a gradual increase to 0.05 copies/ μ g during the 3th hour, moving to 0.09 copies/ μ g at the 4 hours of incubation. During the 6th hour of incubation the level of mRNA was indicated to be approx 0.062 copies/ μ g, which is a decreased of 31% from the level recorded at 4 hour incubation. The mRNA level continued to decline and recorded 0.019 copies/ μ g at - 24 hours of incubation (Figure 20).

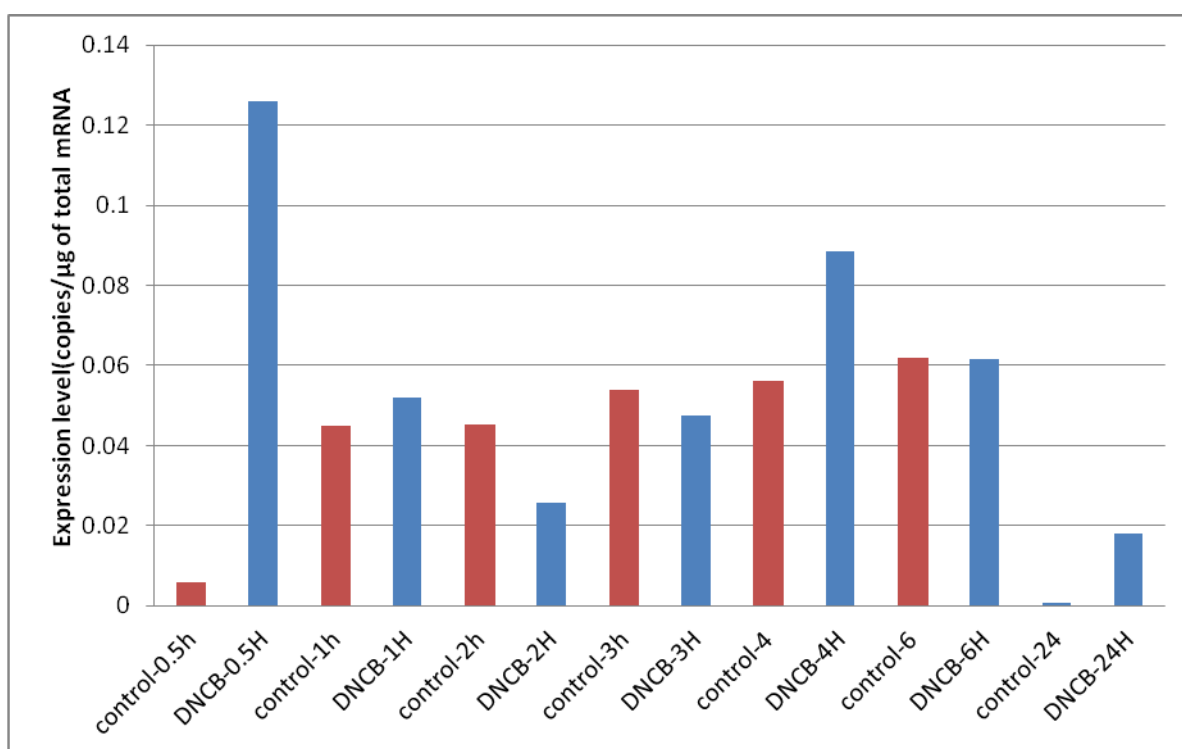


Figure 20. mRNA expression level of Glutathione-S-transferase (Pi), phase II metabolic enzyme (GST-pi) of keratinocytes (HaCaTa cell line) using qRT-PCR treated with DNCB at different incubation time (Raw data Table 7 Appendix) .

The mRNA level of HaCaT cells treated with phthalic anhydride (PA) did not show a sharp change in the mRNA level across the 24-hour incubation. The mRNA level was recorded at around 0.017 copies/ μ g with a higher mRNA level recorded at 24 hours incubation (0.027 copies/ μ g) (Figure 21).

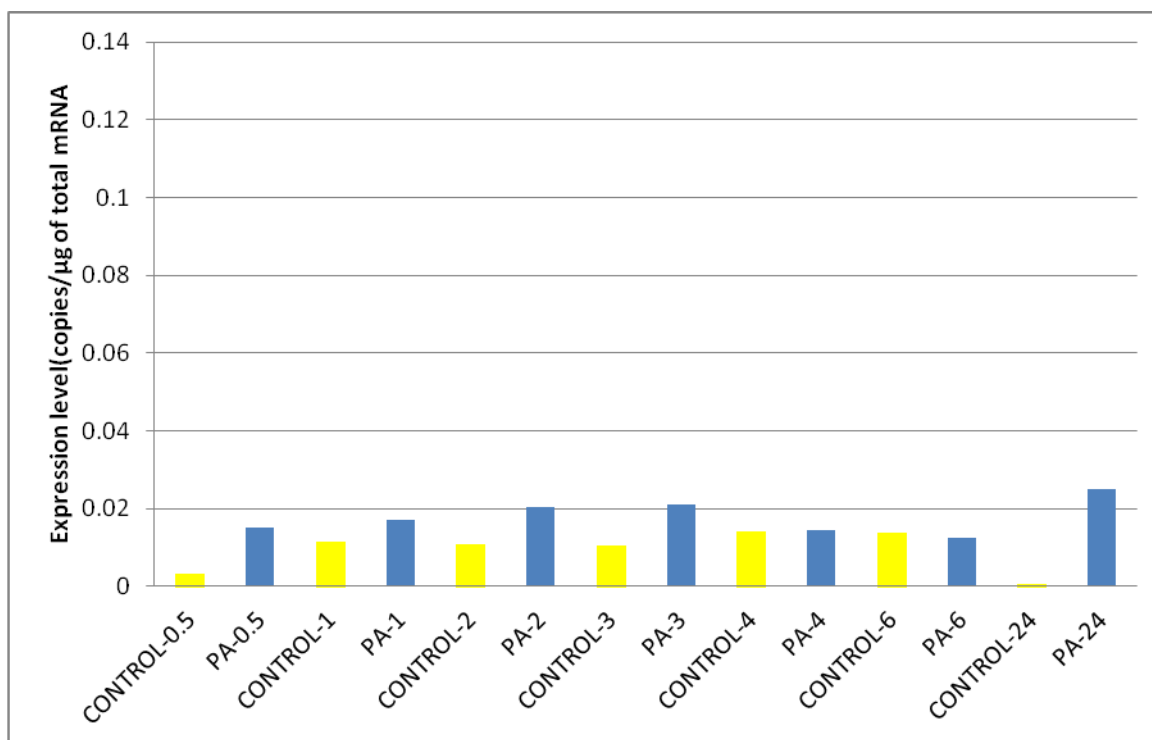


Figure 21. mRNA expression level of Glutathione-S-transferase (Pi), phase II metabolic enzyme (GST-pi) of keratinocytes (HaCaT cell line) using qRT-PCR treated with PA at different time incubation. Raw data Table 8 Appendix.

Untreated HaCaT cells were used as a control for comparing the level of mRNA expression.

4.4. Discussion

4.4.1. *In vitro* examination of induced metabolic enzymes (XME phase II)

Many studies have proved that keratinocytes and/or fibroblasts can be used as a promising tool to examine the immune responses, and molecular signalling together with metabolic conversion of sensitisers. GST phase II enzymes were proved to have the ability to reduce the electrophilic potential of chemicals (Lutz et al., 2001). Modification of signalling proteins involved in the molecular response to different sensitisers has been directly associated with the detoxification process. The Keap1-Nrf2-ARE signalling pathway was found to be the main cellular defence against cellular stress, enhancing the expression of phase II XME.

Research have shown that metabolic enzymes in keratinocytes are involved in preventing tissue damage from oxidative stress. *In vivo* assays have suggested that GST P and Mu metabolic enzymes can be highly expressed in response to contact allergens, in addition to their ability to be detected in HaCaT cells at the genomic and proteomic level (Hewitt et al.,2013). The Study by Jacquoilleot et al., 2015 looked at the expression of glutathione, a prominent antioxidant and cofactor for an important metabolic enzyme Glutathione-S-Transferase, as a response to an exposure to extreme sensitisers such as 1-chloro-2,4-dinitrobenzene (DNCB), 1-fluoro-2,4-dinitrobenzene (DNFB) and 1-bromo-2,4-dinitrobenzene (DNBB). The investigation involved measuring the level of glutathione (GSH) in HaCaT cells and 3D Reconstructed Human Epidermis (RHE), as a result of which DNCB showed the higher potency. DNCB led to depletion of GSH within the first two hours, followed by a gradual increase with the highest level of GSH being recorded at 24h (Jacquoilleot et al. ,2015).

In the current study, the expression of the GST P isoform was determined using the qRT-PCR molecular technique. The mRNA level was measured following incubation of keratinocytes (HaCaT cells) with two different potential chemicals: DNCB (2,4-Dinitrochlorobenzene) and PA (Phthalic anhydride). Both DNCB and PA are well known contact sensitisers. DNCB is known as an extreme sensitiser able to cause skin allergy, where as PA is strong sensitiser where the level of damage depends on the length of contact. The study was carried out using the well-established qRT- PCR technique to monitor the level of GST P mRNA expression as a result of exposure to extreme and strong skin sensitisers (Natsch et al., 2013). HaCaT cells were treated with 10 μ M DNCB and PA where GST Pi mRNA level of expression was monitored at different time intervals.

The current study attempts to build a potential foundation for the use of *in vitro* techniques, in particular qRT-PCR, to monitor the extent of expression of the GST P gene in mRNA in response to treatment with DNCB and PA over different time periods. In addition to their different potencies DNCB and PA have different binding mechanisms: DNCB is known to bind to lysine and cysteine residues, whereas PA binds preferentially to lysine residues. The covalent modification of the Keap-1 protein by different electrophiles has been proved to increase the expression of various XME phase II enzymes, resulting in the induction of ARE-dependent genes responsible for antioxidant regulation including GST (Migdal et al., 2013; Natsch et al., 2013).

During the first 30 min of exposure with DNCB (an extreme sensitiser), GST P has shown a high expression in comparison with the control (uninduced sample). During the first hour of incubation the level of GST P sharply dropped down, reaching its lowest level after 2 hours of incubation, but it remained higher in comparison with the uninduced control sample. The level of GST P expression was higher after each different incubation time period across all the samples treated with DNCB. Clearly DNCB was able to modify the KEAP 1 protein and induce GST P gene expression as a response. The research study by Chia et al., 2010; Wakabayashi et al., 2004 investigated the fact that the modification of only certain residues is required in order to observe Keap-1 modification and dissociation from Nrf2, where the latter translocates to the nucleus. During the third to the fourth hour of incubation the activation of a recovery mechanism was indicated and the expression of the GST P gene started to increase again. The large decrease after the sixth hour of incubation suggests the possibility of the activation of an additional mechanism after prolonged incubation with the extreme chemical DNCB. Chia et al., 2010 studied the NF-kb inflammatory pathway in response to drug treatments. The NF-kb pathway has been proved to control the expression of inflammatory genes, cytokines and to contribute to cell survival. In the presence of a drug,

the NF-kb protein is inhibited, preventing it from binding to the kb regulatory element, interrupting the transcription of anti-apoptotic and antioxidant genes, causing cell death. These lead to cell protection by the Keap1-Nrf2 pathway. The decrease in the level of GST gene expression suggested that, if cell protection by the Keap1-Nrf2 pathway is overwhelmed, cell death may be induced due to the inhibition of NFkb (Figure 11-Supplement data).

Phthalic anhydride is a strong sensitiser, known to bind specifically to lysine residues. PA treated cells showed more constant GST P transcription across the different incubation time periods, but a higher expression in comparison with the untreated samples.

The Keap-1 protein consists of 624 amino acid residues, of which 4% are cysteine and 2.4% are lysine amino acids. In other words, the number of cysteine residues is almost double that of lysine (National Centre For Biotechnology Information). Further experiment focusing on the 3D tertiary structure of the Keap-1 protein is suggested in order to identify possible lysine residues that could be targeted by PA. DNCB appeared to be a more potent Nrf2 activator in compare to with PA. Modification of the Keap-1 protein by DNCB has been investigated by Capple, 2012, but according to my knowledge the same investigation has not been applied to PA.

The present investigation suggested the possibility of using RT-qPCR in order to distinguish between chemicals with different potencies and binding mechanisms. In order to make a final conclusion and confirm the above results, additional experiments need to be carried out, and the effect of DNCB and PA on Nrf2 and NFkb should be investigated further using keratinocytes (HaCaT cells). Secondly, studying the 3D tertiary structure of Keap-1 can be carried out, possibly leading to an understanding of how it is modified by PA. On the another hand an assessment should be carried out of the effect on the expression of the GST P gene of additional chemicals with known potencies and binding mechanisms.

Chapter 5

Final Discussion and Future Studies

5.1. Characterisation of the human skin proteome

The data obtained from protein profiling of human skin showed that proteins from both fractions (S9 and non-S9) are involved in various toxicological pathways such as inflammation, IL-1/4/6 signalling, KEAP 1-NRF2, oxidative stress, EGFR1 signalling, MAPK signalling, prostaglandin synthesis and regulation. In my investigation I have used the information obtained from the skin proteome to identify the proteins involved in toxicological pathways using the available up-to-date publications. These proteins can be used as model proteins for further investigation by tracking their expression on gene and protein level as a result of treatments with chemicals of different categories. *In vitro* techniques such as DNA microarray; qPCR; SDS-Page and Western Blotting can be used to identify and record any changes in the expression of selected genes and/or proteins between treated and untreated samples. As a future plan the same quantified and analysed skin samples can be treated with chemicals with different potency (time and dose dependent) and GelC-MS/MS analysis can be used to track any shift of the MS spectrum between treated and untreated samples. The analysis may provide valuable insights into the levels of nucleophilic residues of a key proteins; these residues are potential targets for electrophilic chemicals or metabolites, the product(s) of which lead(s) to skin sensitisation. I could not think of taking this approach as it requires continuous access to MS apparatus and its accompanying MS data analyser to study the obtained results. Unfortunately the University of Bedfordshire does not have these facilities available.

On the another hand the research can be further extended and the experiment repeated by the identification, quantification and analysis of the skin proteome from a larger number of skin donors. In this way a better picture can be obtained and further confirmation of the human skin proteome composition will become available. Protein Discoverer is a peptide characterisation software provided by Thermo Scientific, which is able to identify and study

protein molecules in depth using mass spectrometry data. Information can be obtained at the protein and peptide level, providing protein characterisation, relative quantification and fast analysis of complex protein mixtures including any post translational modification (PTM). Protein Discoverer can be used for the analysis of the identified proteins, providing meaningful information about gene ontology (GO) classification and literature references. In this way, a larger amount of data can be analysed at the same time using MS raw data (Mass Informatics Platform for Protein Scientists, 2017).

These findings may lead to deeper studies of these proteins and target them *in vitro* as specific “sensors-markers” at a specific toxicological endpoint.

5.2. *In chemico* approach by Top-down mass spectrometry

New results have shown more sites on APG able to bind DNCB under physiological condition (32 °C). An additional experiment has been performed, where 25 chemicals (with various sensitising potencies and binding mechanisms (which bind preferentially either to cysteine or lysine or to both) were incubated with APG under physiological conditions, in order to identify the chemicals that would bind to APG, and possibly to identify their binding locations on the protein. In this way we can obtain a wider picture of the potential to use this analytical technique to predict the sensitising potency of chemicals.

In order to develop reactivity assay it is very important to consider whether the studied chemical will be used as pure (on its own) or with a combination with other chemicals that can be present in a trace or higher quantities. In order to screen a chemical in samples of multi-component products, the reactivity assay has to be developed with the excess of the sample. In this case if the chemical of interest is not very reactive a significant nucleophilic depletion will still be observed. However if the chemical is used as a pure substance within a

sample, an excess of the nucleophile has to be used. In this case any minor impurity in the sample will not interfere with the final results (David and Basketter, 2009).

Further experiments can be performed on APG incubated with those chemicals (showing positive results in the above experiment) over time or dose course under physiological conditions, to quantitatively elucidate haptenisation pathways under different starting conditions

A different model protein, such as albumin or keratin, could be selected for additional study.

These studies would provide more understanding of the mechanism of protein-hapten formation and any specific bindings between sensitisers and proteins, to achieve better quantification to predict skin sensitisation.

The study of the binding mechanisms of biological molecules of known structure to chemicals of different potencies is one of the main stages of identifying a potential drug as a therapeutic agent. Computational (biological) methods underline the ability of developing visual computer models that explain how the compounds bind to the target molecules (proteins). Molecular docking can be used to suggest the conformation of the compound and give information on its 3D orientation and all the possible binding sites. If the structure of the target molecule is known, then a series of virtual chemicals can be screened in order to identify those that can provide a good shape for binding (Ruiz Carmona et al., 2014). With knowledge of the 3D appearance of a target protein and its possible binding sites, virtual screening can be used to test a series of candidate compounds that are expected to bind to the target molecule. The data can be further validated by other experimental methods ([Biesiada et al., 2011](#); Yin and Loo, 2010). Computational biology as a part of the *in silico* approaches for testing skin sensitisers will facilitate future determination of protein-hapten interaction. Since the structure of the protein-hapten complex is of great importance in toxicology, virtual

screening can help not only to identify the binding site, but also to study the mechanism of interaction between proteins and haptens, which can be used to categorise different chemicals based on their potency .

5.3. *In vitro* examination of induced metabolic enzymes

Research in this area has shown that metabolic enzymes in keratinocytes are involved in bio-activation, and conversely deactivation of contact allergens. *In vivo* assays have suggested that GST metabolic enzymes can play a major role in generating immune-reactive intermediates, in parallel with direct detoxification of immunogenic substances (Jacquilleot et. al., 2015).

Future research can focus on examining the induced expression of other metabolic enzymes (phase II and even phase I) at mRNA level by chemicals with different binding mechanisms and sensitising potency. The RT-qPCR technique, SDS-PAGE, Immunoblotting assays and LC-MS/MS can be utilised to quantify mRNA and protein levels between control and chemical treated cells over a dose and/or time course.

Chemicals and different substances compose the basis of various personal care and cosmetic products. The addition of these chemicals and substances are usually to enhance the quality of the products and preserve them for longer period of time. Assessing the potential hazard of any chemical used by consumers is a crucial step before releasing these products to the market. It is important to remember that the sustainability of different individuals towards the chemicals used in cosmetic and personal care products is different usually affected by different factors. These factors are based on how the products are used, consumers' age, skin condition and even genetic factors.

With the implementation of the 7th amendment of the EU Cosmetic Directive in 2013, different approaches have been studied in order to reduce, refine, replace (3R's) the

current *in vivo* approaches for assessing chemical potencies. The obtained results from this and other experiments proved that the allergic contact dermatitis is a complex skin disorder that involves many different cells, toxicological pathways, genes and proteins. In order to understand all the skin biology and the mechanism of allergy in response to chemicals, an integrated *in vitro*, *in chemico* and *in silico* techniques have to be brought together for a possible more accurate characterisation of chemical potency.

6. REFERENCES

About the OECD - OECD (2017). *Oecd.org*.(accessed on 7th July 2017) <http://www.oecd.org/about/>

Aeby, P., Ashikaga, T., Diembeck, W., Eschrich, D. and Gerberick, F. (2007), The COLIPA strategy for the development of *in vitro* alternatives: Skin sensitisation. *Proc. 6th World Congress on Alternatives & Animal Use in the Life Sciences*, 375-379.

Aleksic, M., Pease, K. C., Basketter, A. D. and Panico, M. (2007), Investigating protein haptenation mechanisms of skin sensitisers using human serum albumin as a model protein, *Toxicology in Vitro* **21**, 723-733.

Aleksic, M., Pease, C., Basketter, D. A., Panico, M., Morris, H. R. and Dell, A. (2008), Mass spectrometric identification of covalent adducts of the skin allergen 2,4-dinitro-1-chlorobenzene and model skin proteins, *Toxicology in Vitro* **22**, 1169-1176.

Anderson, S. E., Siegel, P. D. and B.J. Meade, B. (2011). The LLNA: A brief review of recent advances and limitations. *J Allergy (Cairo)* doi: **10.1155/2011/424203**,.

Assuring Safety without Animal Testing: Skin Allergy Case Study - Overview *Assuring Safety without Animal Testing: Skin Allergy Case Study - Overview*.

Asturiol, D. and Worth, A. (2011): The use of chemical reactivity assays in toxicity prediction. *JCR scientific and technical report*, doi 10.2788/32962

Ban on Animal Testing - Growth - European Commission (2017). *Growth*. accessed on 24th September 2017

Basova, L. V., Tiktopulo, E. I., Kashparov, I. A. and Bychkova, V. E. (2004). The Conformational State of Apomyoglobin in the Presence of Phospholipid Vesicles at Neutral pH. *Molecular Biology*, **38**, 272–280.

Basketter, D. A., Evans, P., R.J.Fielder, R. J., Gerberick, G. F., Dearman, R. J. and Kimbere, I. (2002). Local lymph node assay — validation, conduct and use in practice. *Food Chem Toxicol*, **40**, 593-598.

Basketter, A. D. (2012), Non-animal approaches in skin toxicology, *Arch Toxicol* **86**, 1159-1160.

Bensouilah, J. and Buck, P. (2006), *Skin Structure and Function*, pp. 4-11. UK: Radcliffe Publishing

Biesiada J, Porollo A, Velayutham P, Kouril M, Meller J. (2011) Survey of public domain software for docking simulations and virtual screening. *Human genomics*, **5** (5), 497-505

Blacker, K. L., Olson, E., Vessey, D. A. and Boyer, T. D. (1991). Characterization of Glutathione S-Transferase in Cultured Human Keratinocytes. *Journal of Investigative Dermatology*, **97**, 442–446.

Bonifas, J., Hennen, J., Dierolf, D., Kalmes, M., Blomeke, B. (2010), Evaluation of cytochrom P450 (CYP1) and N-acetyltransferase 1 (NAT1) activities in HaCaT cells : implications of development of *in vitro* techniques for predictive testing of contact sensitizers, *Toxicology in vitro* **24**, 973-980

Brohem, C. A., Cardeal, L. B. D. S., Tiago, M., Soengas, M. S., Barros, S. B. D. M. and Maria-Engler, S. S. (2010). Artificial skin in perspective: concepts and applications. *Pigment Cell & Melanoma Research*, **24**, 35–50.

Busheri, K., Marcoux Y., Tredget E., Li L., Zheng J., Ghoreishi M., Weinfeld M., Ghahary A. (2002), Expression of a releasable form of annexin II by human keratinocytes. *J. Cell Biochem*, **86(4)**:737-47

Casati, S., Worth, A., Amcoff, P., Whelan, M., (2013), EURL ECVAM Strategy for Replacement of Animal Testing for Skin Sensitisation Hazard Identification and Classification, *Joint Research Centre of the European Commission*

Chapin, R. E., Boekelheide, K., Cortvrindt, R., Duursen, M. B. V., Gant, T., Jegou, B., Marczylo, E., Pelt, A. M. V., Post, J. N., Roelofs, M. J., (2013). Assuring safety without animal testing: The case for the human testis in vitro. *Reproductive Toxicology*, **39**, 63–68.

Chia, A. J., Goldring, C. E., Kitteringham, N. R., Wong, S. Q., Morgan, P. and Park, B. K. (2010). Differential effect of covalent protein modification and glutathione depletion on the transcriptional response of Nrf2 and NF- κ B. *Biochemical Pharmacology*. **80**, 410–421.

Chipinda, I., Hettick, J. M. and Siegel, D. P. (2011), Haptenisation: Chemical reactivity and protein binding *Journal of Allergy*, doi:10.1155/2011/839682.

Collet JF, Messens J. (2010), Structure, function, and mechanism of thioredoxin proteins, *Antioxid Redox Signal*. **13(8)**:1205-16

Compton, D. P. and Kelleher, L. N. (2012), Spinning up mass spectrometry for whole protein complexes, *Nature method*, **9(11)**, 1065-1066.

Copple, I. M. (2012). The Keap1–Nrf2 Cell Defense Pathway – A Promising Therapeutic Target? *Adv. Pharmacol*, **63**, 43–79.

Corsini, E., Roggen, L. L. E., Galbiati, V., Gibbs, S. (2016) Alternative Approach for Potency Assessment: In Vitro Methods. *Cosmetics* **3(7)**, doi:10.3390

Cronin, M. T., Bajot, F., Enoch, S. J., Madden, J. C., Roberts, D. W. and Schwöbel, J. (2009). The *in Chemico–In silico*Interface: Challenges for integrating experimental and computational chemistry to identify toxicity *ATLA*, **37**, 513-521.

Denecker, G., Ovaere, P., Vandenabeele, P. Declercq, W., (2009) Caspase-14 reveals its secrets. *Department of molecular biology research*, **180(3)**, 451-458

Dietz L, Esser PR, Schmucker SS, Goette I, Richter A, Schnolzer M, Martin SF and Thierse HJ (2010), Tracking human contact allergens: from mass spectrometric identification of peptide-bound reactive small chemicals to chemical-specific native human T cell priming. *Toxicological Sciences* **117** (2):336-347.

Esser, C., Gotz, C., (2013), Filling the gaps: need for research on cell specific xenobiotic metabolism in the skin, *Arc.Toxicol*, 10.1007/s00204-013-1031-7

Eilstein J, Léreaux G, Budimir N, Hussler G, Wilkinson S, Duché D (2014). Comparison of xenobiotic metabolizing enzyme activities in ex vivo human skin and reconstructed human skin models from SkinEthic, *Arch toxicol*, **88(9)**, 1681-1694.

Fouquier, J. and Guedj, M. (2015). Analysis of drug combinations: current methodological landscape. *Pharmacology Research & Perspectives*.**3(3)** doi: 10.1002/prp2.149

From data set to meaningful biology (2017). TMT UK: *Protein Center, Thermo scientific*

Janeway, C. A. (2003). *Immunobiologie: le système immunitaire fondamental et pathologique*. 5th ed. Paris: De Boeck.

Jacquilleot, S., Sheffield, D., Olayanju, A., Sison-Young, R., Kitteringham, N. R., Naisbitt, D. J. and Aleksic, M. (2015). Glutathione metabolism in the HaCaT cell line as a model for the detoxification of the model sensitizers 2,4-dinitrohalobenzenes in human skin. *Toxicology Letters*, **237**, 11–20.

Jong, W. H. D., Arts, J. H., Klerk, A. D., Schijf, M. A., Ezendam, J., Kuper, C. F. and Loveren, H. V. (2009). Contact and respiratory sensitizers can be identified by cytokine profiles following inhalation exposure. *Toxicology*, **261**, 103–111.

Haniffa, M., Gunawan, M., Jardine, L. (2015). Human skin dendritic cells in health and disease. *Journal of Dermatological Science*, **77**, 85-92

Hewitt N., Edward, R., Fritche,E., Gobel, C., Aeby B., Scheel, J., Reisinger, K., Ouidraogo, G., Duche, D., Eilstein, J., Latel, A., Kinny, J., Moore, C., Kuehln, J., Barroso, J., Fautz, R., Pfuhler, S.,(2013), Use of human *in vitro* skin models for accurate and ethical risk assessment: metabolic consideration, *Toxicological science*, **133(2)**, 209-217

Ioannides, C. (2002). Xenobiotic Metabolism: An Overview. *Enzyme Systems that Metabolise Drugs and Other Xenobiotics* 1–32.

Gerberick, F. G., Vassallo, D. J., Foertsch, L. M., Price, B. B. and Chaney, G. J. (2007), Quantification of chemical peptide reactivity for screening contact allergens: A classification tree model approach, *Toxicological Science*, **97**(2), 417-427.

Gerberick, G. F., Troutman, J. A., Foertsch, L. M., Vassallo, J. D., Quijano, M., Dobson, R. L. M., Goebel, C. and Lepoittevin, J.-P. (2009). Investigation of Peptide Reactivity of Pro-hapten Skin Sensitizers Using a Peroxidase-Peroxide Oxidation System. *Toxicological Sciences*, **112**, 164–174.

Goebel, C., Aeby, P., Ade, N., Alépée, N., Aptula, A., Araki, D., Dufour, E., Gilmour, N. Hibatalla, J., Keller, D., Kern, P., Kirst, A., Marrec-Fairley, M., Maxwell, G., Rowland, J., Safford, B., Schellauf, F., Schepky, A., Seaman, C., Teichert, T.

Gotz, C., Pfeiffer, R., Tigges, J., Blatz, V., Jackh, C., Freytag, E., Fabien, E., Landsiedel, R., Merk, H., Krutmann, J., Edwards, R., Pease, C., Joebel, C., Hewitt, N., Fritsche, E. (2012a), Xenobiotic metabolism capacity of human skin in comparison with a 3D epidermis model and keratinocytes- based cell culture as in vitro alternative for chemical testing: activating enzymes (Phase I). *Experimental Dermatology*, **21**, 358-363

Gotz, C., Pfeiffer, R., Tigges, J., Ruwiedel, K., Hubbenthal, U., Merk, H., Krutmann, J., Edwards, R., Abel, G., Pease, C., Joebel, C., Hewitt, N., Fritsche, E. (2012b). Xenobiotic metabolism capacity of human skin in comparison with a 3D epidermis model and keratinocytes- based cell culture as in vitro alternative for chemical testing: phase II enzymes. *Experimental Dermatology*, **21**, 364-369

Hewitt, N. J., Edwards, R. J., Fritsche, E., Goebel, C., et al., (2013), Use of human in vitro skin models for accurate and ethical risk assessment: metabolic considerations. *Toxicological Science*, **133**(2): 209-217.

Hulleste, B. C., Gerberick, G. F. and Ryan, C. A. (2002), Elucidating changes in surface markers expression of dendritic cells following chemical allergen treatment. *Toxicol. Appl. Pharmacol.*, **182**, 226-233.

Jayaprakash P, Dong H, Zou M, Bhatia A, O'Brien K, Chen M, Woodley DT, Li W. (2015) Hsp90 α and Hsp90 β Co-Operate a Stress-Response Mechanism to Cope With Hypoxia and Nutrient Paucity during Wound Healing, *J Cell Sci.*

Jeonge, Y., An, S., Shin, K. and Lee, T. (2013). Peptide reactivity assay using spectrophotometric method for high-throughput screening of skin sensitisation potential of chemical hapten. *Toxicology in Vitro* **27**, 264-271.

Kelleher NL (2004), Top-down proteomics. *Analytical Chemistry*: 197A-203A.

Kellie, J. K., Tran, J. C., Lee, J., Ahlf, D. R., Thomas, H. M., Ntai, I., Catherman, A. C., Durbin, K. R., Zamdborg, L., Vellaichamy, A. et al. (2010). The emerging process of top down mass spectrometry for protein analysis: Biomarkers, protein-therapeutics, and achieving high throughput *Mol. Biosyst* **6**(9), 1532-1539.

Kimura, J., Hayakari, M., Kumano, T., Nakano, H., Satoh, K. and Tsuchida, S. (1998). Altered glutathione transferase levels in rat skin inflamed due to contact hypersensitivity: Induction of the alpha-class subunit **1**. *Biochem J.* **335**(3), 605-610.

Lodygin, D., Yazdi, A., Sander, C., Herzinger, T., Hermeking, H., (2003). Analysis of 14-3-3 σ expression in hyperproliferative skin diseases reveals selective loss associated with CpG-methylation in basal cell carcinoma. *Oncogene*, **22**,5519-5524

Lutz, W., Tarkowski, M., Nowakowska, E. (2001). Genetic polymorphism of glutathione s-transferase as a factor predisposing to allergic dermatitis. *Med.Pro*, **52**, 45–51

Luu-The, V., Duche, D., Ferraris, C., Meunier, J. R., Leclaire, J. and Labrie, F. (2009). Expression profiles of phases 1 and 2 metabolizing enzymes in human skin and the reconstructed skin models episkin and full thickness model from episkin.. *J Steroid Biochem Mol Biol* **116**(3-5), 178-186.

Maheshwari, S. (2013). The cosmetic market current and future outlook. *Business consultancy service, RNCOS*

Mass Informatics Platform for Protein Scientists (2017). TMT UK: *Protein Discoverer, Thermo scientific.*

Maxwell, G. and MacKay, C. (2011). *Skin sensitisation. Modelling the human adverse response.* Bedford, MK: Unilever.

Migdal, C., Botton, J., Ali, Z. E., Azoury, M.-E., Guldemann, J., Gimenez-Arnau, E., Lepoittevin, J.-P., Kerdine-Romer, S. and Pallardy, M. (2013). Reactivity of Chemical Sensitizers Toward Amino Acids In Cellulo Plays a Role in the Activation of the Nrf2-ARE Pathway in Human Monocyte Dendritic Cells and the THP-1 Cell Line. *Toxicological Sciences*, **133**, 259–274.

Millington P.F. and Wilkinson R. (2009) *Skin*. New York: Cambridge University press

Misra, R. V. and Gaulton, T. (2015). Tandem Mass Spectrometry Analysis as an Approach to Delineate Genetically Related Taxa, with Specific Implication for Differentiating *Escherichia coli* from amongst the Complex Enterobacteriaceae Family. *Journal of Proteomics & Enzymology*, **4**.

Montagna, W. (1974). *The Structure and Function of Skin*. 3rd ed. New York: Academic press.

National Center For Biotechnology Information. *Ncbi.nlm.nih.gov*. N.p., 2016. Web. 01 Oct. 2016.

Natsch A (2010), The Nrf2-Keap1-ARE toxicity pathway as a cellular sensor for skin sensitizers—functional relevance and a hypothesis on innate reactions to skin sensitizers, *Toxicological Sciences*, **113** (2): 284-292.

Natsch, A., Ryan, C. A., Foertsch, L., Emter, R., Jaworska, J., Gerberick, F. and Kern, P. (2013). A dataset on 145 chemicals tested in alternative assays for skin sensitization undergoing prevalidation. *Journal of Applied Toxicology*, **33**, 1337-1352

Parkinson, E., Skipp, P., Aleksic, M., Garrow, A., Dadd, T., Hughes, M., Clough, G. and O'connor, C. D. (2014). Proteomic Analysis of the Human Skin Proteome after In Vivo Treatment with Sodium Dodecyl Sulphate. *PLoS ONE* **9**.

Pease, C., Thain, E. and Zazzeroni, R. (2010), Reactivity assays – dealing with substances and samples in anworld – the solution and the real problem *in vitro*. *Contact Dermatitis*, **62**, 256-257

Piersma, S.R., Warmoes, M.O., de Wit, M., de Reus,I., Knol, J.C., Jiménez, C.R. (2013). Whole gel processing procedure for GeLC-MS/MS based proteomics. *Proteome Science*,**11**:17

Pigors M, Schwieger-Briel A, Cosgarea R, Diaconeasa A, Bruckner-Tuderman L, Fleck T, Has C.(2014),Desmoplakin mutations with PalmoplantarKeratoderma, Woolly Hair and Cardiomyopathy,*Acta.Derm.Venereol*, **95**(2), 337-340

Ramadoss, P., Marcus, G., Perdew, G., (2005), Role of the aryl hydrocarbon receptor in drug metabolism. *Expert Opin.DrugMetab.Toxicol.*, **1**(1), 1-13

REACH - Growth - European Commission (2017). *Growth*, (accessed on 15th September 2017), https://ec.europa.eu/growth/sectors/chemicals/reach_bg

Roberts, D. W. and Basketter, D. A. (2009), Reactivity assays, substances, samples and alternatives: Why should we care? *Contact Dermatitis*, **61**, 310-311.

Rose, J. R., Damoc, E., Denisov, E., Makarov, A., Albert, J. R. and Heck, A. J. R. (2012), High-sensitivity Orbitrap mass analysis of intact macromolecular assemblies, *Nature method*, **9**(11), 1084-1088.

Ryan, A.C., Kimber, I., Basketter, D.A., Pallardy, M., Gildea, L.A., Frank Gerberick, G., (2007). Dendritic cells and skin sensitization: Biological roles and uses in hazard identification, *Toxicology and applied pharmacology*, **221**, 384-394

Ru, Q. C., Zhu. L.A., Siberman, J., Shriver, C.D. (2006). Label-free Semiquantitative Peptide Feature Profiling of Human Breast Cancer and Breast Disease Sera via Two-dimensional Liquid Chromatography-Mass Spectrometry. *Molecular & Cellular Proteomics*, **5**, 1095–1104.

Saint-Mezard,P., Rosieres, A., Krasteva,M Berard,V Budois,B., Kaiserlian, D., Nicolas, J., (2004)), Allergic contact dermatitis, *Eur J Dermatol*, **14**, 284-95

(SCHER) Scientific Committee on Health and Environmental Risks (2011). Toxicity and Assessment of Chemical Mixtures. *European commission*.

Schnuch A, Geier J, Lessmann H, Uter W, Arnold R, Mackiewicz, M (2004): Untersuchungen zur Verbreitung umweltbedingter Kontaktallergien mit Schwerpunkt im privaten Bereich, Forschungsbericht 29961219, Umweltbundesamt, Berlin

Schouest, J. M., Luu, T. K. and Moy, R. L. (2010). Improved texture and appearance of human facial skin after daily topical application of barley produced, synthetic, human-like epidermal growth factor (EGF) serum. *J Drugs Dermatol*. **11(5)**, 613-620.

Sergio Ruiz-Carmona, Daniel Alvarez-Garcia, Nicolas Foloppe, A. Beatriz Garmendia-Doval, Szilveszter Juhos, Peter Schmidtke, Xavier Barril , Roderick E. Hubbard ,S. David Morley (2014) rDock: A Fast, Versatile and Open Source Program for Docking Ligands to Proteins and Nucleic Acids. *PLOS Computational Biology*

Siemionow, M. and Einsenmann-Klein, M. (2016). *PLASTIC AND RECONSTRUCTIVE SURGERY*. Springer London LTD.

Stacey E. Anderson, ES., Siegel, D.P., Meade, J.B., (2011), The LLNA: A Brief Review of Recent Advances and Limitations. *Journal of Allergy*, doi:10.1155/2011/424203

Taverna, D., Nanney, B., Pollins, A. C., Sindona, G. and Caprioli, R. (2011), Spatial mapping by imaging mass spectrometry offers advancements for rapid definition of human skin proteomic signatures*PubMed*, **20(8)**, 642-647

Tessier, N., Teissier, S. Weltzien, H.U., Winkler, P., Scheel, J. (2012). Guiding principles for the implementation of non-animal safety assessment approaches for cosmetics: Skin sensitisation, *Regulatory toxicology and pharmacology*, **63**, 40-52

The Adverse Outcome Pathway for Skin Sensitisation Initiated by Covalent Binding to Proteins (2014). *OECD Series on Testing and Assessment*. doi: 10.1787/9789264221444-en

Thyssen, J. P., Giménez-Arnau, E., Lepoittevin, J.-P., Menné, T., Boman, A. and Schnuch, A. (2012). The critical review of methodologies and approaches to assess the inherent skin sensitization potential (skin allergies) of chemicals Part III. *Contact Dermatitis*, **66**, 53–70.

Tigges, J., Weighardt, H., Wolff, S., Gotz,C.,Forsets,I., Kohne,Z., Huebenthal, U., Merk,H., Abel,J., Haarmann-Stemmann,T., Krutmann,J., Fritsche,E., (2013). Aryl Hydrocarbon receptor repressor (AhRR) function revisited: repression of CYP1 activity in human skin fibroblasts is not related to AhRR expression. *The society of investigative dermatology*, 87-95

Troutman, A. J., Foertsch, M. L., Kern, S. P., Jian Dai, H., Quijano, M., Dobson, R. L. M., Lalko, J. F., Lepoittevin, J. and Gerberick, G. F. (2011). The incorporation of lysine into the peroxidase peptide reactivity assay for skin sensitization assessments *Toxicological Science*, **122**(2), 422-436

Tortora GJ. and Grabowski SR. (1993) *Principles of Anatomy and Physiology*. HarperCollins College Publishers.

Tončić, R.J., Lipozenčić, J., Martinac, I., Gregurić, S. (2011). Immunology of Allergic Contact Dermatitis, *Acta Dermatovenereol Croat*, **19**(1), 51-68

Vandebriel, R.J. and van Loveren, H. (2010), Non-animal sensitization testing: State-of-the-art. *Critical Review in Toxicology*, **40**(5), 389-404.

Van der Veen, J. P.T., van Loveren, H. and Ezendam, J. (2012), Applicability of keratinocytes gene signature to predict skin sensitising potential, *Toxicology in Vitro*, **27**(1), 314-322

van Eijl, S., Zhu Z., Cupitt, J., Gierula, M., Götz, C., Fritsche, E., Edwards, E (2012), Elucidation of Xenobiotic Metabolism Pathways in Human Skin and Human Skin Models by Proteomic Profiling. *PloS One*, **7**(7), 1-13

Wakabayashi, N., Dinkova-Kostova, A. T., Holtzclaw, W. D., Kang, M.-I., Kobayashi, A., Yamamoto, M., Kensler, T. W. and Talalay, P. (2004). Protection against electrophile and oxidant stress by induction of the phase 2 response: Fate of cysteines of the Keap1 sensor modified by inducers. *Proceedings of the National Academy of Sciences*, **101**, 2040–2045.

Yin S, Loo JA. (2010) Elucidating the site of protein-ATP binding by top-down mass spectrometry. *J Am Soc Mass Spectrom*, **21**(6), 899-907

Zaidi, Z. and Lanigan, S. W. (2010). *Dermatology in clinical practice*. Dordrecht: Springer.

Zhu, Z, Boobis, A.R. and Edwards, R. J. (2008a), Identification of estrogen-responsive proteins in MCF-7 human breast cancer cells using label-free quantitative proteomics, *Proteomics*, **8**:1987-2005

Zhu Z, Edwards, R. J. and Boobis, A. R. (2008b), Proteomic analysis of human breast cell lines using SELDI-TOF-MS shows that mixtures of estrogenic compounds exhibit simple similar action (concentration additivity). *Toxicology Letters*, **181**:93-103

Zuang, V., Schäffer, M., Tuomainen, A.M., Amcoff, P., Bernasconi, C., Bremer, S., Casati, S., Castello, P., Coecke, P., Corvi, R., Griesinger, C., Roi, A.J., Kirmizidis, G., Prieto, P., Worth, A., Munn, S., Berggren, E., Whelan, M. (2010-2013), EURL ECVAM progress report on the development, validation and regulatory acceptance of alternative methods. *Joint Research Centre of the European –Commission*

7. List of Abbreviations

ACD Allergic Contact Dermatitis

ACN Acetonitrile

AOP Adverse outcome pathways

APG Apomyoglobin

BC Benzalkonium chloride

BCA assay

BZ Benzaldehyde

CB Chlorobenzene

CD4⁺ Cluster of differentiation 4

CD83 Cluster of differentiation 83

CD86 Cluster of differentiation 86

CID Collision-induced dissociation

CM Coumarin

CMIR Cell mediated immune reaction

COLIPA European Cosmetic, Toiletry and Perfumery Association

DC Dendritic cells

DC Dihydrocoumarin

DM 2-Mercaptobenzothiazole

DMEM Dulbecco's Modified Eagle's Medium

DMSO Dimethyl sulfoxide

DNBC 2,4-dichloronitrobenzene

DNCB 2,4-Dinitrochlorobenzen

DP Dibenzoyl peroxide

DPRA Direct peptide reactivity assay

EA Ethyl acrylate

EDTA Ethylenediaminetetraacetic acid

EG Eugenol

EURL ECVEM European Union Reference Laboratory for alternatives to animal testing

FA Formaldehyde

GAPDH Glyceraldehyde 3-phosphate dehydrogenase (Housekeeping gene)

GST- Glutathione -S-transferase

GST P Glutathione -S-transferase pi isoform

GST M Glutathione -S-transferase mu isoform

GST O Glutathione -S-transferase omega isoform

GST A Glutathione -S-transferase alfa isoform

h-CALT Human Cell Line Activation test

HPA Health protecting agency

HPLC High performance liquid chromatography

HPLC/MS High performance liquid chromatography, mass spectrometry

HSA Human serum albumin

IE Isoeugenol

IgG, IgM, IgE Immunoglobulin G,M,E

IL-12 Interleukin 12

IL 2 Interleukin 2

IL1 Interleukin 1

IL6 Interleukin 6

IFN γ Interferon gamma

K14 Cytokeratine 14

KC keratinocytes

LTQ Linear ion trap mass spectrometer

MA Maleic acid

MASCOT Protein identification software of mass spectrometry data

MB 2-Mercaptobenzothiazole

MHC major histocompatibility complex

MM Methyl methacrylate

MS Methyl salicylate

MTT assay [3-(4,5-Dimethylthiazol-2-yl)-2,5-Diphenyltetrazolium Bromide]

MW Molecular weight

NCBI National Center for Biotechnology Information

Non-S9 Non soluble protein fraction

OECD Organisation for Economic Co-operation and Development

PA Phthalic anhydride

PBS Phosphate buffer saline

PD p-Phenylenediamine

PS Phenyl Salicylate

qPCR Quantitative polymerase chain reaction

QSAR quantitative Structure activity relationship

REACH Registration, Evaluation and Authorisation of Chemicals

SAR Structure activity relationship

S9 Soluble protein fraction

SDS Sodium dodecyl sulphate

SDS-PAGE Sodium dodecyl sulphate polyacrylamide gel electrophoresis

TNF Tumour Necrosis factor

U937/CD86 assay Myeloid U937 skin sensitisation test

Uniprot Universal protein knowledgebase

XME Xenobiotic metabolic enzymes

8. Supplementary Data

BIOPREDIC
INTERNATIONAL

FDL FRA900022 vJ BEDF

CERTIFICATE OF ANALYSIS

Human

SKIN S9 FRACTIONS, SINGLE

Catalog number: FRA900

Batch number: FRA900022

1. BIOLOGICAL MATERIAL

ORIGIN OF PRODUIT	
Number of donors	Single
Sex	Female
Age	31 years old
Ethnicity	African
Other information	/
Tissue	Skin

SAFETY DATA

Serological screening is negative for hepatitis B, hepatitis C and HIV viruses.
Caution: although controls were performed, human material has to be considered as potentially dangerous, take maximum care in order to protect yourself and your colleagues.

2. PRODUCT

DESCRIPTION	
Buffer	100mM Tris-HCl, 1mM EDTA, 250mM Sucrose, protease inhibitors, pH 7.4
Last control date	August, 2013
Expiry date	December 31, 2013

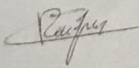
PACKAGING	
Criteria	Results
Protein concentration after thawing (mg/ml) #	8.9
Volume per vial (ml/vial)	1
Protein content per vial (mg/vial)	8.9
Cap color	white

The protein concentration is determined by using the Pierce® BCA Protein Assay Kit from Pierce Biotechnology.

3. STORAGE AND DELIVERY

Storage	In liquid nitrogen
Delivery	In liquid nitrogen

4. VISA FOR BATCH RELEASE

Name	Signature	Date
Nathalie ROUGIER, PhD		September 13, 2013

8-18 Rue Jean Pecker - 35000 Rennes, FRANCE
Tél. (33) 02 99 14 36 14 - Fax (33) 02 99 54 44 72

S.A.R.L. au capital de 98 500€
R.C.S. Rennes B - SIRET 391 701 232 00012 - APE 332B - VAT n°FR 21 391 701 232

CERTIFICATE OF ANALYSIS

Human

SKIN S9 FRACTIONS, SINGLE

Catalog number: FRA900

Batch number: FRA900023

1. BIOLOGICAL MATERIAL

ORIGIN OF PRODUIT	
Number of donors	Single
Sex	Female
Age	43 years old
Ethnicity	African
Other information	/
Tissue	Skin
SAFETY DATA	
Serological screening is negative for hepatitis B, hepatitis C and HIV viruses. <i>Caution: although controls were performed, human material has to be considered as potentially dangerous, take maximum care in order to protect yourself and your colleagues.</i>	

2. PRODUCT

DESCRIPTION	
Buffer	100mM Tris-HCl, 1mM EDTA, 250mM Sucrose, protease inhibitors, pH 7.4
Last control date	August, 2013
Expiry date	December 13, 2013

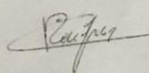
PACKAGING	
Criteria	Results
Protein concentration after thawing (mg/ml) *	14
Volume per vial (ml/vial)	1
Protein content per vial (mg/vial)	14
Cap color	grey

* The protein concentration is determined by using the Pierce® BCA Protein Assay Kit from Pierce Biotechnology.

3. STORAGE AND DELIVERY

Storage	In liquid nitrogen
Delivery	In liquid nitrogen

4. VISA FOR BATCH RELEASE

Name	Signature	Date
Nathalie ROUGIER, PhD		September 13, 2013

CERTIFICATE OF ANALYSIS

Human

SKIN S9 FRACTIONS, SINGLE

Catalog number: FRA900

Batch number: FRA900024

1. BIOLOGICAL MATERIAL

ORIGIN OF PRODUIT	
Number of donors	Single
Sex	Female
Age	61 years old
Ethnicity	Caucasian
Other information	/
Tissue	Skin
SAFETY DATA	
Serological screening is negative for hepatitis B, hepatitis C and HIV viruses. <i>Caution: although controls were performed, human material has to be considered as potentially dangerous, take maximum care in order to protect yourself and your colleagues.</i>	

2. PRODUCT

DESCRIPTION	
Buffer	100mM Tris-HCl, 1mM EDTA, 250mM Sucrose, protease inhibitors, pH 7.4
Last control date	August, 2013
Expiry date	December 13, 2013

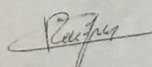
PACKAGING	
Criteria	Results
Protein concentration after thawing (mg/ml) #	10
Volume per vial (ml/vial)	1
Protein content per vial (mg/vial)	10
Cap color	yellow

The protein concentration is determined by using the Pierce® BCA Protein Assay Kit from Pierce Biotechnology.

3. STORAGE AND DELIVERY

Storage	In liquid nitrogen
Delivery	In liquid nitrogen

4. VISA FOR BATCH RELEASE

Name	Signature	Date
Nathalie ROUGIER, PhD		September 13, 2013

CERTIFICATE OF ANALYSIS

Human

SKIN S9 FRACTIONS, SINGLE

Catalog number: FRA900

Batch number: FRA900025

1. BIOLOGICAL MATERIAL

ORIGIN OF PRODUIT	
Number of donors	Single
Sex	Female
Age	51 years old
Ethnicity	Caucasian
Other information	/
Tissue	Skin
SAFETY DATA	
<p>Serological screening is negative for hepatitis B, hepatitis C and HIV viruses. <i>Caution: although controls were performed, human material has to be considered as potentially dangerous, take maximum care in order to protect yourself and your colleagues.</i></p>	

2. PRODUCT

DESCRIPTION	
Buffer	100mM Tris-HCl, 1mM EDTA, 250mM Sucrose, protease inhibitors, pH 7.4
Last control date	August, 2013
Expiry date	December 13, 2013

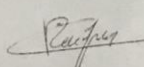
PACKAGING	
Criteria	Results
Protein concentration after thawing (mg/ml) #	13
Volume per vial (ml/vial)	1
Protein content per vial (mg/vial)	13
Cap color	white

The protein concentration is determined by using the Pierce® BCA Protein Assay Kit from Pierce Biotechnology.

3. STORAGE AND DELIVERY

Storage	In liquid nitrogen
Delivery	In liquid nitrogen

4. VISA FOR BATCH RELEASE

Name	Signature	Date
Nathalie ROUGIER, PhD		September 13, 2013

CERTIFICATE OF ANALYSIS

Human SKIN S9 FRACTIONS, SINGLE Catalog number: FRA900 Batch number: FRA900026

1. BIOLOGICAL MATERIAL

ORIGIN OF PRODUIT	
Number of donors	Single
Sex	Female
Age	52 years old
Ethnicity	Caucasian
Other information	/
Tissue	Skin
SAFETY DATA	
Serological screening is negative for hepatitis B, hepatitis C and HIV viruses. <i>Caution: although controls were performed, human material has to be considered as potentially dangerous, take maximum care in order to protect yourself and your colleagues.</i>	

2. PRODUCT

DESCRIPTION	
Buffer	100mM Tris-HCl, 1mM EDTA, 250mM Sucrose, protease inhibitors, pH 7.4
Last control date	August, 2013
Expiry date	December 13, 2013

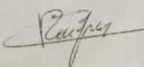
PACKAGING	
Criteria	Results
Protein concentration after thawing (mg/ml) #	14
Volume per vial (ml/vial)	1
Protein content per vial (mg/vial)	14
Cap color	grey

The protein concentration is determined by using the Pierce® BCA Protein Assay Kit from Pierce Biotechnology.

3. STORAGE AND DELIVERY

Storage	In liquid nitrogen
Delivery	In liquid nitrogen

4. VISA FOR BATCH RELEASE

Name	Signature	Date
Nathalie ROUGIER, PhD		August 13, 2013

8-18 Rue Jean Pecker - 35000 Rennes, FRANCE
 Tél. (33) 02 99 14 36 14 - Fax (33) 02 99 54 44 72

S.A.R.L. au capital de 98 500€
 R.C.S. Rennes B - SIRET 391 701 232 00012 - APE 332B - VAT n°FR 21 391 701 232

CERTIFICATE OF ANALYSIS

Human

SKIN S9 FRACTIONS, SINGLE

Catalog number: FRA900

Batch number: FRA900027

1. BIOLOGICAL MATERIAL

ORIGIN OF PRODUIT	
Number of donors	Single
Sex	Female
Age	34 years old
Ethnicity	African
Other information	/
Tissue	Skin
SAFETY DATA	
Serological screening is negative for hepatitis B, hepatitis C and HIV viruses. <i>Caution: although controls were performed, human material has to be considered as potentially dangerous, take maximum care in order to protect yourself and your colleagues.</i>	

2. PRODUCT

DESCRIPTION	
Buffer	100mM Tris-HCl, 1mM EDTA, 250mM Sucrose, protease inhibitors, pH 7.4
Last control date	August, 2013
Expiry date	December 13, 2013

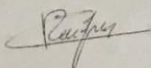
PACKAGING	
Criteria	Results
Protein concentration after thawing (mg/ml) [#]	10
Volume per vial (ml/vial)	1
Protein content per vial (mg/vial)	10
Cap color	yellow

[#] The protein concentration is determined by using the Pierce[®] BCA Protein Assay Kit from Pierce Biotechnology.

3. STORAGE AND DELIVERY

Storage	In liquid nitrogen
Delivery	In liquid nitrogen

4. VISA FOR BATCH RELEASE

Name	Signature	Date
Nathalie ROUGIER, PhD		September 13, 2013

CERTIFICATE OF ANALYSIS

Human

SKIN S9 FRACTIONS, SINGLE

Catalog number: FRA900

Batch number: FRA900028

1. BIOLOGICAL MATERIAL

ORIGIN OF PRODUIT	
Number of donors	Single
Sex	Female
Age	43 years old
Ethnicity	Caucasian
Other information	/
Tissue	Skin
SAFETY DATA	
<p>Serological screening is negative for hepatitis B, hepatitis C and HIV viruses. <i>Caution: although controls were performed, human material has to be considered as potentially dangerous, take maximum care in order to protect yourself and your colleagues.</i></p>	

2. PRODUCT

DESCRIPTION	
Buffer	100mM Tris-HCl, 1mM EDTA, 250mM Sucrose, protease inhibitors, pH 7.4
Last control date	August, 2013
Expiry date	December 13, 2013

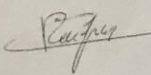
PACKAGING	
Criteria	Results
Protein concentration after thawing (mg/ml) #	17
Volume per vial (ml/vial)	1
Protein content per vial (mg/vial)	17
Cap color	white

The protein concentration is determined by using the Pierce® BCA Protein Assay Kit from Pierce Biotechnology.

3. STORAGE AND DELIVERY

Storage	In liquid nitrogen
Delivery	In liquid nitrogen

4. VISA FOR BATCH RELEASE

Name	Signature	Date
Nathalie ROUGIER, PhD		September 13, 2013

CERTIFICATE OF ANALYSIS

Human

SKIN S9 FRACTIONS, SINGLE

Catalog number: FRA900

Batch number: FRA900029

1. BIOLOGICAL MATERIAL

ORIGIN OF PRODUIT	
Number of donors	Single
Sex	Female
Age	48 years old
Ethnicity	African
Other information	/
Tissue	Skin
SAFETY DATA	
Serological screening is negative for hepatitis B, hepatitis C and HIV viruses. <i>Caution: although controls were performed, human material has to be considered as potentially dangerous, take maximum care in order to protect yourself and your colleagues.</i>	

2. PRODUCT

DESCRIPTION	
Buffer	100mM Tris-HCl, 1mM EDTA, 250mM Sucrose, protease inhibitors, pH 7.4
Last control date	August, 2013
Expiry date	December 13, 2013

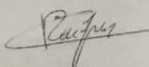
PACKAGING	
Criteria	Results
Protein concentration after thawing (mg/ml) #	18
Volume per vial (ml/vial)	1
Protein content per vial (mg/vial)	18
Cap color	grey

The protein concentration is determined by using the Pierce® BCA Protein Assay Kit from Pierce Biotechnology.

3. STORAGE AND DELIVERY

Storage	In liquid nitrogen
Delivery	In liquid nitrogen

4. VISA FOR BATCH RELEASE

Name	Signature	Date
Nathalie ROUGIER, PhD		September 13, 2013

8-18 Rue Jean Pecker - 35000 Rennes, FRANCE
Tél. (33) 02 99 14 36 14 - Fax (33) 02 99 54 44 72

S.A.R.L. au capital de 98 500€
R.C.S. Rennes B - SIRET 391 701 232 00012 - APE 332B - VAT n°FR 21 391 701 232

Figure 22. The certificates of analysis of the 8 human skin samples provided by Biopredict International, France used in the skin proteome analysis

Table 5. Identification and quantitative expression overview of all proteins identified in S9 & NS9 fractions, based on the presence of ≥ 2 different tryptic peptides identified in all the 8 donors.

Proteins in S9 fraction	Peptide	Mol Weight	NCBI identification
Keratin, type II cytoskeletal 2 epidermal	18	65,433.90	NP_000414.2
Histone H4	6	11,269.60	NP_778224.1
Ig gamma-1 chain C region	6	36,105.00	PT0368
Glyceraldehyde-3-phosphate dehydrogenase	3	36,053.40	CAA25833.1
Ig kappa chain C region	3	11,608.60	P01834.1
Histone H2B type 1-N	4	13,950.80	NP_003511.1
Keratin, type II cytoskeletal 1	17	66,040.30	NP_006112.3
Hemoglobin subunit beta	2	15,998.00	NP_000509.1
Serum albumin	24	69,366.90	NP_000468.1
Ig alpha-1 chain C region	2	37,754.70	B45874
Keratin, type I cytoskeletal 10	14	58,828.80	NP_000412.3
Actin, cytoplasmic type 5	6	41,851.00	
Myosin-9	2	226,537.50	NP_002464.1
Ubiquitin-40S ribosomal protein S27a	3	17,965.60	NP_001129064.1
Gelsolin	4	85,697.80	NP_000168.1
Phosphatidylethanolamine-binding protein 1	2	21,056.90	NP_002558.1
Keratin, type I cytoskeletal 14	8	51,562.50	NP_000517.2
Peptidyl-prolyl cis-trans isomerase A	5	18,012.90	NP_066953.1
Transaldolase	2	37,541.70	NP_006746.1
14-3-3 protein sigma	7	27,774.80	NP_006133.1
Bleomycin hydrolase	3	52,562.60	NP_000377.1
60S acidic ribosomal protein P0	3	34,371.40	NP_444505.1
Keratin, type I cytoskeletal 9	2	62,065.90	NP_000217.2
Serpin B12	3	46,277.70	NP_536722.1
40S ribosomal protein S3	3	29,945.30	NP_001243731.1
L-lactate dehydrogenase A chain	3	36,689.20	NP_005557.1
Proteasome subunit beta type-1	2	26,490.50	NP_002784.1
Prelamin-A/C	4	74,140.70	NP_733821.1
Zinc-alpha-2-glycoprotein	5	34,258.60	NP_001176.1
60S ribosomal protein L5	4	34,363.50	NP_000960.2
40S ribosomal protein SA	3	33,021.30	NP_001012321.1
Annexin A2	12	38,606.10	AAH68065.1
Fructose-bisphosphate aldolase C	2	39,420.60	NP_005156.1
40S ribosomal protein S18	3	17,719.30	NP_072045.1
60S ribosomal protein L12	4		NP_000967.1
Alpha-1-antichymotrypsin	3	47,653.00	NP_001076.2
Pyruvate kinase PKM	7	57,937.50	NP_001193728.1
Junction plakoglobin	10	81,801.90	NP_068831.1
Epiplakin	13	555,615.40	NP_112598.3

Peptidyl-prolyl cis-trans isomerase B	4	18,012.90	NP_000933.1
Malate dehydrogenase, cytoplasmic	2	36,426.90	NP_001186040.1
Alpha-2-macroglobulin	2	163,289.90	NP_000005.2
Protein disulfide-isomerase A3	4	56,784.60	NP_005304.3
Complement C3	3	187,149.10	NP_000055.2
Collagen alpha-1(XVIII) chain	3	178,187.70	NP_001846.3
Protein disulfide-isomerase	5	57,118.10	NP_000909.2
60S ribosomal protein L10a	3	24,832.00	NP_009035.3
Fructose-bisphosphate aldolase A	3	39,420.60	CAA30270.1
Hemopexin	2	51,676.50	NP_000604.1
14-3-3 protein zeta/delta	5	27,745.90	NP_001129174.1
Actin-related protein 3	3	47,371.90	NP_065178.1
Gamma-glutamylcyclotransferase	4	21,008.00	NP_076956.1
Heat shock 70 kDa protein 1B	12	70,230.20	NP_005337.2
14-3-3 protein epsilon	4	29,175.00	NP_006752.1
Transitional endoplasmic reticulum ATPase	7		NP_009057.1
Elongation factor 2	5	50,119.40	NP_001952.1
Peroxiredoxin-1	7	22,110.90	NP_859048.1
Glutathione S-transferase Mu 3	5	25,746.50	NP_000840.2
Alpha-2-macroglobulin-like protein 1	3	161,108.20	NP_653271.2
Triosephosphate isomerase	5	30,790.80	NP_000356.1
Periostin	4	93,318.00	NP_006466.2
Alpha-enolase	8	47,170.20	NP_001419.1
Plectin	13	531,783.90	NP_112598.3
Serotransferrin	22	77,064.30	NP_001054.1
Tripartite motif-containing protein 29	5	65,835.70	NP_036233.2
Glucose-6-phosphate isomerase	3	31,085.70	NP_001171651.1
Desmocollin-1	6	99,988.10	NP_077739.1
WD repeat-containing protein 1	2	66,193.20	NP_059830.1
Caspase-14	6	27,679.80	NP_036246.1
Thioredoxin	2	11,737.30	AAF87085.1
Myosin light polypeptide 6	2	16,929.80	NP_066299.2
Proteasome subunit alpha type-7	4	29,586.00	NP_002783.1
Annexin A7	2	52,740.50	AAH02632.1
Complement C3	7	187,149.10	NP_000055.2
Cathepsin D	4	44,553.00	NP_001900.1

Serpin B5	8	42,101.80	NP_002630.2
Calpain-1 catalytic subunit	5	81,892.60	NP_001185798.1
Protein-glutamine gamma-glutamyltransferase E	7	89,786.00	NP_003236.3
Alpha-actinin-4	14	41,851.00	NP_004915.2
Heat shock protein HSP 90-beta	3	84,778.20	NP_031381.2
Ribonuclease inhibitor	5	49,974.40	NP_976320.1
Dihydrolipoyl dehydrogenase, mitochondrial	2	61,399.70	
Fibrinogen beta chain	5	55,928.60	NP_005132.2
Annexin A1	7	38,715.90	NP_000691.1
Collagen alpha-3(VI) chain	20	343,667.40	NP_476508.2
Transforming growth factor-beta-induced protein ig-h3	3	74,682.90	NP_000349.1
Fibronectin	4	262,616.90	
Ig mu chain C region	3	49,305.70	S37768
Fatty aldehyde dehydrogenase	4	54,849.80	NP_001026976.1
Phosphoglycerate kinase 1	5	44,615.30	NP_000282.1
Glutamate dehydrogenase 1, mitochondrial	10	61,399.70	NP_005262.1
Annexin A5	4	35,938.60	NP_001145.1
Annexin A4	6	35,884.30	NP_001144.1
Heterogeneous nuclear ribonucleoprotein U-like protein 1	2	96,003.10	NP_008971.2
X-ray repair cross-complementing protein 6	5	69,846.40	NP_001460.1
Catalase	10	59,756.50	NP_001743.1
Rab GDP dissociation inhibitor beta	7	50,584.10	NP_001108628.1
Ubiquitin-like modifier-activating enzyme 1	4	117,850.30	NP_003325.2
Ras GTPase-activating-like protein IQGAP1	4	189,258.60	NP_003861.1
Ceruloplasmin	3	122,207.90	NP_000087.1
Isocitrate dehydrogenase [NADP], mitochondrial	3	46,660.50	NP_008830.2
Adenosylhomocysteinase	3	47,717.10	NP_001229602.1
Malate dehydrogenase, mitochondrial	8	35,566.00	NP_005909.2
Aldehyde dehydrogenase, mitochondrial	12	56,381.40	NP_000683.3
Heat shock cognate 71 kDa protein	14	70,806.60	NP_006588.1
Proteasome subunit alpha type-4	7	29,586.00	NP_001096137.1
Aspartate aminotransferase, mitochondrial	5	47,518.60	NP_002071.2
			NP_005338.1
78 kDa glucose-regulated protein	8	21,008.00	
Proteasome subunit beta type-5	4	26,490.50	
Fatty acid synthase	7	273,427.10	NP_004095.4
Heterogeneous nuclear ribonucleoprotein R	3	34,225.40	NP_001095868.1
Serpin B6		42,622.90	NP_001258754.1

Integrin beta-1	3	88,415.10	NP_391988.1
Desmoplakin	32	331,781.40	NP_004406.2
Clathrin heavy chain 1	5	191,592.90	NP_004850.1
Very long-chain specific acyl-CoA dehydrogenase, mitochondrial	4	70,391.60	NP_000009.1
T-complex protein 1 subunit theta	6	59,621.00	NP_006576.2
Collagen alpha-1(XIV) chain	2	193,516.10	NP_004361.3
Spectrin alpha chain, non-erythrocytic 1	15	284,542.70	NP_001123910.1
Filamin-B	16	278,158.80	AAL68442.1
Sodium/potassium-transporting ATPase subunit alpha-1	8	112,899.50	NP_001153706.1
4-trimethylaminobutyraldehyde dehydrogenase	6	54,849.80	NP_000687.3
Puromycin-sensitive aminopeptidase	7	103,279.10	NP_006301.3
Filamin-A	13	280,729.40	BAJ83965.1
Envoplakin	2	231,604.40	NP_001979.2
Collagen alpha-1(VII) chain	12	295,217.50	NP_000085.1
Hexokinase-1	5	102,488.40	NP_000179.2
Tenascin-X	12	464,307.20	NP_061978.6
Fibrillin-1	2	312,226.00	NP_000129.3

Proteins in non S9 fraction	Peptide	Mol Weight	NCBI identification
Histone H4 type VIII	4	11439.8	NP_003486.1
Galectin-7	3	15074.7	NP_002298.1
Keratin, type II cytoskeletal 2 epidermal	15	0	NP_000414.2
ATP synthase subunit beta, mitochondrial	2	137923.7	NP_001677.2
Keratin, type II cytoskeletal 1	17	66040.3	NP_006112.3
Keratin, type I cytoskeletal 10	20	58828.8	NP_000412.3
Annexin A2	20	38606.1	AAH68065.1
Desmoglein-3	4	113748.9	NP_001935.2
Desmoglein-1	14	99970.6	NP_001933.2
Guanine nucleotide-binding protein G(I)/G(S)/G(T) subunit beta-2	2	37331.8	
Ig gamma-1 chain C region	4	36105	PT0368
Fatty aldehyde dehydrogenase	6	54849.8	NP_001026976.1
Desmocollin-1	18	61399.7	NP_077739.1
Plakophilin-1	13	82862.7	NP_000290.2
Annexin A1	10	54391.7	NP_000691.1
Keratin, type II cytoskeletal 5	14	62379.6	NP_000415.2
Annexin A5	5	35938.6	NP_001145.1
Annexin A4	6	35884.3	NP_001144.1
Synaptic vesicle membrane protein VAT-1 homolog	2	41919.8	NP_006364.2
Capsid protein	3	58774.9	

Plasma membrane calcium-transporting ATPase 4	2	137923.7	NP_001675.3
Annexin A8-like protein 2	4		NP_001677.2
Cytochrome b-c1 complex subunit 2, mitochondrial	3	48443.4	NP_003357.2
Sodium/potassium-transporting ATPase subunit alpha-1	15	112899.5	NP_001153706.1
Junction plakoglobin	4	81822.1	NP_002221.1
Serum albumin	12	69366.9	NP_000468.1
Voltage-dependent anion-selective channel protein 1	5	30773.9	NP_003365.1
			NP_001191184.1
Lysosome membrane protein 2	2	54291.7	
Protein disulfide-isomerase A3	7	56784.6	NP_005304.3
NADH-cytochrome b5 reductase 1	5	34096.1	NP_057327.2
Cathepsin D	3	44553	NP_001900.1
Prohibitin	5	29804.6	AAB21614.1
Integrin beta-1	4	88415.1	NP_391988.1
Copine-3	7	60131.6	NP_003900.1
Glutamate dehydrogenase 1, mitochondrial	9	331781.4	NP_005262.1
			NP_004125.3
Stress-70 protein, mitochondrial	2	73742.4	
Glycine amidinotransferase, mitochondrial	2	48456.6	NP_001473.1
Cytochrome b-c1 complex subunit Rieske, mitochondrial	2	29651.8	NP_005994.2
Keratin, type I cytoskeletal 9	6	62065.9	NP_000217.2
			NP_057381.3
Prenylcysteine oxidase 1	4	56642.2	
Protein disulfide-isomerase	6	57118.1	NP_000909.2
Aspartate aminotransferase, mitochondrial	2	47434.6	NP_001273149.1
Cytochrome b-c1 complex subunit 1, mitochondrial	4	52645.9	NP_003356.2
Clathrin heavy chain 1	2	61055.7	NP_004850.1
Alpha-actinin-4	9	104857.2	NP_004915.2
Annexin A7	6	52740.5	AAH02632.1
Voltage-dependent anion-selective channel protein 2	5	31620.5	NP_003366.2
Ras GTPase-activating-like protein IQGAP1	2	189258.6	
Trifunctional enzyme subunit beta, mitochondrial	4	83001.9	NP_001268441.1
Adipocyte plasma membrane-associated protein	3	46481.5	NP_065392.1
78 kDa glucose-regulated protein	12	72334.7	NP_005338.1
Very long-chain specific acyl-CoA	4	70391.6	NP_001029031.1

dehydrogenase, mitochondrial			
Malate dehydrogenase, mitochondrial	6	35566	NP_001269332.1
Heat shock 70 kDa protein 1A/1B	5	70054	NP_005336.3
Ras-related C3 botulinum toxin substrate 1	3	48443.4	P63000.1
Integrin alpha-6	4	126609	NP_000201.2
Aldehyde dehydrogenase, mitochondrial	7	56381.4	NP_001191818.1
60 kDa heat shock protein, mitochondrial	3	44553	NP_002147.2
Sulfide:quinone oxidoreductase, mitochondrial	3	49962	NP_067022.1
Desmoplakin	12	60131.6	AAI40803.1
Endoplasmic reticulum resident protein 29	4	28994.9	NP_006808.1
NADH-ubiquinone oxidoreductase 75 kDa subunit, mitochondrial	7	79468.5	NP_001186910.1
Lanosterol synthase	5	83310	AAB36220.1
Endoplasmin	8		NP_003290.1
Protein disulfide-isomerase A4	5	72934	NP_004902.1
Dolichyl-diphosphooligosaccharide--protein glycosyltransferase subunit 1	6	68571	NP_002941.1
Aconitate hydratase, mitochondrial	4	85428	NP_001089.1
Integrin beta-4	8	202166.7	NP_000204.3
Glycerol-3-phosphate dehydrogenase, mitochondrial	9	80854.6	NP_000399.3
Calcium-binding mitochondrial carrier protein Aralar1	2	191592.9	Q6NUK1.2
Peptidyl-prolyl cis-trans isomerase A	5	18012.9	NP_066953.1
Transmembrane protein 43	5	44876.8	NP_077310.1
Integrin alpha-2	6	129297.9	NP_002194.2
Acyl-CoA dehydrogenase family member 9, mitochondrial	4	68762.8	NP_054768.2
Endoplasmic reticulum aminopeptidase 1	5	107237.9	AIY60633.1
Hexokinase-1	14	102488.4	NP_000179.2
Trifunctional enzyme subunit alpha, mitochondrial	13	83001.9	NP_000173.2
Epidermal growth factor receptor	4	134279.2	ADZ75461.1
Alpha-2-macroglobulin-like protein 1	12	161108.2	NP_653271.2
Serotransferrin	6	77064.3	NP_001054.1
Sarcoplasmic/endoplasmic reticulum calcium ATPase 2	4	114793.9	P16615.1
Myosin-9	24	226537.5	NP_002464.1
Cytosolic phospholipase A2 zeta	2	95084.2	
Golgi apparatus protein 1	6	134553.9	NP_036333.2
Myosin-14	15	227872.6	NP_001139281.1
Prominin-2	3	91883.1	NP_001159449.1
Myoferlin	13	234715.6	AAF27176.1

Synaptophysin-like protein 1	3	28566.1	EAL24402.1
Filamin-A	8	280729.4	NP_001447.2
UDP-glucose:glycoprotein glucosyltransferase 1	5	177195	NP_064505.1
NAD(P) transhydrogenase, mitochondrial	6	113899.2	NP_892022.2
NADH dehydrogenase [ubiquinone] flavoprotein 1, mitochondrial	3	50817.8	NP_009034.2
Myosin-10	5	229002	NP_001243024.1
Profilin-1	2	15054.3	NP_005013.1
Keratin, type II cytoskeletal 3	2	64418.9	NP_476429.2
Spectrin alpha chain, non-erythrocytic 1	2	274613.4	NP_001123910.1
Cation-independent mannose-6-phosphate receptor 3	9	274372.7	NP_000867.2
Serpin A12	3	47177.8	NP_776249.1
Matrilin-2	2	106836.1	NP_002371.3

Table 6. Quantitative expression overview of all proteins identified in S9 & NS9 fractions, based on the presence of ≥ 2 different tryptic peptides identified in all the 8 donors.

Identified proteins in S9 fraction	Peptide	Mol Weight	NCBI identification	total protein level
14-3-3 protein epsilon	4	29,175.00	NP_006752.1	930133.0375
14-3-3 protein sigma	7	27,774.80		2027747.541
14-3-3 protein zeta/delta	5	27,745.90		941868.7524
Alpha-2-macroglobulin	2	163,289.90	NP_000005.2	1014109.375
Alpha-2-macroglobulin-like protein 1	3	161,108.20		859946.0333
Alpha-1-antichymotrypsin	3	47,653.00	NP_001076.2	1207017.111
Aspartate aminotransferase, mitochondrial	5	47,518.60	NP_002071.2	352056.376
Very long-chain specific acyl-CoA dehydrogenase, mitochondrial	4	70,391.60	NP_000009.1	230,036.12
Actin, cytoplasmic type 5	6	41,851.00		4216398.692
Alpha-actinin-4	14	41,851.00	NP_004915.2	598378.2526
Fatty aldehyde dehydrogenase	4	54,849.80	NP_001026976.1	488745.0125
4-trimethylaminobutyraldehyde dehydrogenase	6	54,849.80	NP_000687.3	143799.3947
Serum albumin	24	69,366.90	NP_000468.1	7814385.116
Aldehyde dehydrogenase, mitochondrial	12	56,381.40	NP_000683.3	370722.0319
Fructose-bisphosphate aldolase A	3	39,420.60	CAA30270.1	960654.7222
Fructose-bisphosphate aldolase C	2	39,420.60		1374402.9
Annexin A1	7	38,715.90	NP_000691.1	532824.8548
Annexin A2	12	38,606.10	AAH68065.1	1499714.794
Annexin A4	6	35,884.30	NP_001144.1	441318.7417
Annexin A5	4	35,938.60	NP_001145.1	452793.0125
Annexin A7	2	52,740.50	AAH02632.1	679794.1

Actin-related protein 3	3	47,371.90	NP_065178.1	940328.5556
Sodium/potassium-transporting ATPase subunit alpha-1	8	112,899.50	NP_001153706.1	154457.8661
Transforming growth factor-beta-induced protein ig-h3	3	74,682.90	NP_000349.1	518188.64
Bleomycin hydrolase	3	52,562.60	NP_000377.1	1973558.667
Calpain-1 catalytic subunit	5	81,892.60	NP_001185798.1	614430.2676
Caspase-14	6	27,679.80	NP_036246.1	701406.8438
Catalase	10	59,756.50	NP_001743.1	426,343.14
Cathepsin D	4	44,553.00	NP_001900.1	636870.7506
Ceruloplasmin	3	122,207.90	NP_000087.1	417680.7889
Clathrin heavy chain 1	5	191,592.90	NP_004850.1	267111.928
Complement C3	3	187,149.10	NP_000055.2	1000123.822
Complement C3	7	187,149.10		666487.8167
Collagen alpha-3(VI) chain	20	343,667.40	NP_476508.2	520390.0695
Collagen alpha-1(VII) chain	12	295,217.50	NP_000085.1	111738.9952
Collagen alpha-1(XIV) chain	2	193,516.10	NP_004361.3	171884.4428
Collagen alpha-1(XVIII) chain	3	178,187.70	NP_001846.3	978245.7556
Desmoplakin	32	331,781.40	NP_004406.2	278568.0003
Glutamate dehydrogenase 1, mitochondrial	10	61,399.70	NP_005262.1	462553.106
Dihydrolipoyl dehydrogenase, mitochondrial	2	61,399.70		536,127.65
Desmocollin-1	6	99,988.10	NP_077739.1	740337.5008
Elongation factor 2	5	50,119.40	NP_001952.1	922921.5104
Alpha-enolase	8	47,170.20	NP_001419.1	833333.6047
Epiplakin	13	555,615.40	NP_112598.3	1107208.309
Envoplakin	2	231,604.40	NP_001979.2	111878.975
Fatty acid synthase	7	273,427.10	NP_004095.4	292577.0612
Fibrillin-1	2	312,226.00	NP_000129.3	33,496.14
Fibrinogen beta chain	5	55,928.60	NP_005132.2	535050.412
Fibronectin	4	262,616.90		512725.0778
Filamin-A	13	280,729.40		118903.6471
Filamin-B	16	278,158.80		160342.5445
Glyceraldehyde-3-phosphate dehydrogenase	3	36,053.40	CAA25833.1	9883716.667
Glucose-6-phosphate isomerase	3	31,085.70	NP_001171651.1	744998.88
Rab GDP dissociation inhibitor beta	7	50,584.10	NP_001108628.1	424112.7316
Gelsolin	4	85,697.80	NP_000168.1	2808048.563
Gamma-glutamylcyclotransferase	4	21,008.00	NP_076956.1	939465.4813
78 kDa glucose-regulated protein	8	21,008.00		339769.0547
Glutathione S-transferase Mu 3	5	25,746.50	NP_000840.2	883964.498
Histone H2B type 1-N	4	13,950.80	NP_003511.1	9276818.419
Histone H4	6	11,269.60	NP_778224.1	2.11E+07
Hemoglobin subunit beta	2	15,998.00	NP_000509.1	8091235.975
Hemopexin	2	51,676.50	NP_000604.1	959554.625
Heterogeneous nuclear ribonucleoprotein U-like protein 1	2	96,003.10	NP_008971.2	435139.8
Heterogeneous nuclear ribonucleoprotein R	3	34,225.40	NP_001095868.1	290640.0111
Heat shock 70 kDa protein 1B	12	70,230.20	NP_005337.2	933790.8938
Heat shock protein HSP 90-beta	3	84,778.20	NP_031381.2	584640.5444

Heat shock cognate 71 kDa protein	14	70,806.60	NP_006588.1	369251.7632
Hexokinase-1	5	102,488.40	NP_000179.2	89,650.54
Isocitrate dehydrogenase [NADP], mitochondrial	3	46,660.50	NP_008830.2	391483.9967
Ig alpha-1 chain C region	2	37,754.70	B45874	6137233
Ig gamma-1 chain C region	6	36,105.00	PT0368	13009588.77
Ig mu chain C region	3	49,305.70	S37768	494947.7222
Ig kappa chain C region	3	11,608.60	P01834.1	9278070.489
Ras GTPase-activating-like protein IQGAP1	4	189,258.60	NP_003861.1	417,682.29
Integrin beta-1	3	88,415.10	NP_391988.1	282986.4922
Keratin, type I cytoskeletal 10	14	58,828.80	NP_000412.3	5.31E+06
Keratin, type I cytoskeletal 14	8	51,562.50	NP_000517.2	2.51E+06
Keratin, type I cytoskeletal 9	2	62,065.90	NP_000217.2	1901922.25
Keratin, type II cytoskeletal 2 epidermal	18	65,433.90	NP_000414.2	2.17E+07
Keratin, type II cytoskeletal 1	17	66,040.30	NP_006112.3	8.30E+06
Pyruvate kinase PKM	7	57,937.50	NP_001193728.1	1203846.175
L-lactate dehydrogenase A chain	3	36,689.20	NP_005557.1	1596937.211
Prelamin-A/C	4	74,140.70	NP_733821.1	1537311.731
Malate dehydrogenase, cytoplasmic	2	36,426.90	NP_001186040.1	1029587.5
Malate dehydrogenase, mitochondrial	8	35,566.00	NP_005909.2	382943.1766
Myosin-9	2	226,537.50	NP_002464.1	3198661.75
Myosin light polypeptide 6	2	16,929.80	NP_066299.2	690064.4
Protein disulfide-isomerase	5	57,118.10	NP_000909.2	977765.152
Protein disulfide-isomerase A3	4	56,784.60	NP_005304.3	1004540.056
Phosphatidylethanolamine-binding protein 1	2	21,056.90	NP_002558.1	2587409.5
Phosphoglycerate kinase 1	5	44,615.30	NP_000282.1	482,026.88
Junction plakoglobin	10	81,801.90	NP_068831.1	1168557.885
Plectin	13	531,783.90	NP_112598.3	822,219.49
Periostin	4	93,318.00	NP_006466.2	838200.5319
Peptidyl-prolyl cis-trans isomerase A	5	18,012.90	NP_066953.1	2227722.52
Peptidyl-prolyl cis-trans isomerase B	4	18,012.90		1052328.563
Peroxiredoxin-1	7	22,110.90	NP_859048.1	913130.0776
Proteasome subunit alpha type-4	7	29,586.00	NP_001096137.1	355092.5367
Proteasome subunit alpha type-7	4	29,586.00		681,252.64
Puromycin-sensitive aminopeptidase	7	103,279.10	NP_006301.3	121,318.42
Proteasome subunit beta type-1	2	26,490.50	NP_002784.1	1595880.55
Proteasome subunit beta type-5	4	26,490.50		314958.1688
Ribonuclease inhibitor	5	49,974.40	NP_976320.1	570,206.47
60S ribosomal protein L10a	3	24,832.00	NP_009035.3	964,035.94
60S ribosomal protein L12	4		NP_000967.1	1313476.569
60S ribosomal protein L5	4	34,363.50	NP_000960.2	1503853.044
60S acidic ribosomal protein P0	3	34,371.40	NP_444505.1	1927008
40S ribosomal protein S18	3	17,719.30	NP_072045.1	1352747.622
Ubiquitin-40S ribosomal protein S27a	3	17,965.60	NP_001129064.1	2988518.144
40S ribosomal protein S3	3	29,945.30	NP_001243731.1	1734167.111
40S ribosomal protein SA	3	33,021.30	NP_001012321.1	1500066.2

Adenosylhomocysteinase	3	47,717.10	NP_001229602.1	388707.7556
Serpin B12	3	46,277.70	NP_536722.1	1879312.567
Serpin B5	8	42,101.80	NP_002630.2	623202.6639
Serpin B6		42,622.90	NP_001258754.1	284568.0063
Spectrin alpha chain, non-erythrocytic 1	15	284,542.70	NP_001123910.1	163538.2191
Transaldolase	2	37,541.70	NP_006746.1	2174310.65
T-complex protein 1 subunit theta	6	59,621.00	NP_006576.2	229140.0861
Tenascin-X	12	464,307.20	NP_061978.6	86319.88958
Transitional endoplasmic reticulum ATPase	7		NP_009057.1	923450.0708
Protein-glutamine gamma-glutamyltransferase E	7	89,786.00	NP_003236.3	605587.9857
Thioredoxin	2	11,737.30		691253.4
Triosephosphate isomerase	5	30,790.80	NP_000356.1	858167.652
Serotransferrin	22	77,064.30	NP_001054.1	812051.7413
Tripartite motif-containing protein 29	5	65,835.70	NP_036233.2	812051.7413
Ubiquitin-like modifier-activating enzyme 1	4	117,850.30	NP_003325.2	422553.4375
WD repeat-containing protein 1	2	66,193.20	NP_059830.1	740171.1175
X-ray repair cross-complementing protein 6	5	69,846.40	NP_001460.1	428459.2008
Zinc-alpha-2-glycoprotein	5	34,258.60	NP_001176.1	1532837.975

Identified proteins in Non S9 fractions	Peptide	Mol Weight	NCBI identification	total protein level
HLA class I histocompatibility antigen, A-34 alpha chain	2	41054.6	CAK22320.1	5,605,276.74
Alpha-2-macroglobulin-like protein 1	12	161108.2	NP_653271.2	54765.86264
Aspartate aminotransferase, mitochondrial	2	47434.6	NP_001273149.1	251,001.76
Acyl-CoA dehydrogenase family member 9, mitochondrial	4	68762.8	NP_054768.2	89,289.24
Very long-chain specific acyl-CoA dehydrogenase, mitochondrial	5	70391.6	NP_001029031.1	171,421.26
Aconitate hydratase, mitochondrial	4	85428	NP_001089.1	99,867.43
Actin-5C	6	104857.2	NP_004915.2	3482303.944
Alpha-actinin-4	10	54849.8	NP_001026976.1	216735.2701
Fatty aldehyde dehydrogenase	7	69366.9	NP_000468.1	1,091,544.14
Serum albumin	13	56381.4	NP_001191818.1	394966.0581
Aldehyde dehydrogenase, mitochondrial	7	54391.7	NP_000691.1	406498.9678
Annexin A11	6	38606.1	AAH68065.1	117205.3053
Annexin A1	11	35884.3	NP_001144.1	985486.9702
Annexin A2	20	35938.6	NP_001145.1	2.42E+06
Annexin A4	6	52740.5	AAH02632.1	744,786.72
Annexin A5	5	46481.5	NP_065392.1	746,993.54
Annexin A7	6	112899.5	NP_001153706.1	337867.045
Adipocyte plasma membrane-associated protein	3	114793.9	P16615.1	190667.5
Sodium/potassium-transporting ATPase subunit alpha-1	15	137923.7	NP_001675.3	398346.0648
Sarcoplasmic/endoplasmic reticulum calcium ATPase 2	7	137923.7	NP_001677.2	33,831.71
Plasma membrane calcium-transporting ATPase 4	2		NP_001677.2	475,924.39
ATP synthase subunit beta, mitochondrial	2	58774.9		3312120.058
Annexin A8-like protein 2	4	44553	NP_001900.1	474139.3
Capsid protein	3	44553	NP_002147.2	879,776.90

Cathepsin D	4	61055.7	NP_004850.1	189,576.13
60 kDa heat shock protein, mitochondrial	3	191592.9	Q6NUK1.2	112203.6533
Clathrin heavy chain 1	2	60131.6	NP_003900.1	48,225.74
Calcium-binding mitochondrial carrier protein Aralar1	2	60131.6	AAI40803.1	256,368.40
Copine-3	7	331781.4	NP_005262.1	268737.6848
Desmoplakin	12	61399.7	NP_077739.1	138255.8405
Glutamate dehydrogenase 1, mitochondrial	9	99970.6	NP_001933.2	282878.0927
Desmocollin-1	11	113748.9	NP_001935.2	1338614.263
Desmocollin-3	7	83001.9	NP_000173.2	2777226.279
Desmoglein-1	18	83001.9	NP_001268441.1	962,801.21
Trifunctional enzyme subunit alpha, mitochondrial	17	134279.2	ADZ75461.1	45,315.12
Epidermal growth factor receptor	4		NP_003290.1	58,183.18
Endoplasmin	8	107237.9	AIY60633.1	272910.3728
Endoplasmic reticulum aminopeptidase 1	5	83310	AAB36220.1	71,304.02
Lanosterol synthase	5	28994.9	NP_006808.1	120,450.83
Endoplasmic reticulum resident protein 29	4	280729.4	NP_001447.2	170,767.56
Electron transfer flavoprotein-ubiquinone oxidoreductase, mitochondrial	3	48456.6		63,245.85
Filamin-A	5	37331.8		28,109.92
Filamin-B	3	80854.6	NP_000399.3	39,331.84
Neutral alpha-glucosidase AB	7	73742.4		177,927.36
Glycine amidinotransferase, mitochondrial	2	72334.7	NP_005338.1	274,621.71
Guanine nucleotide-binding protein G(i) subunit alpha-2	3	134553.9	NP_036333.2	1074524.568
Glycerol-3-phosphate dehydrogenase, mitochondrial	9	11439.8		94754.38938
Stress-70 protein, mitochondrial	2	70054	NP_005336.3	279,802.98
78 kDa glucose-regulated protein	12	102488.4	NP_000179.2	178965.6314
Golgi apparatus protein 1	6	36105		30,047.62
Histone H4 type VIII	4	189258.6		4657862.65
Heat shock 70 kDa protein 1A/1B	5	129297.9	NP_002194.2	157,237.22
Hexokinase-1	14	126609	NP_000201.2	68,065.41
Ig gamma-1 chain C region	4	88415.1		1,500,176.42
Ras GTPase-activating-like protein IQGAP1	2	202166.7	NP_000204.3	196,644.82
Integrin alpha-2	6	58828.8	NP_000412.3	89,768.31
Integrin alpha-6	4	62065.9	NP_000217.2	145,452.89
Integrin beta-1	4	0	NP_000414.2	312,924.35
Integrin beta-4	8	66040.3	NP_006112.3	95,953.18
Keratin, type I cytoskeletal 10	15	64418.9		4,411,763.00
Keratin, type I cytoskeletal 14	5	62379.6	NP_000415.2	7043435
Keratin, type I cytoskeletal 9	6	15074.7		62599
Keratin, type II cytoskeletal 2 epidermal	15	106836.1		3907120.586
Keratin, type II cytoskeletal 1	17	35566	NP_001269332.1	2.97E+06
Keratin, type II cytoskeletal 3	2	274372.7	NP_000867.2	10337
Keratin, type II cytoskeletal 5	14	229002	NP_001243024.1	813997
Galectin-7	3	227872.6	NP_001139281.1	3793824
Matrilin-2	2	226537.5	NP_002464.1	151.5
Malate dehydrogenase, mitochondrial	6	234715.6	AAF27176.1	165039.6297

Cation-independent mannose-6-phosphate receptor	9	34096.1	NP_057327.2	6,972.51
Myosin-10	4	79468.5	NP_001186910.1	12,468.57
Myosin-14	15	50817.8		28,873.39
Myosin-9	24	113899.2	NP_892022.2	29686.72939
Myoferlin	13	95084.2		25099.1887
NADH-ubiquinone oxidoreductase 75 kDa subunit, mitochondrial	7	56642.2		128436.3643
NADH dehydrogenase [ubiquinone] flavoprotein 1, mitochondrial	3	57118.1	NP_000909.2	11036.26111
NAD(P) transhydrogenase, mitochondrial	6	56784.6	NP_005304.3	12,466.14
Nodal modulator 2	2	72934	NP_004902.1	12,422.20
Cytosolic phospholipase A2 zeta	2	29804.6	AAB21614.1	31923.335
Prenylcysteine oxidase 1	4	82862.7	NP_000290.2	269,201.33
Protein disulfide-isomerase	6	81822.1	NP_002221.1	261841
Protein disulfide-isomerase A3	12	18012.9	NP_066953.1	91978
Prohibitin	5	15054.3		314372.632
Plakophilin-1	13	91883.1		900093.6763
Junction plakoglobin	4	52645.9	NP_003356.2	396757.1031
Peptidyl-prolyl cis-trans isomerase B	4	48443.4	NP_003357.2	93,300.21
Profilin-1	2	48443.4	P63000.1	10715.5725
Prominin-2	3	68571	NP_002941.1	28301.10222
Cytochrome b-c1 complex subunit 1, mitochondrial	7	54291.7		150218.81
Ras-related C3 botulinum toxin substrate 1	3	47177.8	NP_776249.1	157021.5156
Dolichyl-diphosphooligosaccharide--protein glycosyltransferase subunit 1	6	274613.4		74,897.30
Lysosome membrane protein 2	2	49962	NP_067022.1	347,699.55
Serpin A12	3	28566.1	EAL24402.1	4812.988889
Immunoglobulin G-binding protein A	2	44876.8	NP_077310.1	145642.865
Spectrin beta chain, non-erythrocytic 1	3	77064.3	NP_001054.1	3805.873333
Sulfide:quinone oxidoreductase, mitochondrial	3	29651.8		140179.9778
Synaptophysin-like protein 1	3	177195	NP_064505.1	17207.54778
Transmembrane protein 43	5	41919.8		91,195.67
Serotransferrin	6	30773.9	NP_003365.1	36856.52104
Cytochrome b-c1 complex subunit Rieske, mitochondrial	2	31620.5	NP_003366.2	274431.75
UDP-glucose:glycoprotein glucosyltransferase 1	5			12879.1984
Synaptic vesicle membrane protein VAT-1 homolog	2			598768.175
Voltage-dependent anion-selective channel protein 1	5			309891
Voltage-dependent anion-selective channel protein 2	5			62486

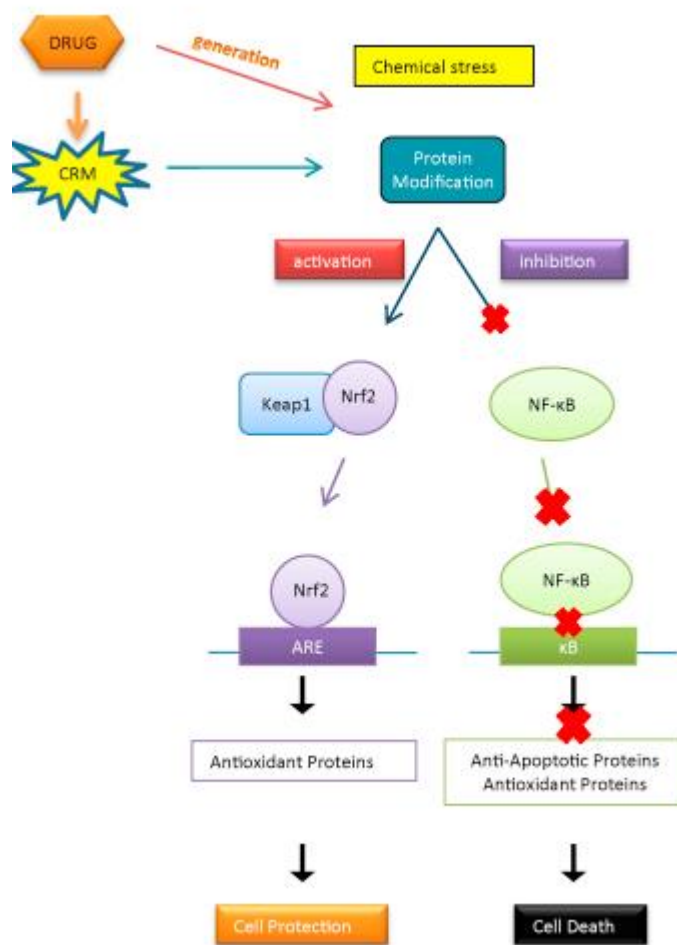


Figure 23. Proposed regulation of Nrf2 and NF-κB by protein modification or GSH depletion (Chia et al.,2010)

Table 7. Summary of the GST Pi gene expression of control and DNCB treated HaCaT cells

Sample	copies/ μ g	Sample	copies/ μ g
control-0.5h	0.00617	DNCB-0.5h	0.11812
control-0.5h	0.00601	DNCB-0.5h	0.14544
control-0.5h	0.00545	DNCB-0.5h	0.11449
average	0.0058767	average	0.1260167
control-1h	0.04175	DNCB-1h	0.0535
control-1h	0.05215	DNCB-1h	0.05165
control-1h	0.04122	DNCB-1h	0.05074
average	0.04504	average	0.0519633
control-2h	0.04472	DNCB-2H	0.02381
control-2h	0.04789	DNCB-2H	0.03031
control-2h	0.04359	DNCB-2H	0.02353
average	0.0454	average	0.0258833
control-3h	0.06284	DNCB-3H	0.0555
control-3h	0.04988	DNCB-3H	0.04624
control-3h	0.04852	DNCB-3H	0.04027
average	0.0537467	average	0.0473367
control-4h	0.05183	DNCB-4H	0.07939
control-4h	0.06176	DNCB-4H	0.09329
control-4h	0.05471	DNCB-4H	0.09235
average	0.0561	average	0.0883433
control-6h	0.07515	DNCB-6H	0.04115
control-6h	0.04368	DNCB-6H	0.04346
control-6h	0.06717	DNCB-6H	0.09981
average	0.062	average	0.0614733
control-24h	0.0012	DNCB-24H	0.01667
control-24h	0.00041	DNCB-24H	0.01377
control-24h	0.00049	DNCB-24H	0.0238
average	0.0007	average	0.01808

Table 8. Summary of the GST Pi gene expression of control and PA treated HaCaT cells

Sample	copies/ μ g	Sample	copies/ μ g
Control 0,5	0.00346	PA-0.5h	0.0152
Control 0,5	0.00336	PA-0.5h	0.01512
Control 0,5	0.00332	PA-0.5h	0.01534
average	0.00338	average	0.01522
Control-1h	0.01074	PA-1h	0.01655
Control -1h	0.0117	PA-1h	0.01735
Control -1h	0.01189	PA-1h	0.01781
average	0.01144333	average	0.01723667
Control-2h	0.0179	PA-2h	0.024598
Control -2h	0.00989	PA-2h	0.020007
Control -2h	0.004999	PA-2h	0.017667
average	0.010911	average	0.020334
Control -3h	0.01023	PA-3h	0.02467
Control -3h	0.01069	PA-3h	0.01933
Control 3h	0.01049	PA-3h	0.01888
average	0.01047	average	0.02096
Control -4h	0.01454	PA-4h	0.01533
Control -4h	0.0146	PA-4h	0.0167
Control -4h	0.01339	PA-4h	0.01148
average	0.01417667	average	0.01450333
Control -6h	0.01182	PA-6h	0.01242
Control -6h	0.01733		
Control -6h	0.01205		
average	0.01373333	PA-24h	0.01778
		PA-24h	0.03092
Control -24	0.00064	PA-24h	0.02642
		average	0.02504

Table 9. Summary of the GAPDH gene expression of control, DNCB and PA treated HaCaT

Sample control	copies/ μ g	Sample	copies/ μ g	Sample	copies/ μ g
C 0.5h	0.004	DNCB 0.5h	0.014	PA 0.5h	0.012
C 0.5h	0.0039	DNCB 0.5h	0.014	PA 0.5h	0.009
C 0.5h	0	DNCB 0.5h	0.023	PA 0.5h	0.023
Average	0.0039	Average	0.0168	Average	0.0147
C 1h	0.02	DNCB 1	0.01	PA 1	0.17
C 1h	0.016	DNCB 1h	0.008	PA 1h	0.0093
C 1h	0	DNCB 1h	0.11	PA 1h	0.101
Average	0.018	Average	0.011	Average	0.0934
C 2h	0.014	DNCB 2h	0.012	PA 2h	0.011
C 2h	0.012	DNCB 2h	0.007	PA 2h	0.007
C 2h	0	DNCB 2h	0.008	PA 2h	0.010
Average	0.013	Average	0.009	Average	0.0094
C 3h	0.013	DNCB 3h	0.02	PA 3h	0.02
C 3h	0.015	DNCB 3h	0.027	PA 3h	0.025
C 3h	0.021	DNCB 3h	0.01	PA 3h	0.015
Average	0.016	Average	0.017	Average	0.02
C 4h	0.039	DNCB 4h	0.09	PA 4h	0.091
C 4h	0.018	DNCB 4h	0.038	PA 4h	0.053
C 4h	0.089	DNCB 4h	0.015	PA 4h	0.015
Average	0.018	Average	0.039	Average	0.055
C 6h	0.04	DNCB 6h	0.032	PA 6h	0.038
C 6h	0.02	DNCB 6h	0.013	PA 6h	0.022
C 6h	0.033	DNCB 6h	0.025	PA 6h	0.027
Average	0.03	Average	0.022	Average	0.029
C 24h	0.12	DNCB 24h	0.02	PA 24h	0.019
C 24h	0.098	DNCB 24h	0.0094	PA 24h	0.0096

C 24h	0.112	DNCB 24h	0.01922	PA 24h	0.01899
Average	0.11	Average	0.015	Average	0.0158

Figure 24. Standard cDNA curve, performed on treated HaCaT cells using the designed GAPDH primers

